On the Multiplicity of Crossing-free Geometric Graphs

DISS. ETH NO. 25204

On the Multiplicity of Crossing-free Geometric Graphs

A thesis submitted to attain the degree of

DOCTOR OF SCIENCES of ETH ZÜRICH

(Dr. sc. ETH Zürich)

presented by

Manuel Wettstein
M.Sc. ETH in Computer Science

born on 29 June 1987
citizen of Switzerland and Italy

accepted on the recommendation of

Prof. Dr. Emo Welzl, examiner
Prof. Dr. Stefan Felsner, co-examiner

2018

Acknowledgments

I wish to express my deepest gratitude to my advisor Emo Welzl; this thesis would not have materialized without his foresight, ingenuity and guidance. Already during my master's studies at ETH, Emo managed to draw my interest to the general topic of this thesis with his lecture about geometric graphs. Shortly after that, I had the privilege of writing my master's thesis under his supervision. He then accepted me into his research group, which I had the pleasure of being part of for the past five years. During that time Emo was indispensable for my research. He kept impressing me with his deep understanding of geometry in particular, and of algorithms and combinatorics in general. Without his constant input and inspiration, it is hard to imagine for any of the three research papers presented in this thesis to have seen the light of day. This holds especially true for our joint paper about wheel sets and polytopes.

Special thanks go to Stefan Felsner, who kindly agreed to serve as the external co-examiner for this thesis. It was always a pleasure to meet him at various conferences and workshops over the years, and he always showed great interest in my work.

I further would like to thank all past and present members of Emo's research group, and everyone else I had the privilege of interacting

with during my time in Zürich. In particular, I want to mention Timon Hertli for helping me get around during my first semester; Vincent Kusters for accompanying me on countless trips to geometry-related conferences and workshops; Antonios Thomas for sharing his office with me for more than three years; Patrick Schnider for the great collaboration when I had the pleasure of supervising his master's thesis; Manuela Fischer for proofreading the first two chapters of this thesis; Alexander Pilz for his contributions to our joint paper about wheel sets and polytopes; Michael Hoffmann for organizing our amazing group workshop every year; and Andrea Salow for being incredibly helpful with any administrative matters.

Last but not least, my thanks go to all co-authors of two additional research papers, which are not included in this thesis. These are Jean Cardinal, Michael Hoffmann, Vincent Kusters and Csaba Tóth for our paper about arc diagrams, flip distances and Hamiltonian triangulations [17]; as well as Oswin Aichholzer, Vincent Kusters, Wolfgang Mulzer and Alexander Pilz for our paper about order types and radial systems [6].

Zürich, May 2018 *Manuel Wettstein*

Contents

Abstract

The subject matter of this thesis are so-called crossing-free geometric graphs. These are simple graphs combined with an embedding on a given set P of n points in the plane, where edges are realized as pairwise non-crossing straight-line segments between the corresponding endpoints. In particular, we are interested in the number of crossing-free geometric graphs, and the investigated problems are of an algorithmic and analytical nature. For example, given P as input, we want to be able to compute the number of crossing-free geometric graphs on P efficiently and to enumerate the corresponding set quickly; or, for any n, we want to understand which point sets P minimize and maximize the corresponding numbers. The contributions of this thesis come in the following three parts.

In the first part, we develop an algorithmic framework for counting and enumeration. The obtained counting algorithms run in time $O(c^n n^4)$, where c depends on the considered graph family, such as triangulations or crossing-free perfect matchings. The obtained enumeration algorithms for crossing-free perfect matchings and convex partitions run with guaranteed polynomial-time delay.

In the second part, we introduce and study a new combinatorial object called the trapezoidal diagram of a crossing-free geometric

graph. In essence, such a diagram records all vertical visibility relations between the vertices and edges of a geometric graph. We give a detailed analysis of the number of such diagrams for perfect matchings and triangulations. We also describe an intriguing connection to higher-dimensional balanced bracket expressions.

In the third part, we study a specific family of point sets $P = H \cup \{w\}$ called wheel sets, with only one non-extreme point w. We obtain explicit formulas for the number of a wide range of families of crossing-free geometric graphs. In the special case of w-embracing triangles, we show how to generalize the obtained formula to higher dimension d, resulting in a $O(n^{d-1})$ time algorithm for computing the simplicial depth of w in $H \subseteq \mathbb{R}^d$.

Zusammenfassung

Gegenstand dieser Arbeit sind sogenannte kreuzungsfreie geometrische Graphen. Dabei handelt es sich um einfache Graphen mit einer Einbettung auf einer Menge P von n Punkten in der Ebene, wobei Kanten als paarweise nichtkreuzende Liniensegmente zwischen den entsprechenden Endpunkten realisiert werden. Im Speziellen interessieren wir uns für die Anzahl kreuzungsfreier geometrischer Graphen, und die untersuchten Fragestellungen sind von algorithmischer und analytischer Natur. Beispielsweise möchten wir für gegebenes P die Anzahl kreuzungsfreier geometrischer Graphen auf P effizient berechnen und die entsprechende Menge schnell enumerieren; oder für alle n möchten wir verstehen welche Punktemenge P die entsprechende Anzahl minimiert und maximiert. Die Beiträge dieser Arbeit kommen in den folgenden drei Teilen.

Im ersten Teil entwickeln wir ein algorithmisches Rahmenwerk zum Zählen und Enumerieren. Die erlangten Zählalgorithmen laufen in Zeit $O(c^n n^4)$, wobei c von der betrachteten Graphenfamilie abhängt, wie beispielsweise Triangulierungen oder kreuzungsfreie perfekte Paarungen. Die erlangten Enumerationsalgorithmen für kreuzungsfreie perfekte Paarungen und konvexe Zerlegungen laufen mit garantiert polynomiellem Zeitverzug.

Im zweiten Teil führen wir ein neues kombinatorisches Objekt ein, welches wir als trapezoidales Diagramm eines kreuzungsfreien geometrischen Graphen bezeichnen. Im Wesentlichen erfasst solch ein Diagramm alle vertikalen Sichtbarkeitsverhältnisse zwischen Knoten und Kanten eines geometrischen Graphen. Wir führen eine detaillierte Analyse der Anzahl solcher Diagramme für perfekte Paarungen und Triangulierungen. Desweiteren beschreiben wir einen verblüffenden Zusammenhang zu höherdimensionalen Klammerausdrücken.

Im dritten Teil untersuchen wir eine spezielle Familie von Punktemengen $P = H \cup \{w\}$, sogenannte Radmengen, mit lediglich einem nichtextremen Punkt w. Wir erhalten explizite Formeln für die Anzahl von einer grossen Auswahl von Familien von kreuzungsfreien geometrischen Graphen. Für den Spezialfall von w-umfassenden Dreiecken zeigen wir, wie die erhaltene Formel auf höhere Dimension d verallgemeinert wird, woraus sich ein $O(n^{d-1})$-Zeit-Algorithmus fürs Berechnen der simplizialen Tiefe von w in $H \subseteq \mathbb{R}^d$ ergibt.

CHAPTER 1

Overview

Our story begins—like countless other stories in mathematics and computer science—with the famous Swiss mathematician Leonhard Euler. In a letter from 1751 to his friend Christian Goldbach he makes the following remark [23]:

> *Ich bin neulich auf eine Betrachtung gefallen, welche mir nicht wenig merkwürdig vorkam. Dieselbe betrifft, auf wie vielerley Arten ein gegebenes polygonum durch Diagonallinien in triangula zerschnitten werden könne.*

In the above passage, Euler considers a polygon with $n = m + 2$ vertices—or, equivalently, with $n = m + 2$ sides. He wants to know the number C_m of different ways that the polygon can be dissected into triangles by joining any non-adjacent vertices with diagonal

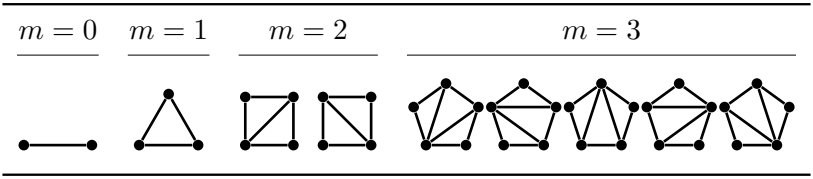

Table 1.1: All possible dissections for $m = 0, 1, 2, 3$.

lines. In the same letter, he gives the following product formula without proof.[1]

$$C_m = \frac{2 \cdot 6 \cdot 10 \cdot 14 \cdot 18 \cdot 22 \cdots (4m-2)}{2 \cdot 3 \cdot 4 \cdot 5 \cdot 6 \cdot 7 \cdots (m+1)} \tag{1.1}$$

Starting with the degenerate case $m = 0$, the numbers C_m thus give rise to the following integer sequence.

$$1, 1, 2, 5, 14, 42, 132, 429, 1430, 4862, \ldots$$

A quick look at Table 1.1 allows easy verification of the first four elements of the sequence.

Besides Euler and Goldbach, the names Johann Segner, Gabriel Lamé and Eugène Catalan are tightly linked to the early development of our understanding of the defined number sequence. In the following we briefly mention their contributions.

In 1761 Segner describes a way of partitioning the set of dissections so that each class comprises all dissections with the same base triangle incident with a fixed base side of the polygon. [56] An example of such a partition is depicted in Figure 1.2. It can then be observed that the number of dissections in a particular class is simply the

[1] In his original letter, Euler (and later also Lamé) formulates all of his observations in terms of n instead of m. From a modern perspective, however, the parameter m turns out to be more natural.

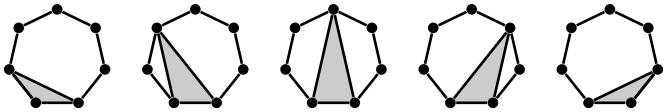

Figure 1.2: Segner's partition for the case $m = 5$. The gray region is the base triangle and the white regions can be dissected arbitrarily.

product of the respective numbers of dissections of the regions to the left and right of the base triangle. This leads to a combinatorial proof of the following recurrence relation.[2]

$$C_m = C_0C_{m-1} + C_1C_{m-2} + C_2C_{m-3} + \cdots + C_{m-1}C_0 \tag{1.2}$$

In 1838 Lamé presents an elegant argument in which dissections are counted in two different ways. [40] The first part of the argument is equivalent to Segner's considerations and also yields the recurrence (1.2). The second part makes use of an idea similar to Segner's; but instead of using base sides with incident base triangles, it uses base vertices with incident base diagonals. For each possible base vertex of the given polygon and each corresponding base diagonal, a product term is added similar to the terms that appear in Segner's sum. Due to overcounting, the sum is finally divided by $2m - 2$, which is twice the number of diagonals in any dissection of the whole polygon.

$$C_m = \frac{(m+2)(C_1C_{m-1} + C_2C_{m-2} + \cdots + C_{m-1}C_1)}{2m-2} \tag{1.3}$$

Combining (1.2) and (1.3) yields the following equation, which now allows easy verification of Euler's product formula.

$$C_{m+1} = \frac{4m+2}{m+2}C_m \tag{1.4}$$

[2]Apparently, since at the time of writing his paper modern index notation is not as common as today, Segner uses the letters $a, b, c, \ldots, o, p, q$ instead of $C_0, C_1, C_2, \ldots, C_{m-3}, C_{m-2}, C_{m-1}$ to formulate the recurrence.

Finally, in Catalan's first among many articles about the defined number sequence[3], he is the first to write down what are nowadays considered standard formulas. [18]

$$C_m = \frac{1}{m+1}\binom{2m}{m} = \frac{(2m)!}{m!(m+1)!} \tag{1.5}$$

Today, the numbers C_m are named after Eugène Catalan. For a more complete account of the history of Catalan numbers, we refer the reader to Igor Pak's very detailed survey on the web. [48]

Catalan numbers are ubiquitous in enumerative combinatorics; they occur in various counting problems concerned with lattice paths, binary trees, balanced bracket expressions, and many more. It is customary at this point to refer to a famous exercise in Richard Stanley's book, which presents no less than sixty-six combinatorial interpretations of the Catalan numbers. [62, Exercise 6.19]

For us, the story about the birth and early development of the Catalan numbers shall serve as motivation for the problems that are considered in this thesis. In many ways, these problems can be seen as generalizations of Euler's question from more than a quarter of a millennium ago. The Catalan numbers themselves and close relatives will reappear in every chapter of this thesis—sometimes in a quite different and even unexpected guise.

1.1 Definitions

Let P be a finite set of n points in the Euclidean plane. Often throughout the thesis, we make the additional assumption that P

[3]Curiously enough, Catalan's article immediately follows Lamé's in the same journal. This coincidence is due to the popularization of Euler's problem by Joseph Liouville among his fellow mathematicians in early 19$^{\text{th}}$ century Paris.

is in *general position*. By this we mean that no three points are contained in a common line, and that no two points share the same x-coordinate. Note right away that the latter condition is not an actual restriction because every finite point set P can be rotated in such a way that the condition is satisfied, and because all problems that we consider are invariant under rotation of P.

A *geometric graph* G on P is a simple graph with vertex set P combined with an embedding into the plane where edges are drawn as straight-line segments between the corresponding endpoints in P. We say that G is *crossing-free* if the drawings of no two edges intersect except possibly at a common endpoint.

It is important to note that crossing-free geometric graphs are not the same as planar graphs, even though there is the following intimate relation. By definition, the abstract graph underlying a crossing-free geometric graph is planar and, due to Fáry's Theorem, every planar graph can be drawn as a crossing-free geometric graph in the plane.

As for a concrete example, let us consider the set $\mathcal{T}(P)$ of all triangulations on P, where by a *triangulation* on P we mean an edge-maximal crossing-free geometric graph on P. Furthermore, let us use the notation $\mathrm{tr}(P) \coloneqq |\mathcal{T}(P)|$ to denote the number of triangulations on P. To be even more concrete, let $P = P_{\mathsf{con}}$ be a set of n points in convex position; for example, the vertex set of a regular n-gon. It can be observed that all n edges along the boundary of the convex hull of P_{con} are *unavoidable*, which means that they are contained as an edge in every triangulation on P_{con}. Therefore, there is a clear bijective correspondence between dissections of a polygon as considered by Euler and the elements of the set $\mathcal{T}(P_{\mathsf{con}})$. For $n \geq 2$ we thus readily obtain the following equation.

$$\mathrm{tr}(P_{\mathsf{con}}) = C_{n-2} = \frac{1}{n-1}\binom{2n-4}{n-2} = \Theta(n^{-3/2}4^n) \tag{1.6}$$

While the special case $P = P_{\mathsf{con}}$ is easy to understand—in particular for triangulations, but also for many other families of crossing-free geometric graphs—much less is known about the general case, where P is an arbitrary point set.

Table 1.3 gives an overview of the different families of crossing-free geometric graphs that are considered throughout the thesis. As a reference, it also gives the notations corresponding to the set $\mathcal{T}(P)$ and the number $\mathrm{tr}(P)$ for all families.

In most cases, the name combined with the example given in Table 1.3 is self-explanatory. However, let us mention explicitly that by $\mathcal{G}(P)$ we mean the set of all crossing-free geometric graphs. Furthermore, by a *convex partition* on P we mean a partition of the set P such that the convex hulls of the individual parts are pairwise disjoint. Similarly, a *convex subdivision* on P is a subdivision of the convex hull of P into convex faces whose vertices belong to P.

It is clear that every convex partition and every convex subdivision on P can be represented uniquely and naturally as a crossing-free geometric graph on P; we simply include all edges along the boundaries of the convex hulls of the individual parts and faces. It can then also be noted for example that a crossing-free matching is a special case of a convex partition, and that a triangulation is a special case of a convex subdivision.

In addition, we use $\mathcal{F}(P)$ and $\mathrm{nf}(P)$ as placeholders whenever we do not wish to specify the graph family.

1.2 Types of Problems

For the most part, the questions that are raised in this thesis—as well as the answers that are given—belong to one of the following three broad categories. Whenever this is not quite true, it still holds

Name	Set	Number	Example
All Graphs	$\mathcal{G}(P)$	$\mathrm{pg}(P)$	
Convex Partitions	$\mathcal{CP}(P)$	$\mathrm{cp}(P)$	
Matchings	$\mathcal{M}(P)$	$\mathrm{ma}(P)$	
Perfect Matchings	$\mathcal{PM}(P)$	$\mathrm{pm}(P)$	
Convex Subdivisions	$\mathcal{CS}(P)$	$\mathrm{cs}(P)$	
Triangulations	$\mathcal{T}(P)$	$\mathrm{tr}(P)$	
Spanning Trees	$\mathcal{ST}(P)$	$\mathrm{st}(P)$	
Spanning Paths	$\mathcal{SP}(P)$	$\mathrm{sp}(P)$	
Spanning Cycles	$\mathcal{SC}(P)$	$\mathrm{sc}(P)$	
Placeholder	$\mathcal{F}(P)$	$\mathrm{nf}(P)$	?

Table 1.3: All considered families of crossing-free geometric graphs.

that the questions and answers arise naturally from the desire to improve our understanding of one of the following points. A short discussion of the state of the art of these problems and a summary of the main references is deferred to Chapter 2.

Formulas for special point sets. For certain concrete point sets P and graph families $\mathcal{F}(P)$ it is possible to give closed formulas—or at least rough asymptotic estimates—for the number $\mathrm{nf}(P) = |\mathcal{F}(P)|$. We have already seen a striking example in (1.6) for the case of triangulations on a point set in convex position, but it is by no means the only one. Point sets that are amenable to such a thorough analysis are usually highly structured with many symmetries ready to be exploited.

Extremal lower and upper bounds. As usual, let $\mathcal{F}(P)$ be any family of crossing-free geometric graphs on P, and let $\mathrm{nf}(P) = |\mathcal{F}(P)|$. In addition, we define the following quantities.

$$\underline{\mathrm{nf}}(n) := \min_{P\colon |P|=n} \mathrm{nf}(P) \qquad \overline{\mathrm{nf}}(n) := \max_{P\colon |P|=n} \mathrm{nf}(P) \tag{1.7}$$

In words, by definition, $\underline{\mathrm{nf}}(n)$ and $\overline{\mathrm{nf}}(n)$ are the best possible extremal lower and upper bounds on $\mathrm{nf}(P)$ in terms of the size n of the underlying point set P. Determining the asymptotic behavior of these quantities as n tends to infinity—leave alone finding exact formulas—proves to be a highly challenging task, often with no resolution in sight to this day. Modern research instead focuses on improving exponential lower and upper bounds of the following kind.

$$\Omega^*(l^n) = \underline{\mathrm{nf}}(n) = O^*(u^n) \text{ for fixed } l \le u \tag{1.8}$$

$$\Omega^*(l^n) = \overline{\mathrm{nf}}(n) = O^*(u^n) \text{ for fixed } l \le u \tag{1.9}$$

Note that the $*$ here indicates that potential subexponential factors are ignored in the Ω- and O-notation. While the gap between the constants l and u often has been made steadily smaller over the past decades, finding the truly best possible values for l and u appears hopeless in many cases.

Algorithms for counting and enumeration. We cannot hope to prove nice closed formulas such as (1.6) for $\mathrm{nf}(P)$ and all possible point sets P. Nevertheless, it is conceivable to construct efficient algorithms which are able to compute the number $\mathrm{nf}(P)$ either exactly or approximately when given P as input. An intriguing question in this context is whether the number $\mathrm{nf}(P)$ can be computed with *exponential speed-up over enumeration*; that is, in time at most $c^{-n} \cdot \mathrm{nf}(P) \cdot \mathrm{poly}(n)$ for some fixed constant $c > 1$. The terminology makes sense after observing that any enumeration algorithm that computes some explicit representation of each element of $\mathcal{F}(P)$ is bound to take time at least $\mathrm{nf}(P) \cdot \mathrm{poly}(n)$.

In the same vein, we cannot hope to get a very deep understanding of the structure of the set $\mathcal{F}(P)$ for all point sets P. However, efficient algorithms for enumerating all elements of $\mathcal{F}(P)$ when given P are within reach. In this context, *efficient* means that the average time spent per enumerated element is polynomial in n; that is, the overall running time is of the form $\mathrm{nf}(P) \cdot \mathrm{poly}(n)$. Additionally, we say that the enumeration is done with *polynomial-time delay* if the time gap between any two enumerated elements—and, in particular, the time until the first output—is bounded by a polynomial in n.

1.3 Contributions

All results presented in this thesis are based on three papers that have been published under the following names.

(i) *Counting and Enumerating Crossing-free Geometric Graphs*, by Manuel Wettstein.

(ii) *Trapezoidal Diagrams, Upward Triangulations, and Prime Catalan Numbers*, by Manuel Wettstein.

(iii) *From Crossing-free Graphs on Wheel Sets to Embracing Simplices and Polytopes with Few Vertices*, by Alexander Pilz, Emo Welzl, and Manuel Wettstein.

Accordingly, and in the same order, Chapters 3 to 5 of this thesis correspond to the three papers above. In the remainder of this chapter, we give a brief summary of these papers.

1.3.1 Framework for Counting and Enumeration

The results presented in (i) rely on earlier work done in the author's master's thesis [70] under the supervision of Emo Welzl. That thesis contains algorithms for counting and enumerating various families of crossing-free geometric graphs. The running times of the counting algorithms are of the form $c^n \cdot \text{poly}(n)$, where c is a constant that depends on the considered graph family. For example, $c \approx 2.83929$ for counting all graphs, $c = 2$ for perfect matchings, $c = 8$ for spanning trees, and $c = 14$ for spanning cycles.

In Chapter 3 we present the content of the later published conference [71] and journal [72] versions of (i). They distinguish themselves from [70] in the following two major ways.

Firstly, we develop a new theoretical framework which captures the common ideas and requirements that are needed for the aforementioned algorithms. The framework shifts our attention from the algorithm itself to a data structure Γ_P, which we call a *combination graph*. Formally speaking, Γ_P is a directed and acyclic graph with unique source and sink vertices so that the set of directed source-sink

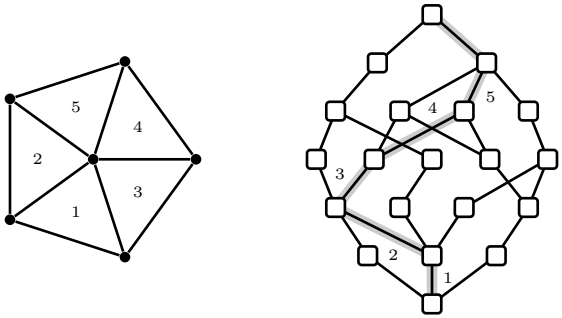

Figure 1.4: On the left, a point set P. On the right, the corresponding combination graph Γ_P. All edges of Γ_P are directed upwards and they are associated with a triangle, except for the upper-most level. Combining the triangles on the highlighted source-sink path of Γ_P yields the corresponding triangulation on P.

paths in Γ_P is in bijective correspondence with the set of crossing-free geometric graphs of a given family on P. A concrete example of such a combination graph Γ_P for the special case of triangulations is displayed in Figure 1.4.

The size of the data structure Γ_P is typically of the form $c^n \cdot \text{poly}(n)$, where again the constant c depends only on the considered graph family. Naturally, by making use of standard graph algorithms, Γ_P then lends itself to the computation of the number $\text{nf}(P)$ in time $c^n \cdot \text{poly}(n)$, or to the efficient enumeration of the elements of the set $\mathcal{F}(P)$ in time $\text{nf}(P) \cdot \text{poly}(n)$.

The developed framework has the effect of making earlier correctness proofs and runtime analyses from [70] a lot more streamlined and simpler. It also makes many of the earlier results more general in the following sense. For a plethora of yet unconsidered graph families, it will be clear at a glance and without any additional work that they are also amenable to the developed techniques.

Secondly, we are able to give a more refined analysis of the size of the data structures Γ_P for the case of spanning trees and spanning cycles. This results in improvements of the corresponding constants from originally $c = 8$ to $c = 7.04313$ for spanning trees, and from originally $c = 14$ to $c = 5.61804$ for spanning cycles.

1.3.2 Trapezoidal Diagrams and Upper Bounds

The material presented in Chapter 4 is solely based on the journal version [73] of (ii).

We introduce and study a new combinatorial object which we call the *trapezoidal diagram* of a crossing-free geometric graph. While originally invented as a potential tool for improving existing extremal upper bounds—a task we have unfortunately not succeeded in so far—these objects have brought forth a range of exciting mathematical connections, which we believe to be of interest in their own right.

Informally speaking, the trapezoidal diagram of a crossing-free geometric graph G is constructed by first taking the trapezoidal decomposition of G and then forgetting the exact coordinates of the vertices of G. Phrased differently, each edge of G knows the identity of the vertices that it can see without obstruction vertically above and below itself, respectively. In addition, the edge also knows the order in which said vertices appear along the x-axis. A more formal definition is given in Chapter 4; for now we use the intuition given by the example displayed in Figure 1.5.

By exploiting a specific way of ordering the trapezoids, we show that trapezoidal diagrams admit a natural encoding as strings over a finite alphabet. In the case of perfect matchings and triangulations, the encodings turn out to be particularly elegant, as they correspond to so-called 3-dimensional balanced bracket expressions.

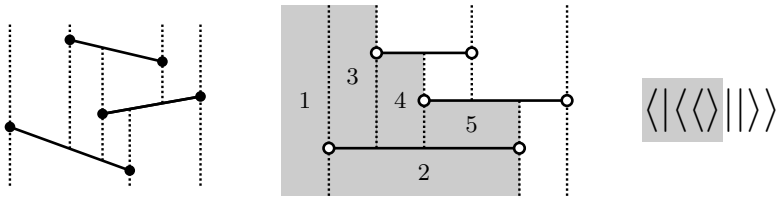

Figure 1.5: On the left, a crossing-free perfect matching and its trapezoidal decomposition. In the middle, the corresponding trapezoidal diagram with some of its trapezoids numbered. On the right, the corresponding encoding as a balanced bracket expression. In this special case, each trapezoid of the trapezoidal diagram corresponds to one particular symbol.

These 3-dimensional balanced bracket expressions form a natural generalization of ordinary balanced bracket expressions, where instead of having only two symbols we now have three symbols. While the latter give rise to the Catalan numbers as their counting sequence, the former give rise to another generalization known as 3-dimensional Catalan numbers.

In the case of perfect matchings, the number of trapezoidal diagrams is easy to analyze because every balanced bracket expression corresponds to a valid trapezoidal diagram. For triangulations the same does not hold. Instead, the expressions corresponding to the trapezoidal diagram of a triangulation form a strict and highly structured subset. For reasons that become clear in Chapter 4, we call such expressions *prime* and we call the emerging counting sequence 3-dimensional *prime Catalan numbers*. Our analysis of this previously unknown number sequence generalizes to arbitrary dimension d; that is, to balanced bracket expressions over d symbols.

Another surprising connection is that trapezoidal diagrams of triangulations are almost the same—in a certain sense—as so-called ab-

stract upward triangulations. Our analysis of the number of trapezoidal diagrams of geometric triangulations thus extends to abstract upward triangulations.

1.3.3 Explicit Formulas for Wheel Sets

At the time of writing, our third paper (iii) is still under review at a journal. However, a conference version of the paper has been published already [50], which forms the basis of Chapter 5.

As already mentioned before, the set of n points in convex position is comparatively easy to analyze. We now investigate what happens if there is just one non-extreme point; that is, we study so-called *wheel sets* $P = H \cup \{w\}$. The defining characteristic is that the point set H is in convex position and that the so-called *extra point* w is contained in the convex hull of H. In contrast to previous convention, we use the letter n to denote the size of H, implying that P has size $n + 1$.

The first important observation is that there is not just one wheel set, but a whole family of wheel sets; by this we mean that the number $\mathrm{nf}(P)$ may change as w moves about. Figure 1.6 shows all different order types that correspond to a wheel set for the special case $n = 7$. In essence, order types group point sets into a finite number of equivalence classes such that any two point sets in the same class behave the same from a combinatorial perspective; precise definitions follow later in Chapter 5.

For many graph families, we show that $\mathrm{nf}(P)$ allows the following simple closed expression.

$$\mathrm{nf}(P) = \sum_{k=0}^{n-1} F_k \Lambda_k \tag{1.10}$$

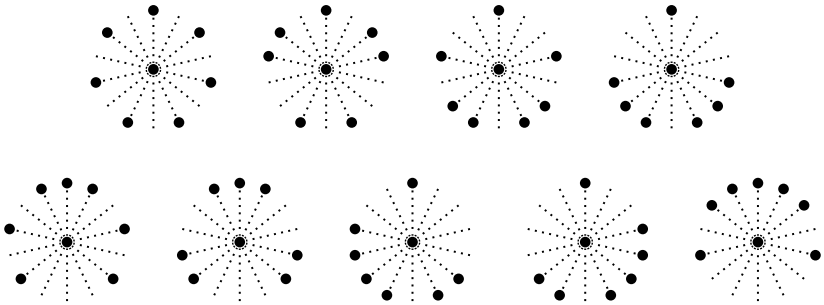

Figure 1.6: All possible order types of wheel sets for $n = 7$.

In the above formula we have an inner product of a vector Λ that only depends on the graph family with what we call the *frequency vector* F, which only depends on the order type of P. Frequency vectors constitute another way of grouping wheel sets into equivalence classes. However, we show that the resulting classes are much coarser than those for order types. Therefore, we deduce that for computing $\mathrm{nf}(P)$ we do not need the full order type information, provided that P is a wheel set.

The developed techniques often make it easy to find extremal configurations. For many graph families, the wheel set P which maximizes $\mathrm{nf}(P)$ turns out to be the symmetric configuration, which can be seen on the top-left of Figure 1.6.

One particular instantiation of (1.10) works for w-embracing triangles; that is, we count unordered triples in H which contain w in their respective convex hull. We generalize this particular result to higher dimensions, where H is a set of n points in $\mathbb{R}^d$ and we are interested in the number of d-simplices spanned by points in H that contain a given query point w. For this higher-dimensional problem we give an exact counting algorithm that runs in time $O(n^{d-1})$.

CHAPTER 2

Background Information

We give a brief account of relevant published literature about the general subject area of this thesis. The focus does not lie on completeness; instead, we give a selection of results and some of their history which allows to better put in perspective our contributions from the upcoming chapters.

2.1 Formulas for Special Point Sets

We review some results for the four special point sets depicted in Figure 2.1, and the graph families defined in Table 1.3 on page 7.

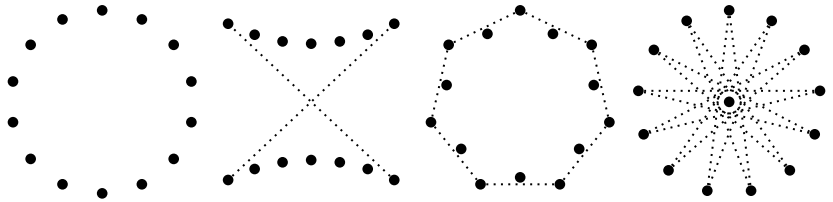

Figure 2.1: From left to right: Convex position, a double chain, a double circle, and a symmetric wheel set with 14 points.

2.1.1 Convex Position

Recall that we write P_{con} to denote a set of n points in convex position. There are two main reasons why this set is comparatively simple to analyze. Firstly, the exact coordinates of the points do not matter as far as the number of crossing-free geometric graphs is concerned. Secondly, the presence of any edge cleanly separates the problem into two independent subproblems, each again defined on a set of points in convex position.

The cases of crossing-free spanning paths and spanning cycles are so simple that we leave them as a warm-up exercise to the reader.

$$\mathrm{sp}(P_{\mathsf{con}}) = 2^{n-3}n \qquad \mathrm{sc}(P_{\mathsf{con}}) = 1 \tag{2.1}$$

For crossing-free perfect matchings and n even, a recurrence akin to Segner's recurrence (1.2) on page 3 can be formulated, leading us once again to the Catalan numbers. Perhaps the first to make this observation is Motzkin in 1948. [46]

$$\mathrm{ma}(P_{\mathsf{con}}) = \sum_{i=0}^{\lfloor n/2 \rfloor} \binom{n}{2i} C_i \qquad \mathrm{pm}(P_{\mathsf{con}}) = C_{n/2} \tag{2.2}$$

The remaining families—all graphs, convex partitions, convex subdivisions and spanning trees—are dealt with by a systematic approach

developed by Flajolet and Noy in 1999. [24] Their approach makes use of tools from analytic combinatorics, such as symbolic methods, generating functions and singularity analysis.

$$\mathrm{pg}(P_{\mathsf{con}}) = \sum_{i=0}^{\lfloor \frac{n-1}{2} \rfloor} (-1)^i \frac{1 \cdot 3 \cdots (2n-2i-5)}{12 \cdot i!(n-2i-1)!} 3^{n-2i} 2^{n-i} \tag{2.3}$$

$$\mathrm{cp}(P_{\mathsf{con}}) = C_n = \frac{1}{n+1}\binom{2n}{n} \tag{2.4}$$

$$\mathrm{cs}(P_{\mathsf{con}}) = \frac{1}{n-1}\sum_{i=0}^{n-2}(-1)^i \binom{n-1}{i}\binom{2n-4-i}{n-2-i} 2^{n-2-i} \tag{2.5}$$

$$\mathrm{st}(P_{\mathsf{con}}) = \frac{1}{2n-1}\binom{3n-3}{n-1} \tag{2.6}$$

2.1.2 Double Chain

The *double chain* P_{dch} is defined for even n only; it consists of two convex chains with $n/2$ vertices each, facing one another with opposed concavity. Both chains must be sufficiently flat, so that no segment connecting two vertices on opposite chains may properly intersect the convex hull of either chain.

The double chain is first introduced in 2000 by García, Noy and Tejel, who observe that this point set has an exceptionally small number of pairs of crossing edges. [27] They prove lower bounds for the following four graph families.

$$\begin{aligned} \mathrm{pm}(P_{\mathsf{dch}}) &= \Omega^*(3^n) & \mathrm{tr}(P_{\mathsf{dch}}) &= \Omega^*(8^n) \\ \mathrm{st}(P_{\mathsf{dch}}) &= \Omega^*(9.35^n) & \mathrm{sc}(P_{\mathsf{dch}}) &= \Omega^*(4.64^n) \end{aligned} \tag{2.7}$$

In 2006 Sharir and Welzl give corresponding lower bounds for convex partitions and matchings. [61]

$$\mathrm{cp}(P_{\mathsf{dch}}) = \Omega^*(5.23^n) \qquad \mathrm{ma}(P_{\mathsf{dch}}) = \Omega^*(4^n) \tag{2.8}$$

One year later, Aichholzer, Hackl, Huemer, Hurtado, Krasser and Vogtenhuber study all crossing-free geometric graphs. [5]

$$\mathrm{pg}(P_{\mathsf{dch}}) = \Omega^*(39.8^n) \tag{2.9}$$

Finally, a more sophisticated analysis from 2015 by Huemer and de Mier further improves the original lower bound for spanning trees as follows. [34]

$$\mathrm{st}(P_{\mathsf{dch}}) = \Omega^*(12.52^n) \tag{2.10}$$

2.1.3 Double Circle

The *double circle* P_{dcr} is constructed by taking the vertices of a regular n-gon for n even, and then pushing every other vertex inwards into the interior of the convex hull by an infinitesimally small distance.

In 1997 Hurtado and Noy give a detailed analysis of the number of triangulations on the double circle. [35] Among other things they prove that, asymptotically speaking, for every vertex that is pushed inwards the number of triangulations decreases by a factor of $3/4$.

$$\mathrm{tr}(P_{\mathsf{dcr}}) = \Theta\left((3/4)^{n/2}\right)\mathrm{tr}(P_{\mathsf{con}}) = \Theta\left(n^{-3/2}\sqrt{12}^{n}\right) \tag{2.11}$$

2.1.4 Wheel Sets

As mentioned in Chapter 1, $P = H \cup \{w\}$ is a wheel set if H is in convex position and w is contained in the convex hull of H. Recall also that we use the convention $n = |H|$ for wheel sets.

Perhaps the first to consider triangulations on wheel sets are Randall, Rote, Santos and Snoeyink in 2001. [51] For odd n they show that the maximizing point set is the *symmetric* wheel set P_{sym}, which

is composed of the vertices of a regular n-gon and one additional vertex at the exact center. They give the following formula.

$$\mathrm{tr}(P_{\mathsf{sym}}) = \frac{1}{2}\left(C_n - n\left(C_{(n-1)/2}\right)^2\right) \tag{2.12}$$

In 2017 Ruiz-Vargas and Welzl study perfect matchings on wheel sets. [55] They give a closed formula for all wheel sets and characterize both the minimizing and maximizing point sets. Based on ideas from that paper, Pilz, Welzl and Wettstein later prove similar formulas for a range of other graph families, such as matchings, triangulations, spanning trees and more. [50]

2.2 Extremal Lower and Upper Bounds

All bounds discussed in this chapter—as well as some additional ones—are summarized in Table 2.2. As a reading example, the top-right entry says that $\mathrm{pg}(P) = O^*(187.53^n)$ holds for all P; the corresponding main reference is [59]. Also recall that the $*$ indicates that potential subexponential factors are ignored.

2.2.1 Minimum

For some graph families, such as perfect matchings and spanning trees, it has been known for a long time that the number $\mathrm{nf}(P)$ is minimized if P is in convex position. In 2007 Aichholzer, Hackl, Huemer, Hurtado, Krasser and Vogtenhuber prove the following much more general statement.

Theorem 2.1 (Theorem 3 in [5])**.** *There exists an injective mapping of all cycle-free plane geometric graphs on top of a set of n points in convex position to isomorphic plane geometric graphs on top of any set of n points.*

	Minimum		Maximum	
	$\forall P\colon \Omega^*(c^n)$	$\exists P\colon O^*(c^n)$	$\exists P\colon \Omega^*(c^n)$	$\forall P\colon O^*(c^n)$
$\mathrm{pg}(P)$	11.65 [5]	11.65 [24]	39.80 [5]	187.53 [59]
$\mathrm{cp}(P)$	3.00 [46]	4.00 [24]	5.23 [61]	12.24 [61]
$\mathrm{ma}(P)$	3.00 [5]	3.00 [46]	4.00 [61]	10.43 [61]
$\mathrm{pm}(P)$	2.00 [5]	2.00 [27]	3.09 [12]	10.05 [61]
$\mathrm{cs}(P)$	2.63 [3]	5.82 [24]	8.65 [20]	187.53 [59]
$\mathrm{tr}(P)$	2.63 [3]	3.46 [35]	8.65 [20]	30.00 [58]
$\mathrm{st}(P)$	6.75 [5]	6.75 [24]	12.52 [34]	141.07 [33]
$\mathrm{sp}(P)$	2.00 [5]	2.00	4.64 [27]	141.07 [33]
$\mathrm{sc}(P)$	1.00	1.00	4.64 [27]	54.55 [60]

Table 2.2: Exponential extremal bounds, where the cells display the respective exponential bases c.

Their use of the word plane is synonymous with how we use the word crossing-free. Furthermore, they also show that $\mathrm{pg}(P)$ is minimized if P is in convex position, and it is an easy exercise to show that the same holds for $\mathrm{sc}(P)$. Combined with the fact that convex position is often easy to analyze, we obtain for many graph families explicit formulas for the overall minimum $\underline{\mathrm{nf}}(n)$. As a consequence for all these families, the corresponding lower and upper bounds in the first and second column of Table 2.2 are identical.

The most notable exception which does not fit well with Theorem 2.1 is the family of triangulations. In fact, judging from (2.11), we already know that the double circle has exponentially fewer triangulations than a point set in convex position. While it is conjectured by many researchers that the double circle is the minimizing point set for triangulations, nobody knows how to go about proving a matching lower bound.

2.2.2 Maximum

In contrast to our reasonable understanding of minimizing configurations, it is not known for any of the considered graph families what the maximizing point set looks like. As far as the maximum number $\overline{\mathrm{nf}}(n)$ itself is concerned, it is a priori not clear at all that it even admits an exponential upper bound such as the one stipulated earlier in equation (1.9) on page 8. Nevertheless, in 1981 Ajtai, Chvátal, Newborn and Szemerédi prove the nowadays well-known Crossing Lemma, which has the following slightly lesser well-known consequence.

Theorem 2.2 (Theorem 2 in [8])**.** *Every planar drawing of every graph with n vertices contains fewer than 10^{13n} crossing-free subgraphs.*

By a subgraph they mean a subset of the drawn edges. Clearly, by applying the above theorem to the complete geometric graph on any given set P of n points, this implies that the number $\mathrm{pg}(P)$ of all crossing-free geometric graphs, and hence every other $\mathrm{nf}(P)$, is also bounded by 10^{13n} from above.

One line of research tries to improve the general upper bound obtained by Theorem 2.2, resulting in better and better individual upper bounds over time. The successive improvements are too numerous; we only list the currently best bounds in the fourth column of Table 2.2.

Coming from the other direction, which corresponds to the third column of Table 2.2, it is attempted to construct new point sets P for which $\mathrm{nf}(P)$ is large. For this purpose, the double chain—or more complicated variants, such as the so-called double zig-zag chain—is often used.

2.3 Algorithms for Counting & Enumeration

2.3.1 Counting

The algorithmic problem of counting crossing-free geometric graphs has been the subject of extensive investigation, in particular for triangulations. [2, 9, 10, 36, 52]

In 2011 Razen and Welzl show for the first time that for some non-trivial family of crossing-free geometric graphs, the corresponding counting problem can be solved with exponential speed-up over enumeration. [53] Namely, they describe an algorithm which computes $\mathrm{pg}(P)$ in time $O^*(\mathrm{tr}(P))$ by first enumerating the set $\mathcal{T}(P)$ and then counting subgraphs in a clever way to avoid repetition. Since they also prove that $\mathrm{pg}(P) = \Omega^*(2.82^n) \cdot \mathrm{tr}(P)$ holds for all P, it is clear that their algorithm runs exponentially faster than any procedure that counts by enumerating the whole set $\mathcal{G}(P)$.

Making use of an unrelated approach, Alvarez and Seidel show in 2013 how to compute the number $\mathrm{tr}(P)$ in time $O(2^n n^2)$. [11] From Table 2.2 we know that $\mathrm{tr}(P) = \Omega^*(2.63^n)$ holds for all point sets P, which implies that this algorithm also runs with exponential speed-up over enumeration.

One year later, Wettstein shows how to generalize the ideas of Alvarez and Seidel. [72] The result is a theoretical framework which gives rise to counting algorithms for all defined families of crossing-free geometric graphs. The corresponding running times are of the form $c^n \cdot \mathrm{poly}(n)$, where the constant c depends on the graph family. In many cases, these algorithms also achieve an exponential speed-up over enumeration.

In a very recent breakthrough from 2016, Marx and Miltzow present a new algorithm that computes the number $\mathrm{tr}(P)$ in sub-exponential time $n^{O(\sqrt{n})}$. [44] By making use of simple annotation systems,

the algorithm is also shown to work for all crossing-free geometric graphs, perfect matchings, spanning trees and spanning cycles, among many others.

2.3.2 Enumeration

A general technique for enumeration called reverse search is developed by Avis and Fukuda in 1996. [13] While solving many unrelated enumeration problems, it can be used for the efficient enumeration of $\mathcal{T}(P)$ and $\mathcal{ST}(P)$. In 2002 Bespamyatnikh describes a particularly efficient implementation of this technique for triangulations, where the time spent per enumerated triangulation is only $O(\log \log n)$. [14]

In 2007 Aichholzer, Aurenhammer, Huemer and Vogtenhuber develop efficient Gray code enumeration schemes for the sets $\mathcal{G}(P)$ and $\mathcal{ST}(P)$. [4] In contrast to reverse search, these schemes have the additional property that any two consecutively enumerated geometric graphs differ only by a constant number of edges.

Another framework for enumerating crossing-free geometric graphs is developed by Katoh and Tanigawa in 2008. [37] It is based on the idea of first enumerating all triangulations and then enumerating all subgraphs of the desired type. Inevitably, the overall running time is always at least $\Omega^*(\mathrm{tr}(P))$. The framework is applied to the sets $\mathcal{G}(P)$, $\mathcal{ST}(P)$ and $\mathcal{PM}(P)$, among others. In the case of $\mathcal{G}(P)$ it yields yet another efficient enumeration algorithm. However, for $\mathcal{ST}(P)$ and $\mathcal{PM}(P)$ the algorithms are not provably efficient since it is unclear how the numbers $\mathrm{st}(P)$ and $\mathrm{pm}(P)$ compare to $\mathrm{tr}(P)$.

The already mentioned theoretical framework for counting developed by Wettstein can also be used for enumeration. [72] In particular, it yields provably efficient enumeration algorithms for the sets $\mathcal{CP}(P)$ and $\mathcal{PM}(P)$ with guaranteed polynomial-time delay.

CHAPTER 3

Framework for Counting and Enumeration

3.1 Introduction

The framework developed here generalizes ideas originally used by Alvarez and Seidel for counting triangulations. [11] Loosely speaking, the technique boils down to the following steps. Fix a set of crossing-free geometric graphs whose elements can be decomposed into reasonably small or simple pieces. For instance, every triangulation can be decomposed into a set of interior-disjoint triangles and, similarly, every crossing-free perfect matching can be decomposed into a set of non-intersecting segments. The aim then is to construct a directed acyclic graph Γ with the following three properties. Firstly, each edge in Γ is labeled with one of the aforementioned pieces. Secondly, there exist distinguished source and sink vertices

in Γ. Thirdly, there is a natural bijection between source-sink paths in Γ and the fixed set of crossing-free geometric graphs; by this we mean that given any source-sink path in Γ, we can collect all the labels appearing on that path and combine them to obtain the corresponding geometric graph. Given such a graph Γ for one particular family of geometric graphs, the corresponding counting and enumeration problems can then be reduced to counting and enumerating source-sink paths in Γ.

Let $\mathcal{G}_P^*$ be the set of crossing-free geometric graphs on all non-empty subsets of P. Elements of $\mathcal{G}_P^*$ are called *units*, and they can be thought of as the simple pieces from the previous paragraph. For a unit $u \in \mathcal{G}_P^*$ we denote by $\mathrm{pts}(u) \subseteq P$ the set of vertex points of u; that is, if u is a geometric graph on a particular subset P' of P, then $\mathrm{pts}(u) = P'$. Let us define a number of useful subsets of $\mathcal{G}_P^*$.

- Let $\mathcal{S}_P$ be the set of *segments* with both endpoints in P. That is, each $u \in \mathcal{S}_P$ is a geometric graph on exactly two points of P with the edge between them.

- Let $\mathcal{CP}_P$ be the set of *convex parts* with vertices in P. That is, for each $u \in \mathcal{CP}_P$ the convex hull of $\mathrm{pts}(u)$ does not contain any points of $P \setminus \mathrm{pts}(u)$; in words, interior points are also vertex points of u. Moreover, u contains all the edges along the boundary of the convex hull of the set $\mathrm{pts}(u)$. Observe that all isolated points and segments with endpoints in P are also elements of $\mathcal{CP}_P$.

- Let $\mathcal{CF}_P$ be the set of *convex faces* with vertices in P. That is, $\mathcal{CF}_P$ contains all $u \in \mathcal{CP}_P$ with $|\mathrm{pts}(u)| \geq 3$ and no interior vertices. The *shape* of any such u is the bounded and closed region delimited by its edges.

- Let $\mathcal{T}_P$ be the set of *empty triangles* with vertices in P. That is, $\mathcal{T}_P$ contains all $u \in \mathcal{CF}_P$ with $|\mathrm{pts}(u)| = 3$.

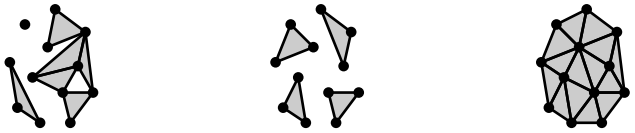

$\mathfrak{C}^{\mathsf{cf}}(\mathcal{T}_P)$ $\mathfrak{C}^{\mathsf{pt}}(\mathcal{T}_P)$ $\mathfrak{C}^{\mathsf{sd}}(\mathcal{T}_P)$

Figure 3.1: The three defined types of crossing-free combinations of $\mathcal{T}_P$. The shaded regions represent the shapes of elements of $\mathcal{T}_P$.

Let us fix a subset $\mathcal{U}$ of $\mathcal{G}_P^*$. For any units $u_1, u_2 \in \mathcal{U}$, if u_1 contains an edge e_1 and u_2 contains a different edge e_2 such that e_1 and e_2 are crossing, then we also say that u_1 and u_2 are *crossing*. Otherwise, u_1 and u_2 are *non-crossing*. A *combination* of $\mathcal{U}$ is a subset C of $\mathcal{U}$, and C is *crossing-free* if the elements of C are pairwise non-crossing.

Let $\mathfrak{C}^{\mathsf{cf}}(\mathcal{U})$ denote the set of crossing-free combinations of $\mathcal{U}$. A combination $C \in \mathfrak{C}^{\mathsf{cf}}(\mathcal{U})$ is called a *partition* of P if the sets $\mathrm{pts}(u)$ of all $u \in C$ are pairwise disjoint and if their union is P. Let $\mathfrak{C}^{\mathsf{pt}}(\mathcal{U})$ denote the set of all such partitions of P. Assuming $\mathcal{U} \subseteq \mathcal{CF}_P$, a combination $C \in \mathfrak{C}^{\mathsf{cf}}(\mathcal{U})$ is called a *subdivision* of the convex hull of P if the shapes of all $u \in C$ are pairwise interior-disjoint and if their union is the convex hull of P. Let $\mathfrak{C}^{\mathsf{sd}}(\mathcal{U})$ denote the set of all such subdivisions of the convex hull of P. We refer to Figure 3.1 for examples for the special case $\mathcal{U} = \mathcal{T}_P$.

For the purpose of this chapter, we no longer consider the sets $\mathcal{G}(P)$, $\mathcal{PM}(P)$, $\mathcal{T}(P)$, and so on, as defined in Section 1.1. Instead, we talk about crossing-free combinations of specific sets of units. For example, since there is an obvious bijection between the sets $\mathfrak{C}^{\mathsf{cf}}(\mathcal{S}_P)$ and $\mathcal{G}(P)$, any counting or enumeration algorithm for one set can be adapted easily for the other. In a similar way, there are bijections for example between the sets $\mathfrak{C}^{\mathsf{pt}}(\mathcal{S}_P)$ and $\mathcal{PM}(P)$, as well as $\mathfrak{C}^{\mathsf{sd}}(\mathcal{T}_P)$ and $\mathcal{T}(P)$.

In the same spirit, we define the sets $\mathfrak{C}_P^{\mathsf{st}}, \mathfrak{C}_P^{\mathsf{sc}} \subseteq \mathfrak{C}^{\mathsf{cf}}(\mathcal{S}_P)$ of all crossing-free combinations of $\mathcal{S}_P$ whose segments form spanning trees and spanning cycles on P, respectively.

Definition 3.1. *Let $\mathcal{U} \subseteq \mathcal{G}_P^*$. A* combination graph (over $\mathcal{U}$) *is a directed and acyclic multigraph Γ with two distinguished vertices $\perp$ and $\top$, called the* source *and* sink *of Γ. All edges in Γ, except for those ending in $\top$, are labeled with an element of $\mathcal{U}$. Moreover, the sink $\top$ has no outgoing edges. The* size *of Γ is the number of vertices and edges in Γ.*

For any combination graph Γ and any set $\mathfrak{C}$ of combinations, we say that Γ *represents* $\mathfrak{C}$ if there is a bijection between the set of directed $\perp$-$\top$ paths in Γ and the set $\mathfrak{C}$ in the following sense. Taking any $\perp$-$\top$ path in Γ and building the set of labels on that path yields the corresponding combination in $\mathfrak{C}$.

The following are comparatively simple applications of a theoretical framework developed in Section 3.2. The corresponding proofs can be found in Section 3.3. Many more, in some cases obvious, applications are possible.

Theorem 3.2 (All geometric graphs)**.** *There exists a combination graph over $\mathcal{S}_P$ of size $O(c^n n^3)$ with $c < 2.83929$ that represents $\mathfrak{C}^{\mathsf{cf}}(\mathcal{S}_P)$.*

Theorem 3.3 (Convex partitions)**.** *There exists a combination graph over $\mathcal{CP}_P$ of size $O(2^n n^3)$ that represents $\mathfrak{C}^{\mathsf{pt}}(\mathcal{CP}_P)$.*

Theorem 3.4 (Perfect matchings)**.** *There exists a combination graph over $\mathcal{S}_P$ of size $O(2^n n^3)$ that represents $\mathfrak{C}^{\mathsf{pt}}(\mathcal{S}_P)$.*

Theorem 3.5 (Convex subdivisions)**.** *There exists a combination graph over $\mathcal{CF}_P$ of size $O(2^n n^3)$ that represents $\mathfrak{C}^{\mathsf{sd}}(\mathcal{CF}_P)$.*

Theorem 3.6 (Triangulations; Theorem 3 in [11])**.** *There exists a combination graph over $\mathcal{T}_P$ of size $O(2^n n^3)$ that represents $\mathfrak{C}^{\mathsf{sd}}(\mathcal{T}_P)$.*

Within our framework we can explain similar results for spanning trees and spanning cycles. However, these two classes are substantially harder to deal with. Section 3.6 is devoted to the corresponding proofs.

Theorem 3.7 (Spanning trees)**.** *There exists a combination graph over $\mathcal{S}_P$ of size $O(c^n n^3)$ with $c < 7.04313$ that represents $\mathfrak{C}_P^{\mathsf{st}}$.*

Theorem 3.8 (Spanning cycles)**.** *There exists a combination graph over $\mathcal{S}_P$ of size $O(c^n n^3)$ with $c < 5.61804$ that represents $\mathfrak{C}_P^{\mathsf{sc}}$.*

To get a bound on the running time for computing an explicit representation of any one of the combination graphs Γ in the above theorems, it suffices to add another factor n to the bound on the size of Γ. See Section 3.4 for details.

Given a representation of Γ, the corresponding counting problem can be solved in time linear in the size of Γ by counting directed $\bot$-$\top$ paths using standard graph algorithms. After removing all dead ends in Γ, which is also possible in time linear in the size of Γ, enumeration of the corresponding set $\mathfrak{C}$ requires time at most linear in the length of the longest $\bot$-$\top$ path per enumerated object. We refer to [11] for an example.

Observe that the exponential bases in Theorems 3.2 to 3.6 are not larger than the exponential bases of the corresponding lower bounds given in the first row of Table 2.2 on page 22. As a corollary we therefore get efficient enumeration algorithms for the sets $\mathcal{G}(P)$, $\mathcal{CP}(P)$, $\mathcal{PM}(P)$, $\mathcal{CS}(P)$ and $\mathcal{T}(P)$ whose overall running times are bounded by the length of the output times a polynomial in n. For $\mathcal{CP}(P)$ and $\mathcal{PM}(P)$, a small adaptation, which is described in Section 3.5, results in enumeration algorithms with polynomial-time delay for every output.

Theorem 3.9. *The sets $\mathcal{CP}(P)$ and $\mathcal{PM}(P)$ can be enumerated such that the delay for any output is bounded by a polynomial in n.*

With the exception of $\mathcal{PM}(P)$, the lower bounds are even strictly larger, meaning that our algorithms compute the numbers $\mathrm{pg}(P)$, $\mathrm{cp}(P)$, $\mathrm{cs}(P)$ and $\mathrm{tr}(P)$ with exponential speed-up over any procedure that counts by enumerating the respective set. For spanning trees it might as well be that the constant c in Theorem 3.7 is smaller than 6.75, but we have been unable to prove it. For spanning cycles we cannot always hope for such an exponential speed-up because for a set P of n points in convex position we have $\mathrm{sc}(P) = 1$.

3.2 Theoretical Framework

Let P be a set of n points in general position. In particular, assume that no two points share the same x-coordinate, which means the points can be ordered as $p_1, \ldots, p_n$ from left to right in a unique way. If a point p_i is to the left of another point p_j, that is, if $i \leq j$, then we write $p_i \preceq p_j$. Recall that $\mathrm{pts}(u) \subseteq P$ is the set of vertex points in any $u \in \mathcal{G}_P^*$. We define $\mathrm{lft}(u) \coloneqq \min_{\preceq}(\mathrm{pts}(u))$ and $\mathrm{rgt}(u) \coloneqq \max_{\preceq}(\mathrm{pts}(u))$, the *left-most* and *right-most point* of u, respectively. For any $u_1, u_2 \in \mathcal{G}_P^*$, if $\mathrm{rgt}(u_1) \preceq \mathrm{lft}(u_2)$ holds then we say that u_1 is *to the left* of u_2 and we also write $u_1 \preceq u_2$.

For each $u \in \mathcal{G}_P^*$ we define $\mathrm{low}(u) \subseteq P$ and $\mathrm{upp}(u) \subseteq P$, the *lower* and *upper shadow* of u, respectively. The set $\mathrm{low}(u)$ contains all points in P from which a vertical ray shooting upwards intersects the relative interior of some segment of u. The set $\mathrm{upp}(u)$ is defined in an analogous way. Whenever we have either $\mathrm{pts}(u_1) \cap \mathrm{low}(u_2) \neq \emptyset$ or $\mathrm{upp}(u_1) \cap \mathrm{pts}(u_2) \neq \emptyset$ for any u_1, u_2, then we say that u_2 *depends on* u_1 and we write $u_1 \sqsubset u_2$. The following lemma aims at making this cryptic definition more intuitive.

Here, and only here, by a *point on* u we mean either a point in $\mathrm{pts}(u)$ or a point in the relative interior of some edge of u.

Lemma 3.10. *Let $u_1, u_2 \in \mathcal{G}_P^*$ be arbitrary. Then, u_2 depends on u_1 if and only if there exists a point on u_2 directly (that is, same x-coordinate) and strictly above a point on u_1. In particular, if u_1 and u_2 are crossing, then they are mutually dependent; that is, we have $u_1 \sqsubset u_2$ and $u_2 \sqsubset u_1$.*

Proof. The "only if" is immediate by definition of $u_1 \sqsubset u_2$. For the "if", let us fix two points on u_1 and u_2, respectively, the one on u_2 directly and strictly above the one on u_1. If either of those points is contained in $\text{pts}(u_1)$ or $\text{pts}(u_2)$, respectively, the conclusion $u_1 \sqsubset u_2$ is again immediate. Otherwise, let e_1 and e_2 be the edges of u_1 and u_2 that contain the two respective fixed points in their relative interiors. Without loss of generality, we assume that e_1 and e_2 diverge and thus do not intersect towards the left, as illustrated on the right hand side. In case 1, the left endpoint of e_1 is below e_2, which means $\text{pts}(u_1) \cap \text{low}(u_2) \neq \emptyset$ and hence $u_1 \sqsubset u_2$. In case 2, the left endpoint of e_2 is above e_1, which means $\text{upp}(u_1) \cap \text{pts}(u_2) \neq \emptyset$ and hence again $u_1 \sqsubset u_2$. □

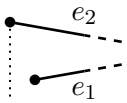

case 1

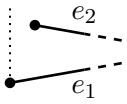

case 2

To ease notation throughout, we write $\text{pts}(C)$ and $\text{low}(C)$ in order to denote the sets $\bigcup_{u \in C} \text{pts}(u)$ and $\bigcup_{u \in C} \text{low}(u)$, respectively.

Besides giving an intuition for the dependence relation, Lemma 3.10 turns out to be absolutely crucial for everything that follows. It suggests a safe and practical way of adding a new segment $u \in \mathcal{S}_P$, say, to a crossing-free combination C of $\mathcal{S}_P$. Safe means that we do not create crossings; that is, $C \cup \{u\}$ is also crossing-free. Practical means that we may, to a great extent, remain ignorant of the exact composition of C. Indeed, as long as we know the sets $\text{pts}(C)$ and $\text{low}(C)$, and provided that we choose u such that $\text{pts}(u) \cap \text{low}(C) = \emptyset$ and $\text{upp}(u) \cap \text{pts}(C) = \emptyset$, then no element of C can possibly depend on u and hence, by Lemma 3.10, $C \cup \{u\}$ is crossing-free.

By extension, this suggests a way of constructing a combination C by adding all elements in a succession where earlier occurrences do not depend on later occurrences. An apparent disadvantage is that this will not work for every conceivable subset $\mathcal{U}$ of $\mathcal{G}_P^*$ and every crossing-free combination C of $\mathcal{U}$. Most importantly, for it to work, there must be no circular dependencies among elements of C. In the following we formalize this requirement.

Let $\mathcal{U} \subseteq \mathcal{G}_P^*$ and let $C \subseteq \mathcal{U}$ be arbitrary. An element u of C is *extreme (in C)* if $u \not\sqsubset u'$ holds for all other elements u' of C. If it exists, the *right-most extreme element* in C is the unique extreme element u in C which satisfies $u' \preceq u$ for all other extreme elements u' in C.

Definition 3.11. *Let $\mathcal{U} \subseteq \mathcal{G}_P^*$ and let $\mathfrak{C}$ be a set of combinations of $\mathcal{U}$. We call* $\mathfrak{C}$ serializable *if it is non-empty and if every non-empty $C \in \mathfrak{C}$ contains a right-most extreme element, which is denoted by* $\mathrm{rex}(C)$*; additionally, $C \setminus \{\mathrm{rex}(C)\}$ must itself be an element of $\mathfrak{C}$.*

Let $\mathfrak{C}$ be serializable, and further let $C, C' \in \mathfrak{C}$. We will often write $C \xrightarrow{u} C'$, which stands for $C = C' \setminus \{u\}$ and $u = \mathrm{rex}(C')$. In a sense, the notation suggests that C can be extended to C' by adding u. Observe that $\mathfrak{C}$ naturally induces a directed and acyclic graph (actually, a tree) with vertex set $\mathfrak{C}$ and edges with labels from the set $\mathcal{U}$; indeed, whenever $C \xrightarrow{u} C'$ holds we simply add an edge from vertex C to vertex C' with label u. A combination graph over $\mathcal{U}$ that represents an arbitrary subset of $\mathfrak{C}$ is obtained by defining $\bot := \emptyset$ and by adding appropriate unlabeled edges which end in an additional vertex $\top$. However, the resulting combination graph is too large as its size is $\Theta(|\mathfrak{C}|)$. In the following we show how to compress it without losing too many of its nice properties.

Definition 3.12. *Let $\mathfrak{C}$ be serializable. An equivalence relation $\sim$ over $\mathfrak{C}$ is called* coherent *if $C_1 \sim C_2$ implies the following; if $C_1 \xrightarrow{u} C_1'$ holds then also $C_2 \xrightarrow{u} C_2'$ for some $C_2' \sim C_1'$.*

Intuitively, to make our combination graph smaller we would like to merge two vertices C_1 and C_2. This makes sense only if the subtrees rooted at C_1 and C_2 are identical when looking at edge labels. As will be proved later, if $C_1 \sim C_2$ holds, coherency of $\sim$ enforces precisely what we want.

In the remainder of this chapter we will always deal with a serializable set $\mathfrak{C}$ of combinations of some $\mathcal{U} \subseteq \mathcal{G}_P^*$, and an equivalence relation $\sim$ over $\mathfrak{C}$. For any $C \in \mathfrak{C}$ we then define the equivalence class $[C] \coloneqq \{C' \in \mathfrak{C} \colon C' \sim C\}$, where the relation $\sim$ will be obvious from the context. We also write $(\mathfrak{C}/\!\sim) \coloneqq \{[C] \colon C \in \mathfrak{C}\}$ to denote the set of all equivalence classes.

Definition 3.13. *A* combination problem *is a tuple* $(\mathcal{U}, \mathfrak{C}, \sim, \mathfrak{T})$ *where* $\mathcal{U} \subseteq \mathcal{G}_P^*$, $\mathfrak{C}$ *is a serializable set of combinations of* $\mathcal{U}$, $\sim$ *is a coherent equivalence relation on* $\mathfrak{C}$, *and* $\mathfrak{T}$ *is a subset of* $(\mathfrak{C}/\!\sim)$.

As will be described below, the set $\mathfrak{T}$ allows us to specify the subset of $\mathfrak{C}$ we are actually interested in.

Every combination problem $(\mathcal{U}, \mathfrak{C}, \sim, \mathfrak{T})$ induces a corresponding combination graph $\Gamma = \Gamma(\mathcal{U}, \mathfrak{C}, \sim, \mathfrak{T})$ over $\mathcal{U}$ as follows. The vertices of Γ are all equivalence classes in $(\mathfrak{C}/\!\sim)$ plus one extra vertex denoted by $\top$. The vertex $[\emptyset]$ is also referred to by $\bot$. Existence of $\bot$ follows from $\emptyset \in \mathfrak{C}$, an easy consequence of serializability of $\mathfrak{C}$. Whenever $C \xrightarrow{u} C'$ holds, then we add an edge from vertex $[C]$ to vertex $[C']$ with label u. We do not, however, add the same labeled edge more than once. Lastly, for every vertex $[C]$ in $\mathfrak{T}$ we add an unlabeled edge which starts in $[C]$ and ends in $\top$. Observe that Γ does not contain any directed cycles because given any such cycle, it would be possible to construct an infinite sequence $C \xrightarrow{u} C', C' \xrightarrow{u'} C'', \ldots$, which cannot exist.

Recall that the notation $C \xrightarrow{u} C'$ stands for $C = C' \setminus \{u\}$ and $u = \operatorname{rex}(C')$. Additionally, we write $[C] \xrightarrow{u} [C']$ if there exists an edge in Γ from vertex $[C]$ to vertex $[C']$ with label u. The following

observations are straight-forward consequences of coherency of $\sim$ and of the way Γ is constructed.

Observation 3.14. *The combination graph $\Gamma = \Gamma(\mathcal{U}, \mathfrak{C}, \sim, \mathfrak{T})$, defined as above, has the following properties.*

- *Completeness; if $C \xrightarrow{u} C'$, then $[C] \xrightarrow{u} [C']$.*
- *Soundness; if $[C] \xrightarrow{u} [C']$, then $C \xrightarrow{u} C''$ for some $C'' \sim C'$.*
- *Determinism; if $[C] \xrightarrow{u} [C']$ and $[C] \xrightarrow{u} [C'']$, then $[C'] = [C'']$.*

By induction it can now be shown that for every vertex $[C]$ there is a natural bijection from $[C]$ to the set of directed $\bot$-$[C]$ paths in Γ, which then gives us the following lemma.

Lemma 3.15. *Let $(\mathcal{U}, \mathfrak{C}, \sim, \mathfrak{T})$ be a combination problem and let Γ be the corresponding combination graph. Then, Γ represents $\bigcup \mathfrak{T}$ and the size of Γ is at most $O(|(\mathfrak{C}/\sim)| \cdot |\mathcal{U}|)$.*

Proof. The upper bound on the size of Γ holds because it has exactly $|(\mathfrak{C}/\sim)| + 1$ vertices and, since it is deterministic as in Observation 3.14 and has no duplicate labeled edges, each vertex has at most $|\mathcal{U}| + 1$ outgoing edges. It only remains to show that Γ represents $\bigcup \mathfrak{T}$.

For each directed path R in Γ let C_R denote the set of all labels on R; that is, C_R is the combination of $\mathcal{U}$ corresponding to the path R. Moreover, for any $C \in \mathfrak{C}$, the *canonical order* of C is the unique sequence over all elements in C which is obtained by successively removing right-most extreme elements from C and then putting the removed elements in reverse order.

For every vertex $[C]$ in Γ we now claim the following. Firstly, there exists a directed $\bot$-$[C]$ path R in Γ with $C_R = C$, irrespective of the choice of the representative C. Secondly, for every directed $\bot$-$[C]$ path R we have that $C_R \in [C]$. Thirdly, the labels on any directed $\bot$-$[C]$ path R with $C_R = C$ appear in canonical order of C. The

proof of these claims is by induction over an arbitrary topological ordering of the vertices in Γ. After that, the lemma follows by combining the claims with the fact that Γ is deterministic.

For the first part of the claim, if $C = \emptyset$ holds, then clearly $[C] = \bot$ and the $\bot$-$\bot$ path without edges works. Otherwise, if $C \neq \emptyset$, then we know that $C' \xrightarrow{u} C$ for some C' and u. By completeness, there is an edge $[C'] \xrightarrow{u} [C]$ in Γ and a $\bot$-$[C]$ path R with $C_R = C$ can be constructed from the $\bot$-$[C']$ path R' with $C_{R'} = C'$ which exists by induction.

For the second part of the claim, let R be a directed $\bot$-$[C]$ path in Γ. If R is of length zero then $[C] = \bot$ and $C_R = \emptyset \in [C]$. Otherwise, let R' be the $\bot$-$[C']$ path that is obtained by removing the last edge $[C'] \xrightarrow{u} [C]$ from R. By induction, and without loss of generality, $C_{R'} = C'$. By soundness, we have $C' \xrightarrow{u} C''$ for some $C'' \sim C$ and hence also $C_R = C'' \in [C]$.

For the third part of the claim, observe that in the previous paragraph, the last label on the path R with $C_R = C''$ is the right-most extreme element in C''. Hence, this also follows by induction. □

3.3 Three Simple Applications

We present three generic kinds of combination problems. They directly correspond to the three types of crossing-free combinations depicted earlier in Figure 3.1.

3.3.1 All Crossing-free Combinations

The aim of this subsection is to give a proof of Theorem 3.2. Still, some of the following insights are fairly general and can be used in many different settings.

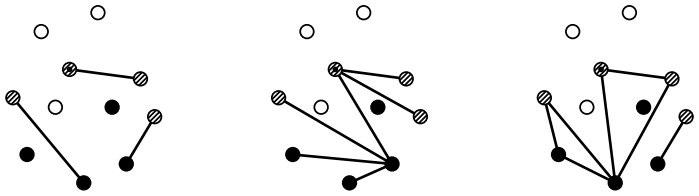

Figure 3.2: Three equivalent elements of $\mathfrak{C}^{\mathsf{cf}}(\mathcal{S}_P)$.

Let us fix a set of units $\mathcal{U} \subseteq \mathcal{G}_P^*$, and let us assume that the set $\mathfrak{C}^{\mathsf{cf}}(\mathcal{U})$ is serializable. Then, as follows, a combination C in $\mathfrak{C}^{\mathsf{cf}}(\mathcal{U})$ can be described by a coloring of the set P with three colors ○, ⊘, ● and a special marking, for example ⊘, on one of the points. A point $p \in P$ is given the color ● if $p \in \mathrm{low}(C)$, it is given the color ⊘ if $p \in \mathrm{pts}(C) \setminus \mathrm{low}(C)$, and it is given the color ○ otherwise. The special marking is put on the left-most point of $\mathrm{rex}(C)$.

Figure 3.2 shows, for the special case $\mathcal{U} = \mathcal{S}_P$, that different combinations can have identical such descriptions. Whenever that is the case, we consider two combinations equivalent. More formally, we put $C \sim C'$ if and only if the following conditions hold.

- $\mathrm{low}(C) = \mathrm{low}(C')$
- $\mathrm{pts}(C) \setminus \mathrm{low}(C) = \mathrm{pts}(C') \setminus \mathrm{low}(C')$
- $\mathrm{lft}(\mathrm{rex}(C)) = \mathrm{lft}(\mathrm{rex}(C'))$

Our goal is to prove that $\sim$ is coherent, as in Definition 3.12. However, this endeavor is doomed to fail because for contrived choices of $\mathcal{U}$ we can have $C \xrightarrow{u} C'$ and, at the same time, $C \sim C'$. In the language of combination graphs this means that we would have to introduce loops, leading to a potentially infinite number of source-sink paths. To avoid this problem, we require for any $C, C' \in \mathfrak{C}^{\mathsf{cf}}(\mathcal{U})$ and any $u \in \mathcal{U}$ that $C \xrightarrow{u} C'$ implies $C \not\sim C'$. If this additional requirement is met, then we say that $\mathfrak{C}^{\mathsf{cf}}(\mathcal{U})$ is *progressive*.

Lemma 3.16. *Let $\mathcal{U} \subseteq \mathcal{G}_P^*$ with $\mathfrak{C}^{\mathsf{cf}}(\mathcal{U})$ both serializable and progressive. Then, the equivalence relation $\sim$ on $\mathfrak{C}^{\mathsf{cf}}(\mathcal{U})$, as defined above, is coherent.*

Proof. Let $C_1, C_2 \in \mathfrak{C}^{\mathsf{cf}}(\mathcal{U})$ be non-empty (otherwise, the proof is trivial) with $C_1 \sim C_2$ and assume that $C_1 \xrightarrow{u} C_1'$ holds for $C_1' \in \mathfrak{C}^{\mathsf{cf}}(\mathcal{U})$ and $u \in \mathcal{U}$. Consider $C_2' \coloneqq C_2 \cup \{u\}$. We show $C_2' \in \mathfrak{C}^{\mathsf{cf}}(\mathcal{U})$, $C_1' \sim C_2'$ and $C_2 \xrightarrow{u} C_2'$, which implies the lemma.

By assumption, $\mathrm{low}(C_1) = \mathrm{low}(C_2)$ and $\mathrm{pts}(C_1) \setminus \mathrm{low}(C_1) = \mathrm{pts}(C_2) \setminus \mathrm{low}(C_2)$. From this and from the fact that u is extreme in C_1', we first derive that u is also extreme in C_2'. Assume the opposite; that is, either $\mathrm{pts}(u) \cap \mathrm{low}(C_2) \neq \emptyset$ or $\mathrm{upp}(u) \cap \mathrm{pts}(C_2) \neq \emptyset$ holds. In the first case, we get $\mathrm{pts}(u) \cap \mathrm{low}(C_1) = \mathrm{pts}(u) \cap \mathrm{low}(C_2) \neq \emptyset$, contradicting that u is extreme in C_1'. In the second case, we get at least one of $\mathrm{upp}(u) \cap \mathrm{pts}(C_1) \supseteq \mathrm{upp}(u) \cap (\mathrm{pts}(C_1) \setminus \mathrm{low}(C_1)) = \mathrm{upp}(u) \cap (\mathrm{pts}(C_2) \setminus \mathrm{low}(C_2)) \neq \emptyset$ and $\mathrm{upp}(u) \cap \mathrm{low}(C_1) = \mathrm{upp}(u) \cap \mathrm{low}(C_2) \supseteq \mathrm{upp}(u) \cap (\mathrm{pts}(C_2) \cap \mathrm{low}(C_2)) \neq \emptyset$. Both possibilities again lead to u not being extreme in C_1'. We conclude that u is extreme in C_2'.

Since u is extreme in C_2', no other element of C_2' can possibly depend on u. By Lemma 3.10, since C_2 is crossing-free, we also have that C_2' is crossing-free. Hence, $C_2' \in \mathfrak{C}^{\mathsf{cf}}(\mathcal{U})$.

Next, by definition of C_2' it is easily seen that $\mathrm{low}(C_1') = \mathrm{low}(C_2')$ and $\mathrm{pts}(C_1') \setminus \mathrm{low}(C_1') = \mathrm{pts}(C_2') \setminus \mathrm{low}(C_2')$ both hold. To prove also $\mathrm{lft}(\mathrm{rex}(C_1')) = \mathrm{lft}(\mathrm{rex}(C_2'))$, and consequently $C_1' \sim C_2'$, it suffices to show $\mathrm{rex}(C_2') = u$. So, for $u' \coloneqq \mathrm{rex}(C_2')$ and assuming that $u' \neq u$, we get $u \preceq u'$ and thus also $\mathrm{rex}(C_2) = u'$. Invoking $C_1 \sim C_2$ yields $u \preceq \mathrm{rex}(C_1)$, which contradicts the assumption $u = \mathrm{rex}(C_1')$.

It remains to prove $C_2 \xrightarrow{u} C_2'$. Observe that $u = \mathrm{rex}(C_2')$ and $C_2 \cup \{u\} = C_2'$ are not sufficient. In addition, we need $C_2 = C_2' \setminus \{u\}$; that is, u must not be contained in C_2. However, assuming $u \in C_2$, we easily derive $C_1 \sim C_2 = C_2' \sim C_1'$, which, when combined with $C_1 \xrightarrow{u} C_1'$, contradicts the assumption that $\mathfrak{C}^{\mathsf{cf}}(\mathcal{U})$ is progressive. □

Let us define $\mathfrak{T} \coloneqq (\mathfrak{C}^{\mathsf{cf}}(\mathcal{U})/\!\sim)$. Using Lemma 3.16 we see that the tuple $(\mathcal{U}, \mathfrak{C}^{\mathsf{cf}}(\mathcal{U}), \sim, \mathfrak{T})$ is a combination problem as long as $\mathfrak{C}^{\mathsf{cf}}(\mathcal{U})$ is both serializable and progressive. For the corresponding combination graph, denoted by $\Gamma^{\mathsf{cf}}_{\mathcal{U}}$, we now obtain the following corollary of Lemma 3.15.

Corollary 3.17. *If $\mathcal{U} \subseteq \mathcal{G}^*_P$ is such that $\mathfrak{C}^{\mathsf{cf}}(\mathcal{U})$ is both serializable and progressive, then $\Gamma^{\mathsf{cf}}_{\mathcal{U}}$ represents $\mathfrak{C}^{\mathsf{cf}}(\mathcal{U})$ and the size of $\Gamma^{\mathsf{cf}}_{\mathcal{U}}$ is at most $O(|(\mathfrak{C}^{\mathsf{cf}}(\mathcal{U})/\!\sim)| \cdot |\mathcal{U}|)$.*

Theorem 3.2 follows by invoking Corollary 3.17 with $\mathcal{U} = \mathcal{S}_P$ and by making use of the next two lemmas. The first one essentially shows that $\mathfrak{C}^{\mathsf{cf}}(\mathcal{S}_P)$ is a well-behaved set. The second one gives us a better upper bound on the size of $\Gamma^{\mathsf{cf}}_{\mathcal{S}_P}$. Observe, however, that a bound of $O(3^n n^3)$ is immediate because we can encode equivalence classes by coloring the n points with three colors and by assigning a marking to one of the n points, and because of $|\mathcal{S}_P| = O(n^2)$.

Lemma 3.18. *For any point set P, $\mathfrak{C}^{\mathsf{cf}}(\mathcal{S}_P)$ is both serializable and progressive.*

Proof (serializable). Let $C \in \mathfrak{C}^{\mathsf{cf}}(\mathcal{S}_P)$ be non-empty but otherwise arbitrary. We prove serializability by exhibiting a right-most extreme element u in C. For this, consider the relative interiors of all segments in C. These segments without endpoints are convex and pairwise non-intersecting. For a set of convex and non-intersecting shapes in the plane it is well-known that at least one of them can be translated in the y-direction to infinity in a continuous motion, without intersecting any other shape in the process. [65] Any segment that has this property corresponds to an extreme element in C. The extreme elements in C now can be ordered from left to right according to their relative positions when projected orthogonally onto the x-axis. The segment u on the far right is a right-most extreme element in C. □

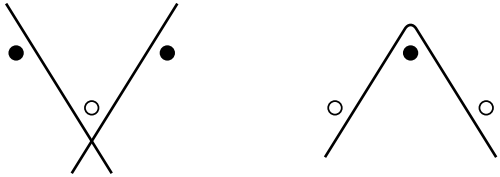

Figure 3.3: Three consecutive points can always be colored in a way that does not correspond to an element of $\mathfrak{C}^{\mathsf{cf}}(\mathcal{S}_P)$.

Proof (progressive). Towards a contradiction, assume $C' \xrightarrow{u} C$ and $C \sim C'$ for $C, C' \in \mathfrak{C}^{\mathsf{cf}}(\mathcal{S}_P)$ and $u \in \mathcal{S}_P$. Let $u' \coloneqq \mathrm{rex}(C')$. We have $\mathrm{lft}(u) = \mathrm{lft}(u')$ and we have to distinguish the two cases illustrated on the right hand side. In case 1, we have $\mathrm{rgt}(u) \in \mathrm{pts}(C) \setminus \mathrm{low}(C)$ but also $\mathrm{rgt}(u) \notin \mathrm{pts}(C') \setminus \mathrm{low}(C')$ as otherwise u' would not be extreme in C'. In case 2, we have $\mathrm{rgt}(u') \in \mathrm{low}(C)$ but also $\mathrm{rgt}(u') \notin \mathrm{low}(C')$ as otherwise u' would not be extreme in C'. Hence, in both cases we get a contradiction to the assumption $C \sim C'$. □

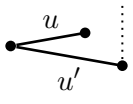

case 1

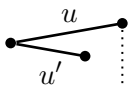

case 2

Lemma 3.19. *For any set P of n points, the relation $\sim$ partitions $\mathfrak{C}^{\mathsf{cf}}(\mathcal{S}_P)$ into at most $O(\alpha^n n)$ equivalence classes; that is, we have $|(\mathfrak{C}^{\mathsf{cf}}(\mathcal{S}_P)/\!\sim)| = O(\alpha^n n)$, where $\alpha \approx 2.83929$.*

The proof of Lemma 3.19 is a bit tedious. We only sketch the main idea here, and postpone a more careful analysis to Section 3.7.

Note that for any three consecutive points p_i, p_{i+1}, p_{i+2} in P, the point p_{i+1} is either below or above the straight line through p_i and p_{i+2}, as depicted in Figure 3.3. In both cases we can show that at least one of the $3^3 = 27$ different ways of assigning colors to p_i, p_{i+1}, p_{i+2} does not describe an actual element of $\mathfrak{C}^{\mathsf{cf}}(\mathcal{S}_P)$. A bound of $O(26^{n/3}n) = O(2.963^n n)$ on the size of $(\mathfrak{C}^{\mathsf{cf}}(\mathcal{S}_P)/\!\sim)$ then follows after partitioning P into $n/3$ consecutive triples.

In the first case, if we assign colors ●, ○, ●, there must be two segments which pass over the points p_i and p_{i+2}, respectively, and which pass under p_{i+1}. Clearly, any two such segments are crossing. In the second case, if we assign colors ○, ●, ○, there must be a segment that passes over p_{i+1} and under p_i and p_{i+2}. Clearly, this is impossible for a straight-line segment.

Note also that if $\Gamma^{\mathsf{cf}}_{\mathcal{S}_P}$ is constructed bottom-up, as will be explained in more detail in Section 3.4, then all these impossible colorings are avoided automatically.

3.3.2 Crossing-free Partitions

Let us again fix a set of units $\mathcal{U} \subseteq \mathcal{G}^*_P$. We define the set $\mathfrak{C}^{\check{\mathsf{pt}}}(\mathcal{U})$ of all crossing-free combinations C of $\mathcal{U}$ for which the sets $\mathrm{pts}(u)$ of all $u \in C$ are pairwise disjoint and for which $\mathrm{low}(C) \subseteq \mathrm{pts}(C)$ holds. Figure 3.4 depicts three such combinations for the special case $\mathcal{U} = \mathcal{CP}_P$. Observe that $\mathfrak{C}^{\mathsf{pt}}(\mathcal{U})$ and $\mathfrak{C}^{\check{\mathsf{pt}}}(\mathcal{U})$ are different sets, and also observe that we have in fact $\mathfrak{C}^{\mathsf{pt}}(\mathcal{U}) \subseteq \mathfrak{C}^{\check{\mathsf{pt}}}(\mathcal{U})$.

Let us assume that $\mathfrak{C}^{\check{\mathsf{pt}}}(\mathcal{U})$ is serializable. Similar to the previous subsection, we use two colors ○, ⊘ and a special marking ⊘ on the points in P to describe an element C of $\mathfrak{C}^{\check{\mathsf{pt}}}(\mathcal{U})$. A point p receives the color ⊘ if $p \in \mathrm{pts}(C)$, and ○ otherwise. The marking is again put on the left-most point of $\mathrm{rex}(C)$. If two combinations have identical such descriptions, then we consider them equivalent. Formally, we put $C \sim C'$ if and only if the following conditions hold.

- $\mathrm{pts}(C) = \mathrm{pts}(C')$
- $\mathrm{lft}(\mathrm{rex}(C)) = \mathrm{lft}(\mathrm{rex}(C'))$

One peculiarity in Figure 3.4 is that some points have been given the color ⊘ even though there are no incident segments and the points are not in the interior of any convex part. The reason for this is

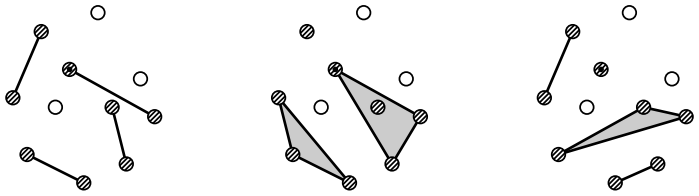

Figure 3.4: Three equivalent elements of $\mathfrak{C}^{\mathsf{p\check{t}}}(\mathcal{CP}_P)$.

that the set $\mathcal{CP}_P$ also contains all isolated points; that is, all $u \in \mathcal{G}_P^*$ with $|\operatorname{pts}(u)| = 1$.

Also observe that $C \xrightarrow{u} C'$ implies $C \not\sim C'$ because $\operatorname{pts}(C)$ is always a proper subset of $\operatorname{pts}(C')$. Consequently, an explicit notion of progressive, as in the previous subsection, is not needed here.

Lemma 3.20. *Let $\mathcal{U} \subseteq \mathcal{G}_P^*$ with $\mathfrak{C}^{\mathsf{p\check{t}}}(\mathcal{U})$ serializable. Then, the equivalence relation $\sim$ on $\mathfrak{C}^{\mathsf{p\check{t}}}(\mathcal{U})$, as defined above, is coherent.*

Proof. Let $C_1, C_2 \in \mathfrak{C}^{\mathsf{p\check{t}}}(\mathcal{U})$ be non-empty (otherwise, the proof is trivial) with $C_1 \sim C_2$ and assume that $C_1 \xrightarrow{u} C_1'$ holds for $C_1' \in \mathfrak{C}^{\mathsf{p\check{t}}}(\mathcal{U})$ and $u \in \mathcal{U}$. Consider $C_2' \coloneqq C_2 \cup \{u\}$. We show $C_2' \in \mathfrak{C}^{\mathsf{p\check{t}}}(\mathcal{U})$, $C_1' \sim C_2'$ and $C_2 \xrightarrow{u} C_2'$, which implies the lemma.

First, observe that since u is extreme in C_1', it is also extreme in C_2'; indeed, $\operatorname{pts}(u) \cap \operatorname{low}(C_2) \subseteq \operatorname{pts}(u) \cap \operatorname{pts}(C_2) = \operatorname{pts}(u) \cap \operatorname{pts}(C_1) = \emptyset$ and $\operatorname{upp}(u) \cap \operatorname{pts}(C_2) = \operatorname{upp}(u) \cap \operatorname{pts}(C_1) = \emptyset$ can be derived immediately. By Lemma 3.10, C_2' is crossing-free. Moreover, deriving $\operatorname{low}(C_2') = \operatorname{low}(C_2) \cup \operatorname{low}(u) \subseteq \operatorname{pts}(C_2) \cup \operatorname{low}(C_1') \subseteq \operatorname{pts}(C_2') \cup \operatorname{pts}(C_1') = \operatorname{pts}(C_2')$ proves that, indeed, $C_2' \in \mathfrak{C}^{\mathsf{p\check{t}}}(\mathcal{U})$. By making use of the marking in the same way as in the proof of Lemma 3.16 we get $\operatorname{rex}(C_2') = u$, and it follows that $C_1' \sim C_2'$ and $C_2 \xrightarrow{u} C_2'$. □

Let us define the set $\mathfrak{T} \subseteq (\mathfrak{C}^{\mathsf{p\check{t}}}(\mathcal{U})/\!\sim)$ which contains all equivalence classes $[C]$ for which $\operatorname{pts}(C) = P$ holds. Observe that then $\bigcup \mathfrak{T} = \mathfrak{C}^{\mathsf{pt}}(\mathcal{U})$. From Lemma 3.20 it follows that $(\mathcal{U}, \mathfrak{C}^{\mathsf{p\check{t}}}(\mathcal{U}), \sim, \mathfrak{T})$

is a combination problem provided that $\mathfrak{C}^{\check{\mathsf{pt}}}(\mathcal{U})$ is serializable. For the corresponding combination graph $\Gamma_{\mathcal{U}}^{\mathsf{pt}}$ we now get the following corollary of Lemma 3.15.

Corollary 3.21. *If $\mathcal{U} \subseteq \mathcal{G}_P^*$ is such that $\mathfrak{C}^{\check{\mathsf{pt}}}(\mathcal{U})$ is serializable, then $\Gamma_{\mathcal{U}}^{\mathsf{pt}}$ represents $\mathfrak{C}^{\mathsf{pt}}(\mathcal{U})$ and the size of $\Gamma_{\mathcal{U}}^{\mathsf{pt}}$ is $O(|(\mathfrak{C}^{\check{\mathsf{pt}}}(\mathcal{U})/\!\sim)| \cdot |\mathcal{U}|)$.*

Theorems 3.3 and 3.4 now follow from Corollary 3.21 and the following two lemmas.

Lemma 3.22. *For any point set P and any subset $\mathcal{U}$ of $\mathcal{CP}_P$, it holds that $\mathfrak{C}^{\check{\mathsf{pt}}}(\mathcal{U})$ is serializable.*

Proof. The proof for the existence of right-most extreme elements is analogous to the first part of the proof of Lemma 3.18. However, proving that $C' := C \setminus \{u\}$, where $u = \mathrm{rex}(C)$, is an element of the set $\mathfrak{C}^{\check{\mathsf{pt}}}(\mathcal{U})$ is not completely trivial since we have to verify that $\mathrm{low}(C') \subseteq \mathrm{pts}(C')$ holds.

For the sake of contradiction, let us assume that there exists a point $p \in \mathrm{low}(C') \setminus \mathrm{pts}(C')$. From $C' \subseteq C$ we get $\mathrm{low}(C') \subseteq \mathrm{low}(C)$ and hence also $p \in \mathrm{low}(C)$. We now make use of $\mathrm{low}(C) \subseteq \mathrm{pts}(C)$, which holds by definition of $\mathfrak{C}^{\check{\mathsf{pt}}}(\mathcal{U})$, to obtain $p \in \mathrm{pts}(C)$. By combining this with $p \notin \mathrm{pts}(C')$ we obtain $p \in \mathrm{pts}(u)$ because $\mathrm{pts}(C) \setminus \mathrm{pts}(C') = \mathrm{pts}(u)$. It follows that the set $\mathrm{low}(C') \cap \mathrm{pts}(u)$ is non-empty since it contains at least the point p. This, however, contradicts the fact that u is extreme in C. □

Note that in the case of convex partitions, the general bound on the size of the resulting combination graph from Corollary 3.21 is insufficient to prove Theorem 3.3 because $\mathcal{U} = \mathcal{CP}_P$ alone can be of size $\Omega(2^n)$. The following lemma is therefore really needed.

Lemma 3.23. *For any point set P of size n and any subset $\mathcal{U}$ of $\mathcal{CP}_P$, the size of $\Gamma_{\mathcal{U}}^{\mathsf{pt}}$ is at most $O(2^n n^3)$.*

Proof. We prove that the number of labeled edges in $\Gamma_{\mathcal{U}}^{\mathsf{pt}}$ can be bounded by $O(2^n n^3)$ from above, which then implies the lemma.

Fix $p_l, p_r \in P$ with $p_l \preceq p_r$, and let $P_l^r \coloneqq \{p_l, p_{l+1}, \ldots, p_{r-1}, p_r\} \subseteq P$ be the set of points between p_l and p_r. Observe that there are at most 2^{r-l+1} convex parts $u \in \mathcal{CP}_P$ for which $p_l = \mathrm{lft}(u)$ and $p_r = \mathrm{rgt}(u)$ holds. Let us also fix such a convex part u. Next, we will give a bound on the number of edges in $\Gamma_{\mathcal{U}}^{\mathsf{pt}}$ with label u. This bound will only depend on the indices l and r.

Suppose that $[C] \xrightarrow{u} [C']$ is an edge in $\Gamma_{\mathcal{U}}^{\mathsf{pt}}$ and assume further that $C \xrightarrow{u} C'$. Then, we easily see that $\overline{\mathrm{low}}(u) = \mathrm{pts}(C) \cap P_l^r$, where $\overline{\mathrm{low}}(u) \coloneqq \mathrm{low}(u) \setminus \mathrm{pts}(u)$. This means that for each point $p \in P_l^r$ it is determined by u whether $p \in \mathrm{pts}(C)$ holds or not. For a point $p \in P \setminus P_l^r$ there are at most two choices, either $p \in \mathrm{pts}(C)$ or $p \notin \mathrm{pts}(C)$. It follows that there are at most $2^{n-(r-l+1)}n$ many vertices $[C]$ with an outgoing edge labeled by u. As usual, the additional factor n comes from the special marking.

The total number of labeled edges in $\Gamma_{\mathcal{U}}^{\mathsf{pt}}$ can therefore be bounded by the following sum.

$$\sum_{l=1}^{n}\sum_{r=l}^{n} 2^{r-l+1} \cdot 2^{n-(r-l+1)}n = \sum_{l=1}^{n}\sum_{r=l}^{n} 2^n n = O(2^n n^3) \qquad \square$$

3.3.3 Subdivisions

Let $\mathcal{U} \subseteq \mathcal{CF}_P$, which means in particular that the *shape* of each unit u is defined. We define the set $\mathfrak{C}^{\mathsf{sd}}(\mathcal{U})$ which contains all combinations C of $\mathcal{U}$ for which the following holds. There exists an x-monotone polygonal chain, denoted by $\mathrm{chn}(C)$, which starts in p_1, ends in p_n, has only points from P as vertices, and satisfies the following with regard to C. The shapes of all u in C form a subdivision of the region between $\mathrm{chn}(C)$ and the lower convex hull of P,

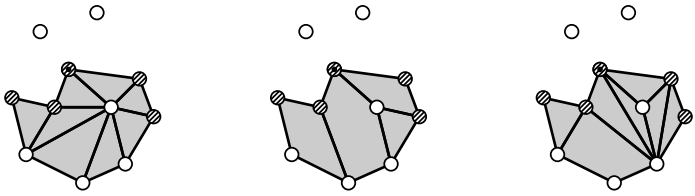

Figure 3.5: Three equivalent elements of $\mathfrak{C}^{\check{\mathrm{sd}}}(\mathcal{CF}_P)$.

by which we mean that the shapes are pairwise interior-disjoint and each point of the plane in the interior of that region is contained in the shape of at least one element u of C.

As depicted in Figure 3.5, we describe such a combination C by giving the vertex points of $\mathrm{chn}(C)$ the color ⊘, by giving all other points the color ○, and by adding the usual marking. Guided by this description, we put $C \sim C'$ if and only if the following holds.

- $\mathrm{chn}(C) = \mathrm{chn}(C')$
- $\mathrm{lft}(\mathrm{rex}(C)) = \mathrm{lft}(\mathrm{rex}(C'))$

Lemma 3.24. *Let $\mathcal{U} \subseteq \mathcal{CF}_P$ with $\mathfrak{C}^{\check{\mathrm{sd}}}(\mathcal{U})$ serializable. Then, the equivalence relation $\sim$ on $\mathfrak{C}^{\check{\mathrm{sd}}}(\mathcal{U})$, as defined above, is coherent.*

Proof. Let $C_1, C_2 \in \mathfrak{C}^{\check{\mathrm{sd}}}(\mathcal{U})$ be non-empty (otherwise, the proof is trivial) with $C_1 \sim C_2$ and assume that $C_1 \xrightarrow{u} C_1'$ holds for $C_1' \in \mathfrak{C}^{\check{\mathrm{sd}}}(\mathcal{U})$ and $u \in \mathcal{U}$. Consider $C_2' \coloneqq C_2 \cup \{u\}$. We show $C_2' \in \mathfrak{C}^{\check{\mathrm{sd}}}(\mathcal{U})$, $C_1' \sim C_2'$ and $C_2 \xrightarrow{u} C_2'$, which implies the lemma.

From the definition of $\mathfrak{C}^{\check{\mathrm{sd}}}(\mathcal{U})$, it is immediate that also $C_2' \in \mathfrak{C}^{\check{\mathrm{sd}}}(\mathcal{U})$ and $\mathrm{chn}(C_2') = \mathrm{chn}(C_1')$. Since u is extreme in C_1', it is also extreme in C_2'. Using the usual argument involving the marking we see that $\mathrm{rex}(C_2') = u$, it follows that $C_1' \sim C_2'$ and $C_2 \xrightarrow{u} C_2'$. □

Let $\mathfrak{T} \subseteq (\mathfrak{C}^{\check{\mathrm{sd}}}(\mathcal{U})/\!\sim)$ be the set that contains $[C]$ if and only if $\mathrm{chn}(C)$ is equal to the upper convex hull of P. Observe that $\bigcup \mathfrak{T} =$

$\mathfrak{C}^{\mathsf{sd}}(\mathcal{U})$. If $\mathcal{U}$ is such that $\mathfrak{C}^{\check{\mathsf{sd}}}(\mathcal{U})$ is serializable, then $(\mathcal{U}, \mathfrak{C}^{\check{\mathsf{sd}}}(\mathcal{U}), \sim, \mathfrak{T})$ is a combination problem and we denote by $\Gamma^{\mathsf{sd}}_{\mathcal{U}}$ the corresponding combination graph.

Corollary 3.25. *If $\mathcal{U} \subseteq \mathcal{CF}_P$ is such that $\mathfrak{C}^{\check{\mathsf{sd}}}(\mathcal{U})$ is serializable, then $\Gamma^{\mathsf{sd}}_{\mathcal{U}}$ represents $\mathfrak{C}^{\mathsf{sd}}(\mathcal{U})$ and the size of $\Gamma^{\mathsf{sd}}_{\mathcal{U}}$ is bounded from above by $O(|(\mathfrak{C}^{\check{\mathsf{sd}}}(\mathcal{U})/\!\sim)| \cdot |\mathcal{U}|)$.*

Theorems 3.5 and 3.6 now follow from Corollary 3.25 and the following two lemmas.

Lemma 3.26. *For any point set P and any subset $\mathcal{U}$ of $\mathcal{CF}_P$, it holds that $\mathfrak{C}^{\check{\mathsf{sd}}}(\mathcal{U})$ is serializable.*

Proof. The proof for the existence of right-most extreme elements is again analogous to Lemma 3.18. Also, it can be seen that $C' := C \setminus \{u\}$, where $u = \mathrm{rex}(C)$, is an element of $\mathfrak{C}^{\check{\mathsf{sd}}}(\mathcal{U})$. Simply observe that the upper convex hull of the shape of u must be contained in $\mathrm{chn}(C)$, which means that $\mathrm{chn}(C')$ is obtained from $\mathrm{chn}(C)$ by replacing the upper hull of u with its lower hull. □

Similar to the previous subsection, the next lemma is not implied by the general bound from Corollary 3.25. However, the proof is analogous to the proof of Lemma 3.23 and thus omitted.

Lemma 3.27. *For any point set P of size n and any subset $\mathcal{U}$ of $\mathcal{CF}_P$, the size of $\Gamma^{\mathsf{sd}}_{\mathcal{U}}$ is at most $O(2^n n^3)$.*

3.4 Representation of Combination Graphs

In the preceding sections, we have treated vertices of a combination graph Γ as equivalence classes over a set of combinations. Of course, this is a very inefficient way to represent them. However, in all cases we have seen how to describe these equivalence classes by an

assignment of a constant number of colors to the points in P and an index to the point with the special marking. It is thus easy to encode vertices of Γ with a linear number of bits for the coloring and a logarithmic number of bits for the index.

The construction of Γ is most easily done bottom-up. That is, we start with the source $\perp$, we enumerate all outgoing edges and add the corresponding new vertices to our representation of Γ. We continue this process, that is, pick a vertex and enumerate all outgoing edges, until we have done so for all vertices in Γ.

In all cases except for convex partitions and convex subdivisions, the enumeration of outgoing edges for a given vertex can be done in the most wasteful way while still staying within the required time bounds. For example, in the case of Theorem 3.2, for every vertex in $\Gamma^{\mathsf{cf}}_{\mathcal{S}_P}$ we can enumerate the whole set $\mathcal{S}_P$ and check for each segment whether it corresponds to an outgoing edge in linear time. In the case of Theorems 3.3 and 3.5 we have to be more careful since we do not have the time to enumerate the whole set $\mathcal{CP}_P$, say, for every vertex in $\Gamma^{\mathsf{pt}}_{\mathcal{CP}_P}$. A simple solution is to enumerate the set $\mathcal{CP}_P$ only once at the beginning and to find for each enumerated $u \in \mathcal{CP}_P$ all vertices in $\Gamma^{\mathsf{pt}}_{\mathcal{CP}_P}$ for which u corresponds to an outgoing edge. That is, instead of constructing $\Gamma^{\mathsf{pt}}_{\mathcal{CP}_P}$ bottom-up, we start with the set of all potential vertices and no edges, and then for every fixed u we add all edges of the form $[C] \xrightarrow{u} [C']$. Since the colors of all points in between $\mathrm{lft}(u)$ and $\mathrm{rgt}(u)$ are predetermined in C and C', the running time of this approach can be bounded by using the same arguments as in the proof of Lemma 3.23.

3.5 Polynomial-Time Delay Enumeration

In this section we sketch an additional trick—originally suggested to the author by Emo Welzl—which allows us to enumerate the

sets of crossing-free convex partitions and perfect matchings with polynomial-time delay. That is, we give algorithms which output the elements of $\mathcal{CP}(P)$ or $\mathcal{PM}(P)$ in some order and without repetitions, and such that the time we have to wait for any new output is not larger than a polynomial in n.

As already discussed in Section 3.1, from Theorems 3.3 and 3.4 we get enumeration algorithms for these two sets that run in time $O^*(\mathrm{cp}(P))$ and $O^*(\mathrm{pm}(P))$, respectively. However, while the time delay *between* any two outputs is bounded by a polynomial, the time delay *before* the first output is exponential. Precisely, there is a preprocessing phase that takes time $\Theta^*(2^n)$ during which we construct representations of the respective combination graphs while not producing any outputs. The trick is to hide this preprocessing phase by outputting $\Theta^*(2^n)$ objects obtained by other means.

Theorem 3.9 (restated)**.** *The sets $\mathcal{CP}(P)$ and $\mathcal{PM}(P)$ can be enumerated such that the delay for any output is bounded by a polynomial in n.*

Proof. We begin by defining a sufficiently large subset $\mathcal{EM}(P)$ of $\mathcal{PM}(P)$. Elements of this set are called *easy perfect matchings*, and they are constructed recursively. If P is the empty set, then $\mathcal{EM}(P) = \emptyset$. Otherwise, let p_1 be the left-most point and let p_i be any other point. Let P_i be the set of points that are to the left of the directed line through p_1 and p_i, and let P_i' be the set of points that are to the right of that line. The set $\mathcal{EM}(P)$ contains all perfect matchings that, for any choice of i, are composed of the edge p_1p_i and two easy perfect matchings on P_i and P_i', respectively.

Clearly, easy perfect matchings are crossing-free. Furthermore, note that efficient enumeration and recognition algorithms for the set $\mathcal{EM}(P)$ are easy to obtain from the definition. Lastly, the number of easy perfect matchings on even-sized point sets satisfies the Catalan recurrence, and thus $|\mathcal{EM}(P)| = C_{n/2} = \Theta(n^{-3/2}2^n)$. We refer to

[27] for more details, where these objects are used to prove a lower bound on the number of perfect matchings.

We now have everything that we need. In order to enumerate the set $\mathcal{PM}(P)$ with polynomial-time delay, we start the construction of $\Gamma^{\mathsf{pt}}_{\mathcal{S}_P}$. During this preprocessing phase, we output elements of $\mathcal{EM}(P)$ in appropriate time intervals. Once we have an explicit representation of $\Gamma^{\mathsf{pt}}_{\mathcal{S}_P}$, we continue the enumeration by outputting arbitrary elements of $\mathcal{PM}(P)$. Of course, whenever we have a new potential output, we have to check first whether it is an easy perfect matching, which means that it has been output before. If that is the case, then we simply discard it.

One final caveat now is that there might be a long period where we have to discard all potential outputs, which might again lead to a delay that is no longer polynomially bounded. However, this is easily fixed for example by only using up half of the set $\mathcal{EM}(P)$ during the preprocessing phase, and by using the other half as a substitute for every other discarded output during the second phase.

The enumeration of $\mathcal{CP}(P)$ with polynomial-time delay is done completely analogously. Since every crossing-free perfect matching is also a crossing-free convex partition, we can even reuse the set $\mathcal{EM}(P)$ for this purpose. □

3.6 Spanning Trees and Spanning Cycles

In this section we show that it is possible to construct non-trivial combination graphs for the sets of crossing-free spanning trees and spanning cycles.

3.6.1 Preliminaries

Spanning trees and spanning cycles are harder to deal with than anything that we have encountered before. The reason is that these graphs have properties which hold globally. For example, the construction of $\Gamma^{\mathsf{pt}}_{\mathcal{S}_P}$ in Section 3.3.2 can be adapted in such a way that source-sink paths correspond to 2-regular (instead of 1-regular) crossing-free geometric graphs. We simply have to keep track of the degree of each vertex (whether it is currently 0, 1 or 2, which means we need three instead of two colors) and in the end enforce that every vertex has degree 2. However, if we want that source-sink paths correspond only to crossing-free spanning cycles, then we also need to enforce that each such path corresponds to a connected geometric graph. Being connected is a property that holds globally, and there is no obvious and efficient way to deal with it. To get rid of this problem, at least for spanning trees and spanning cycles, we next state an auxiliary lemma. It allows us to translate connectivity into simpler features which can be enforced on a local level.

Let G be an abstract directed multigraph and let v be a vertex in G. G is *root-oriented towards* v if all vertices in G have exactly one outgoing edge, except for v, which has no outgoing edges. If G is root-oriented towards v, then v is called the *root* of G. Observe that being root-oriented implies that G has exactly $n-1$ edges, where n is the number of vertices in G. It does however not imply that G is connected or, in other words, a tree. The reason is that there might be a connected component with a directed cycle. Such components are always disconnected from the root.

A *plane drawing* of G is a drawing which maps all vertices of G to distinct points in the plane and which draws all edges as simple curves such that no two edges intersect except possibly in a common endpoint. Given two respective plane drawings of directed multigraphs G_1 and G_2, we say the drawings are *disjoint* if they do

not use any common points in the plane. Moreover, the drawings are *entangled* if for each cycle in either drawing, both its interior and exterior contain a point used by the other drawing. Finally, for fixed vertices v_1 in G_1 and v_2 in G_2 we say the two drawings are *tangent* in v_1 and v_2 if the points corresponding to v_1 and v_2 can be connected by an additional curve without intersecting any points already used in either drawing.

Lemma 3.28. *Let G_1 and G_2 be finite, directed multigraphs that are root-oriented towards v_1 and v_2, respectively. Then, there exist plane drawings of G_1 and G_2 that are disjoint, entangled and tangent in v_1 and v_2 if and only if both G_1 and G_2 are trees.*

Proof. If G_1 and G_2 are trees, then the desired drawings exist. To prove the other direction of the lemma, it suffices to show that both G_1 and G_2 do not contain any cycles.

Let us thus fix plane drawings of G_1 and G_2 with the desired properties and assume that G_1 contains a cycle C. Without loss of generality, the root v_2 of G_2 is contained in the exterior of C. Since the drawings of G_1 and G_2 are tangent in v_1 and v_2, also the root v_1 of G_1 is contained in the exterior of C. Now, from all cycles of either G_1 or G_2 that are contained in the interior of C, let us select a minimal cycle C'. Minimal means that C' does itself not contain any other cycles in its interior. Such a cycle exists since G_1 and G_2 are finite. We assume that C' again belongs to G_1, the other case being analogous. Since the drawings of G_1 and G_2 are entangled, we get a vertex of G_2 in the interior of C'. Starting from this vertex we now follow directed edges in G_2. Since the drawings of G_1 and G_2 are disjoint, we never leave the interior of C', which in particular means that we never reach v_2. However, since G_2 only has a finite number of vertices and all except for v_2 have an outgoing edge, we are bound to get into a cycle eventually. Clearly, this new cycle of G_2 is still contained in the interior of C', in contradiction to minimality. □

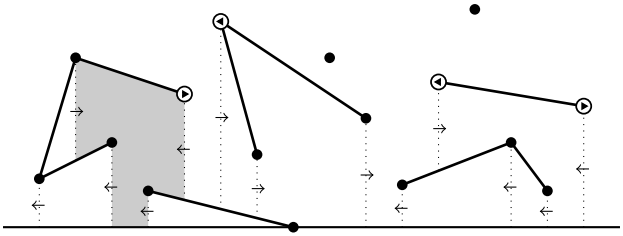

Figure 3.6: The horizontal line is the bottom. Dotted lines are borders. The shaded region is a face with out-degree 1. Points which expose a drain to the left are marked with ⊙. Points which expose a drain to the right are marked with ⊙.

We make two adaptations to the framework from Section 3.2. However, we note that all definitions and lemmas from that section extend naturally to the following setting.

The set $\mathcal{U}$ is no longer understood as a simple subset of $\mathcal{G}_P^*$. Firstly, we restrict units to be segments from the set $\mathcal{S}_P$. Secondly, a unit can have additional information attached to it. As an example, $\mathcal{U}$ could be defined as the set of directed segments. That is, each u in $\mathcal{U}$ would correspond to an element of $\mathcal{S}_P$, but it would also have a direction. In particular, this means that multiple elements of $\mathcal{U}$ can correspond to the same geometric graph. A combination C of $\mathcal{U}$ is still understood as a subset of $\mathcal{U}$. However, we do not allow the same geometric graph to appear twice in C. That is, in the above example, the elements of C are pairwise distinct as segments.

We conclude by giving some definitions and conventions that will be used in the following two subsections. We refer to Figure 3.6 for illustrations.

We assume there are unique points $\hat{p}, \check{p} \in P$ with largest and smallest y-coordinates, respectively. The horizontal line through $\check{p}$ is called the *bottom*.

For every crossing-free combination C of some set of units $\mathcal{U}$ we define a set of faces as follows. From the endpoints of each segment u in C we draw vertical rays (called *borders*) downwards until we hit either the bottom or the relative interior of another segment contained in C. Then, a *face* in C is a maximal connected region in the plane. There is one unbounded region above the bottom, which is called the *infinite face*. The unbounded region below the bottom is not a face and will be ignored. Furthermore, we say that two faces in C are *adjacent* if they share a (vertical) border.

Borders are always directed either left-to-right or right-to-left. In a combination C, the *out-degree* of a face is the number of borders directed away from that face. We further say that a point p *exposes a drain to the left* if the border below p is directed left-to-right and the region directly to the left of that border belongs to the infinite face. An analogous definition is given for *exposing a drain to the right*. If a point exposes a drain either to the left or to the right, we simply say that it *exposes a drain*.

3.6.2 Spanning Trees

We define a very special set $\mathcal{S}_P^{\mathsf{st}}$ of units. Each u in $\mathcal{S}_P^{\mathsf{st}}$ is a segment from the set $\mathcal{S}_P$ with a direction. Additionally, below either endpoint of u a border might be attached that is directed either left-to-right or right-to-left.

We also define the set $\mathfrak{C}_P^{\mathsf{st}}$, which contains all crossing-free combinations C of $\mathcal{S}_P^{\mathsf{st}}$ with the following additional properties. In what follows, the *out-degree* of a point $p \in P$ in C denotes the number of segments in C that have p as an endpoint and are directed away from p.

- The point $\hat{p}$ has out-degree 0 in C.
- Every point $p \in P$ has out-degree at most 1 in C.

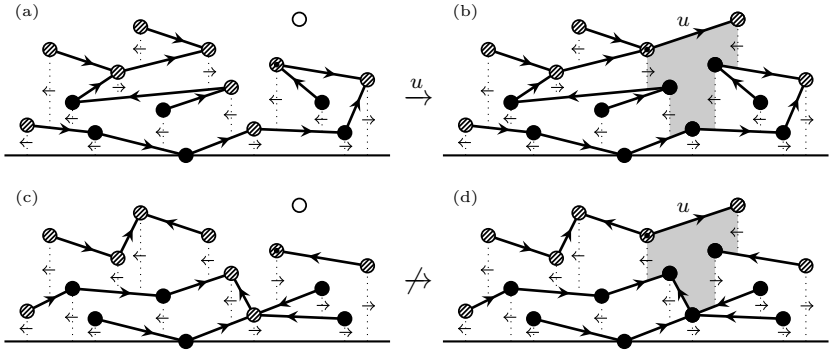

Figure 3.7: The elements of $\mathfrak{C}_P^{\text{st}}$ in (a) and (c) cannot be considered equivalent.

- Every point $p \in \text{low}(C)$ has out-degree 1 in C.
- Every finite face in C has out-degree 1.

Examples can be seen in Figure 3.7 (a), (b) and (c). The combination in (d) violates the last three properties.

Note that all of the above properties are maintained when removing the right-most extreme element from a combination from the set $\mathfrak{C}_P^{\text{st}}$. We thus get the following lemma.

Lemma 3.29. *For any point set P, $\mathfrak{C}_P^{\text{st}}$ is serializable.*

We reuse the three colors ○, ⊘, ● and the special marking from Section 3.3.1 with their original meaning to describe elements of $\mathfrak{C}_P^{\text{st}}$, as already depicted in Figure 3.7. However, that same figure illustrates that we cannot reuse the old equivalence relation as it is not coherent. There are the following three problems. Firstly, the out-degree of a point can become larger than 1. Secondly, a point with out-degree 0 can disappear in the lower shadow of a segment. Thirdly, a finite face with out-degree not equal to 1 can be created.

To make the equivalence relation coherent, it suffices to partition the points with color ⊘ into six smaller categories. That is, we have to replace the color ⊘ with 6 new colors, resulting in a total of 8 colors, and then consider two combinations equivalent if they agree in that new coloring and also in the special marking. We do not define the colors explicitly here, but only explain what information we have to keep track of.

For each point with color ⊘ we keep track of its out-degree, that is, whether it is currently 0 or 1. This allows us to avoid the first two problems mentioned earlier. Furthermore, for each point with color ⊘ we keep track of whether it exposes a drain and whether it is to the left or right. This allows us to avoid the third problem because whenever a new segment u is added to a combination C, a new finite face is created below u, and the out-degree of that face is determined by the number of exposed drains in the lower shadow and at the endpoints of u. Indeed, observe that borders corresponding to exposed drains in the lower shadow of u become out-borders of the new finite face. Also, an exposed drain at the left endpoint, say, of u becomes an out-border of the new face if and only if it is exposed to the right.

As usual, we define an equivalence relation $\sim$ over $\mathfrak{C}_P^{\mathsf{st}}$ based on the $2+2\cdot 3 = 8$ colors from the preceding discussion, and with the usual marking. The above intuition can be made precise and the following can be proved.

Lemma 3.30. *The equivalence relation $\sim$ on $\mathfrak{C}_P^{\mathsf{st}}$, as defined above, is coherent.*

We define the set $\mathfrak{T} \subseteq (\mathfrak{C}_P^{\mathsf{st}}/\!\sim)$ which contains $[C]$ if and only if every point (except for $\hat{p}$) has out-degree 1 in C and the infinite face has out-degree 0. Let Γ_P^{st} be the combination graph corresponding to the combination problem $(\mathcal{S}_P^{\mathsf{st}}, \mathfrak{C}_P^{\mathsf{st}}, \sim, \mathfrak{T})$. Theorem 3.7 with $c = 8$ now follows from Lemma 3.15 and from the following insight.

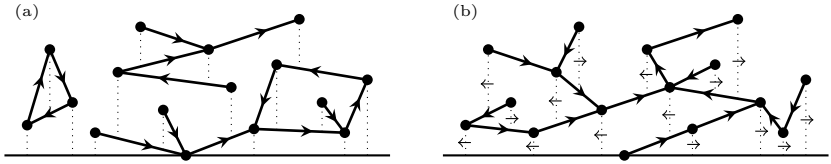

Figure 3.8: Illustrations for the proof of Lemma 3.31.

Lemma 3.31. *There is a natural bijection between the sets* $\bigcup \mathfrak{T}$ *and* $\mathcal{ST}(P)$ *in the following sense. For any combination* C *in* $\bigcup \mathfrak{T}$*, building the geometric graph on* P *with edges that correspond to the segments in* C *yields the corresponding crossing-free spanning tree in* $\mathcal{ST}(P)$*.*

Proof. Any combination C in $\bigcup \mathfrak{T}$ induces two directed multigraphs G_1 and G_2 with corresponding plane drawings, as follows.

G_1 is the graph with vertex set P and with edges that correspond to the directed segments in C. By definition of both $\mathfrak{C}_P^{\mathfrak{st}}$ and $\mathfrak{T}$, we at least know that G_1 is root-oriented towards $\hat{p}$, as exemplified in Figure 3.8 (a).

For the vertices of G_2 we choose one arbitrary point in the interior of each face in C. Two vertices in G_2 are connected if their corresponding faces in C are adjacent. The direction of that edge is chosen in accordance with the direction of the corresponding border in C. Again by definition of $\mathfrak{C}_P^{\mathfrak{st}}$ and $\mathfrak{T}$, G_2 is root-oriented towards the vertex corresponding to the infinite face in C, as exemplified in Figure 3.8 (b).

The drawings of G_1 and G_2 can be chosen such that they are disjoint, entangled, and tangent in $\hat{p}$ and the infinite face. The proof is concluded by applying Lemma 3.28 and by observing that any spanning tree on P can be root-oriented towards $\hat{p}$ in a unique way. □

One can prove that $c < 8$ by adapting the arguments from Section 3.3.1. With some more work, we get $c < 7.04313$, as will be shown in Section 3.7.

3.6.3 Spanning Cycles

We define a slightly different set of units $\mathcal{S}_P^{\mathsf{sc}}$. In the same way as in the previous subsection, below the endpoints of any segment u in $\mathcal{S}_P^{\mathsf{sc}}$ directed borders can be attached. Here, however, the segment u itself does not have a direction.

We also define the set $\mathfrak{C}_P^{\check{\mathsf{sc}}}$, which contains all crossing-free combinations C of $\mathcal{S}_P^{\mathsf{sc}}$ with the following additional properties. In what follows, the *degree* of a point $p \in P$ in C stands for the number of segments in C that have p as an endpoint. Also, if the size of C is n, the *last finite face* in C is defined as the face directly below the right-most extreme element of C. All other finite faces are called *normal*.

- If $|C| = n$, the last finite face in C has out-degree 0.
- Every point $p \in P$ has degree at most 2 in C.
- Every point $p \in \mathrm{low}(C)$ has degree 2 in C.
- Every normal finite face in C has out-degree 1.

Note again that the above properties are maintained when removing the right-most extreme element from a combination from the set $\mathfrak{C}_P^{\check{\mathsf{sc}}}$.

Lemma 3.32. *For any point set P, $\mathfrak{C}_P^{\check{\mathsf{sc}}}$ is serializable.*

We have to keep track of the degrees of all points. For one last time, we change the meaning of the colors ○, ⊘, ● and use them to identify points of degree 0, 1 and 2, respectively.

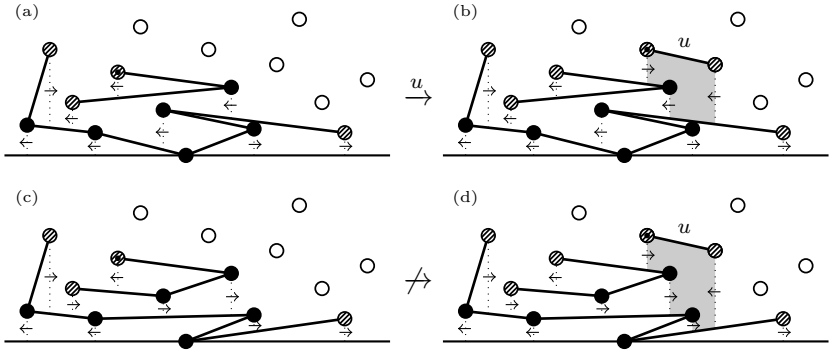

Figure 3.9: The elements of $\mathfrak{C}_P^{\text{sc}}$ in (a) and (c) cannot be considered equivalent.

Unsurprisingly, and similar to the previous subsection, an equivalence relation based only on these three colors and the usual marking is not coherent, see Figure 3.9. The only problem, however, is that finite faces with bad out-degrees can be created. A by now routine proof shows that these three colors are already sufficient to avoid crossings.

To avoid finite faces with bad out-degrees, we split ⊘ into 3 subcolors, and we split ● into 2 subcolors, for a total of 6 different colors which are then used to define an equivalence relation $\sim$ on $\mathfrak{C}_P^{\text{sc}}$. For each point with color ⊘ we keep track of whether it exposes a drain; if yes, we also keep track of whether it is to the left or right. Remember, this extra information is relevant if and only if the point in question is one of the endpoints of a new segment. For a point with color ● we only keep track of whether it exposes a drain or not. The reason why this is sufficient is that such a point has, by definition, degree 2 already and cannot be an endpoint of a new segment.

Lemma 3.33. *The equivalence relation $\sim$ on $\mathfrak{C}_P^{\text{sc}}$, as defined above, is coherent.*

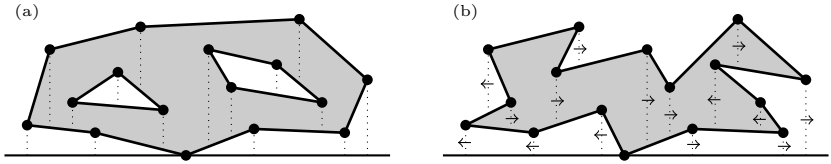

Figure 3.10: White faces are vertices in G_E. Shaded faces are vertices in G_O.

We define a set $\mathfrak{T} \subseteq (\mathfrak{C}_P^{\mathsf{sc}}/\!\sim)$ that contains $[C]$ if and only if each point has degree 2 in C and the infinite face has out-degree 0. Let Γ_P^{sc} be the combination graph corresponding to $(\mathcal{S}_P^{\mathsf{sc}}, \mathfrak{C}_P^{\mathsf{sc}}, \sim, \mathfrak{T})$. Theorem 3.8 with $c = 6$ follows from Lemma 3.15 and from the following insight. The better bound $c < 5.61804$ will be proved later in Section 3.7.

Lemma 3.34. *There is a natural bijection between the sets* $\bigcup \mathfrak{T}$ *and* $\mathcal{SC}(P)$ *in the following sense. For any combination* C *in* $\bigcup \mathfrak{T}$*, building the geometric graph on* P *with edges that correspond to the segments in* C *yields the corresponding spanning cycle in* $\mathcal{SC}(P)$*.*

Proof. For any combination C in $\bigcup \mathfrak{T}$ we know that each point is of degree 2, which means that C is a set of disjoint cycles, as exemplified in Figure 3.10 (a). Similar to the proof of Lemma 3.31, C induces two directed multigraphs G_E and G_O.

The vertex set of G_E is the set of faces in C which are contained in an even number of cycles. The vertex set of G_O is the set of faces in C which are contained in an odd number of cycles. In both G_E and G_O, two vertices are connected by an edge if the corresponding faces in C are adjacent. The direction of each edge reflects the direction of the corresponding border in C. By definition of $\mathfrak{C}_P^{\mathsf{sc}}$ and $\mathfrak{T}$, G_E and G_O are root-oriented towards the infinite face and the last finite face in C, respectively, as exemplified in Figure 3.10 (b).

Clearly, there exist plane drawings of G_E and G_O which are disjoint, entangled, and also tangent in the respective roots. Applying Lemma 3.28 hence concludes the proof. □

3.7 Bounds on Size of Combination Graphs

In this final section, we show how to prove the bounds on the constants c in Theorems 3.2, 3.7 and 3.8. Recall that vertices of combination graphs can be interpreted as colorings of P with a finite number of colors. The following proofs make use of the fact that certain patterns cannot occur in these colorings because of geometric constraints. Also, in the case of spanning trees and spanning cycles, we can improve the bounds further by identifying and discarding vertices from which the sink $\top$ can no longer be reached.

3.7.1 All Geometric Graphs

Recall the definition of the set $\mathfrak{C}^{\mathsf{cf}}(\mathcal{S}_P)$ and the corresponding equivalence relation $\sim$ from Section 3.3.1. We are left to prove the following lemma.

Lemma 3.19 (restated)**.** *For any set P of n points, the relation $\sim$ partitions $\mathfrak{C}^{\mathsf{cf}}(\mathcal{S}_P)$ into at most $O(\alpha^n n)$ equivalence classes; that is, we have $|(\mathfrak{C}^{\mathsf{cf}}(\mathcal{S}_P)/\!\sim)| = O(\alpha^n n)$, where $\alpha \approx 2.83929$.*

Proof. We encode equivalence classes $[C]$ in $(\mathfrak{C}^{\mathsf{cf}}(\mathcal{S}_P)/\!\sim)$ by a string s_C of length n over the alphabet $\{\bullet, \oslash, \circ\}$ and by an index k_C. The i-th entry in s_C is $\bullet$ if $p_i \in \mathrm{low}(C)$, it is $\oslash$ if $p_i \in \mathrm{pts}(C) \setminus \mathrm{low}(C)$, and it is $\circ$ otherwise. The index k_C is equal to the number i which satisfies $p_i = \mathrm{lft}(\mathrm{rex}(C))$. From this encoding we immediately get a bound of $O(3^n n)$ on the size of $(\mathfrak{C}^{\mathsf{cf}}(\mathcal{S}_P)/\!\sim)$.

Our proof strategy is as follows. We ignore the index k_C and give an upper bound of $O(\alpha^n)$ on the number of strings s_C corresponding to a combination C in $\mathfrak{C}^{\mathsf{cf}}(\mathcal{S}_P)$. From this, the desired upper bound follows after adding an additional factor n. We do so by defining an injective function from a set A to a set B. Set A contains all strings s_C. Set B contains all strings from $\{\bullet, ⊘, ○\}^n$ which do not contain any subsequences of the form $(\bullet, ○, \ldots, ○, \bullet)$; that is, *one or more* consecutive symbols ○ enclosed by two symbols $\bullet$. Such subsequences are called *forbidden* henceforth. The bound on $|A|$ then follows from $|B| = \Theta(\alpha^n)$. The latter is an elementary counting problem whose proof we omit, see for example [25, Chapter I.4].

Let us define $f\colon A \to B$. For any $a \in A$ we construct $f(a)$ by the following process. We iterate over a from left to right, and whenever we find a forbidden subsequence $(\bullet, ○, \ldots, ○, \bullet)$ we replace it by $(⊘, \bullet, \ldots, \bullet, ⊘)$. For example, if $a = (\bullet, ○, \bullet, \bullet, \bullet, ○, \bullet)$ then $f(a) = (⊘, \bullet, ⊘, \bullet, ⊘, \bullet, ⊘)$; however, if $a = (\bullet, ○, \bullet, ○, \bullet)$ then $f(a) = (⊘, \bullet, ⊘, ○, \bullet)$ because the second forbidden subsequence in a is no longer a forbidden subsequence after the first has been replaced. It only remains to prove injectivity of f.

Towards a contradiction, assume thus that $a \neq a'$ satisfy $f(a) = f(a') =: b$. Let i be the smallest index with $a_i \neq a'_i$. We distinguish the three cases $b_i = ○$, $b_i = ⊘$ and $b_i = \bullet$.

For $b_i = ○$, observe that the function f never uses the symbol ○ to replace an entry in a or a'. Hence, $a_i = a'_i = ○$, a contradiction.

For $b_i = ⊘$, we assume without loss of generality that $a_i = \bullet$ and $a'_i = ⊘$. Moreover, a_i is either the first or last letter in a forbidden subsequence in a that is replaced under f. From minimality of i we get that it is the first letter. Since the following argument generalizes to larger subsequences, we now assume for simplicity that we have $(a_i, a_{i+1}, a_{i+2}) = (\bullet, ○, \bullet)$ and $(b_i, b_{i+1}, b_{i+2}) = (⊘, \bullet, ⊘)$. There are two possibilities for the corresponding letters in a'.

- If $(a'_i, a'_{i+1}, a'_{i+2}) = (\circledcirc, \bullet, \circledcirc)$, then observe that the points p_i, p_{i+1}, p_{i+2} from the set P must form a left turn; that is, p_{i+1} is strictly below the segment with endpoints p_i and p_{i+2}. The reason is that $a' = s_{C'}$ corresponds to a combination C' in $\mathfrak{C}^{\mathsf{cf}}(\mathcal{S}_P)$, and there must be a segment in C' which has p_{i+1}, but neither p_i nor p_{i+2}, in its lower shadow. On the other hand, $(a_i, a_{i+1}, a_{i+2}) = (\bullet, \circ, \bullet)$ implies that the points p_i, p_{i+1}, p_{i+2} form a right turn; that is, p_{i+1} is strictly above the segment with endpoints p_i and p_{i+2}. Again, this holds because also $a = s_C$ corresponds to a combination C, and there must be a segment in C which has both p_i and p_{i+2}, but not p_{i+1}, in its lower shadow. We have derived a contradiction because these two arrangements of p_i, p_{i+1} and p_{i+2} are mutually exclusive.

- If $(a'_i, \ldots, a'_{i+3}) = (\circledcirc, \bullet, \bullet, \circ)$ and $(b_i, \ldots, b_{i+3}) = (\circledcirc, \bullet, \circledcirc, \bullet)$, that is, index $i+2$ is the beginning of a forbidden subsequence in a', then we further obtain $(a_i, \ldots, a_{i+3}) = (\bullet, \circ, \bullet, \bullet)$. A contradiction can be derived similar to the previous case. The symbols in a' imply that the points p_i, p_{i+1} and p_{i+3} form a left turn because there exists a segment which has p_{i+1} and p_{i+2}, but neither p_i nor p_{i+3}, in its lower shadow. The symbols in a imply that p_i, p_{i+1} and p_{i+3} form a right turn because there exists a segment which has p_i, p_{i+2} and p_{i+3}, but not p_{i+1}, in its lower shadow.

For $b_i = \bullet$, we may assume that $a_i = \circ$, $a'_i = \bullet$, and that in a there exists a forbidden subsequence that starts before index i and ends after index i and that is replaced under f. Again for simplicity, we assume $(a_{i-1}, a_i, a_{i+1}) = (\bullet, \circ, \bullet)$ and $(b_{i-1}, b_i, b_{i+1}) = (\circledcirc, \bullet, \circledcirc)$ and note that longer sequences can be treated similarly. By minimality of i we get $a'_{i-1} = a_{i-1} = \bullet$. The only possible way for $a'_{i-1} = \bullet$ to be replaced by $b_{i-1} = \circledcirc$ under f is if a'_{i-1} is the last letter in a forbidden subsequence in a'. Therefore, $(a'_{i-3}, a'_{i-2}, a'_{i-1}) = (\bullet, \circ, \bullet)$ and $(b_{i-3}, b_{i-2}, b_{i-1}) = (\circledcirc, \bullet, \circledcirc)$, again without loss of generality. By

minimality of i we get $(a_{i-3}, a_{i-2}, a_{i-1}) = (●, ○, ●)$. In summary, we have derived $(a_{i-3}, \ldots, a_{i+1}) = (●, ○, ●, ○, ●)$ and $(b_{i-3}, \ldots, b_{i+1}) = (⊘, ●, ⊘, ●, ⊘)$. This is a contradiction because at most one of these two forbidden subsequences in a is replaced under f. □

3.7.2 Spanning Trees

Recall the definition of Γ_P^{st} from Section 3.6.2. The following lemma is all that is left to complete the proof of Theorem 3.7.

Lemma 3.35. *For any P, there exists a subgraph of Γ_P^{st} induced by a vertex subset $V \subseteq (\mathfrak{C}_P^{\mathsf{st}}/\!\sim)$ satisfying $|V| = O(\alpha^n n)$, where $\alpha \approx 7.04313$, and such that V contains all vertices that appear on at least one $\bot$-$\top$ path in Γ_P^{st}. Moreover, given a vertex of Γ_P^{st}, we can decide in time $O(n)$ whether it belongs to V.*

Proof. We specify eight colors ①, …, ⑧ that were introduced only informally in Section 3.6.2. Given C in $\mathfrak{C}_P^{\mathsf{st}}$, the colors are assigned to the points in P as follows. If $p \in \mathrm{low}(C)$ then p has color ①, meaning that ① = ● in the original color scheme. Otherwise, and if additionally $p \notin \mathrm{pts}(C)$, then p has color ⑧, which means that ⑧ = ○. All remaining points are assigned one of the colors ②, …, ⑦, which thus correspond to the original color ⊘. Color ② means that p has out-degree 0 and exposes no drain. Color ③ means that p has out-degree 0 and exposes a drain to the left. Color ④ means that p has out-degree 0 and exposes a drain to the right. Color ⑤ means that p has out-degree 1 and exposes no drain. Color ⑥ means that p has out-degree 1 and exposes a drain to the left. Color ⑦ means that p has out-degree 1 and exposes a drain to the right.

Let now s_C be the string from $\{①, \ldots, ⑧\}^n$ that corresponds to a given combination C in $\mathfrak{C}_P^{\mathsf{st}}$. The present lemma is a consequence of the following three observations.

- For two consecutive points p_i and p_{i+1}, it cannot be that both p_i and p_{i+1} have out-degree 1 and, at the same time, p_i exposes a drain to the left and p_{i+1} exposes a drain to the right. As illustrated on the right hand side, if that were the case then there would be either a crossing or a finite face of out-degree 0, both in contradiction with the definition of $\mathfrak{C}_P^{\mathfrak{st}}$. Hence, in s_C we will never observe the pattern (⑥, ⑦); that is, color ⑥ directly followed by color ⑦. Additionally, if p_i and p_{i+k} (taking the role of p_{i+1}) are separated by any number of points of degree 0, the same argument still applies. Hence, we can further rule out the pattern (⑥, ⑧, . . . , ⑧, ⑦).

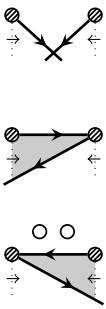

- Similarly, for two consecutive points p_i and p_{i+1}, it cannot be that both p_i and p_{i+1} have out-degree 0 and, at the same time, p_i exposes a drain to the left and p_{i+1} exposes a drain to the right. Since both points have out-degree 0 they cannot possibly be connected by an edge, and thus we necessarily get a crossing, as illustrated on the right hand side. Hence, the pattern (③, ④) cannot occur in s_C. Using the same argument we can further rule out the pattern (③, ②, . . . , ②, ④), since in such a configuration there will always be two consecutive points p_i and p_{i+1} of out-degree 0 such that p_i is the left endpoint of an edge and p_{i+1} is the right endpoint of another edge. Similar to the first observation, any additional points with degree 0 do not interfere with this argument. The same can be said for any points that are in the lower shadow of C. Hence, we can rule out the pattern (③, ①|②|⑧, . . . , ①|②|⑧, ④), where "|" indicates an arbitrary choice between several options.

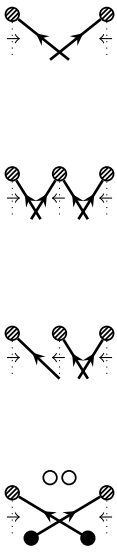

In our last observation, we describe a pattern that actually occurs in s_C. However, for any occurrence it can be seen that the corresponding vertex $[C]$ is not contained in any $\bot$-$\top$ path in Γ_P^{st}. Therefore, the set V from the lemma may safely be defined as the subset of all vertices of Γ_P^{st} that do not contain this final pattern.

- Let p_i and p_{i+1} be two consecutive points such that p_i exposes a drain to the right and p_{i+1} exposes a drain to the left. Then, clearly, the out-degree of the infinite face in C is different from 0 and thus there is no direct connection from $[C]$ to $\top$ in Γ_P^{st}. Moreover, any new segment u that consumes the drain exposed by p_i (that is, the border below p_i becomes an out-border of the new face directly below u) must also consume the drain exposed by p_{i+1}, as illustrated on the right hand side. However, the face below u having out-degree at least 2 contradicts the definition of $\mathfrak{C}_P^{\mathsf{st}}$. Therefore, the two drains exposed by p_i and p_{i+1} can never be consumed and the sink $\top$ can thus never be reached. Hence, we can safely discard any vertices with the pattern (④|⑦, ③|⑥). Additionally, suppose that p_i and p_{i+k} (taking the role of p_{i+1}) are separated by any number of points of degree 0 or points in the lower shadow of C. Then, no matter how a new segment u is added, we again get a pair of drains facing each other and all points in between are either of degree 0 or in the lower shadow. Hence, we can further discard any vertices with the pattern (④|⑦, ①|⑧, . . . , ①|⑧, ③|⑥).

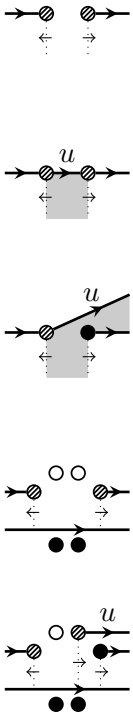

Let A be the subset of $\{①, \ldots, ⑧\}^n$ containing only strings without subsequences belonging to the three patterns from the above observations. Then, it can be shown that $|A| = \Theta(\alpha^n)$ using standard techniques [25, Chapter I.4], and the lemma follows. □

3.7.3 Spanning Cycles

Finally, recall the definition of Γ_P^{sc} from Section 3.6.3. The following lemma concludes the proof of Theorem 3.8.

Lemma 3.36. *For any P, there exists a subgraph of Γ_P^{sc} induced by a vertex subset $V \subseteq (\mathfrak{C}_P^{\check{\mathsf{sc}}}/\!\sim)$ satisfying $|V| = O(\alpha^n n)$, where $\alpha \approx 5.61804$, and such that V contains all vertices that appear on at least one $\bot$-$\top$ path in Γ_P^{sc}. Moreover, given a vertex of Γ_P^{sc}, we can decide in time $O(n)$ whether it belongs to V.*

Proof. We again give specifications for the colors $①, \ldots, ⑥$ that are assigned to the points in P for any C in $\mathfrak{C}_P^{\check{\mathsf{sc}}}$. Color ① means that the corresponding point p has degree 2 and exposes no drain. Color ② means that p has degree 2 and exposes a drain. Color ③ means that p has degree 1 and exposes no drain. Color ④ means that p has degree 1 and exposes a drain to the left. Color ⑤ means that p has degree 1 and exposes a drain to the right. Color ⑥ means that p has degree 0.

The following observation is similar to the third observation in the proof of the preceding lemma. Let C be a combination in $\mathfrak{C}_P^{\check{\mathsf{sc}}}$ and let p_i and p_{i+1} be two consecutive points. If p_i exposes a drain to the right and p_{i+1} exposes a drain to the left in C, then C cannot be augmented in such a way that the infinite face has out-degree 0 without creating finite faces with out-degree larger than 1. In other words, the vertex $[C]$ does not appear on any $\bot$-$\top$ path in Γ_P^{sc} and may safely be discarded. The same holds for two not necessarily consecutive points p_i and p_{i+k} such that again p_i exposes a drain to

the right and p_{i+k} exposes a drain to the left, and such that all points in between p_i and p_{i+k} have either degree 0 or 2. No matter how a new segment u is added to C, we again end up with a combination with two exposed drains facing each other and only points of degree 0 or 2 in between.

The subset V of vertices is defined as follows. We exclude all vertices with the patterns $(⑤, ④)$ or $(⑤, ①|②|⑥, \ldots, ①|②|⑥, ④)$. Let now A be the subset of $\{①, \ldots, ⑥\}^n$ which contains only strings without subsequences belonging to the above patterns. Then, it can be shown that $|A| = \Theta(\alpha^n)$, see again [25, Chapter I.4], and the lemma follows. □

CHAPTER 4

Trapezoidal Diagrams and Upper Bounds

4.1 Introduction

Let us introduce the two main notions to be studied in this chapter, namely *trapezoidal diagrams* and *prime Catalan numbers*. The latter is a purely combinatorial concept related to balanced bracket expressions; it is, as such, of independent interest to combinatorialists. The former is a simple and natural structure which encodes the vertical visibility relations between segments in a geometric graph; it is studied as a potential tool for proving better upper bounds on the maximum number of crossing-free geometric graphs.

Prime Catalan Numbers. A *balanced bracket expression (of dimension d)* is a finite string c over an alphabet $\{b_1, \ldots, b_d\}$ of d *brackets* such that all brackets occur in equal numbers in c, and such that every prefix of c contains at least as many occurrences of b_i as of b_{i+1}, for $1 \leq i \leq d-1$. The *size* $m = |c|$ of c is defined as the number of occurrences of b_1. As an example, let us enumerate all balanced bracket expressions of dimension $d = 3$ with brackets $b_1 =$ '$\langle$', $b_2 =$ '|', and $b_3 =$ '$\rangle$' and of size $m = 2$.

$$\langle|\rangle|\rangle \qquad \langle\langle||\rangle\rangle \qquad \langle|\langle|\rangle\rangle \qquad \langle\langle|\rangle|\rangle \qquad \langle|\rangle\langle|\rangle$$

We call a balanced bracket expression of dimension d *prime* if it does not contain any non-empty, contiguous and proper substrings that are themselves balanced bracket expressions of dimension d over the same bracket alphabet. Note that in the above enumeration, only the first two expressions are prime, whereas the other three all contain "$\langle|\rangle$" as a proper substring.

The m-th d-dimensional Catalan number $C_m^{(d)}$ can be defined as the number of balanced bracket expressions of dimension d and of size m. [31, 63] The most prominent instantiation of this family of sequences is of course given by the customary (2-dimensional) Catalan numbers $C_m = C_m^{(2)}$. In this chapter, however, the focus is on the 3-dimensional case. [41] For easy reference, below we enumerate the first ten entries in the sequence corresponding to $C_m^{(3)}$, starting with $m = 0$.

$$1, 1, 5, 42, 462, 6006, 87516, 1385670, 23371634, 414315330, \ldots$$

Explicit product formulas for the numbers $C_m^{(d)}$ are known and can be obtained by employing the famous hook-length formula for standard Young tableaux of shape (m^d). See [47] for a precise statement and an insightful proof of the hook-length formula. For example,

for dimension $d = 3$ we obtain the following rather elegant formula.

$$C_m^{(3)} = \frac{2(3m)!}{(m+2)!(m+1)!m!} \tag{4.1}$$

By employing Stirling's approximation for factorials, we further get the following asymptotic estimate.

$$C_m^{(3)} = \Theta\left(m^{-4}27^m\right) \tag{4.2}$$

In a similar vein, we denote by $P_m^{(d)}$ the number of balanced bracket expressions of dimension d and of size m which are prime. We call $P_m^{(d)}$ the m-th d-dimensional *prime Catalan number*. In spite of the natural definition, we are not aware of any previous work that studies these numbers or acknowledges their existence. Below we enumerate the first ten entries in the sequence corresponding to $P_m^{(3)}$, starting again with $m = 0$.

$$1, 1, 2, 12, 107, 1178, 14805, 203885, 3002973, 46573347, \ldots$$

This sequence stands in contrast to the customary 2-dimensional case. Indeed, by reusing the brackets $b_1 = \text{`}\langle\text{'}$ and $b_2 = \text{`}\rangle\text{'}$, we see that the empty string ε and "$\langle\rangle$" are the only prime balanced bracket expressions of dimension $d = 2$. Hence, $P_m^{(2)} = 0$ for $m \geq 2$.

In Section 4.4 we study various aspects of the numbers $P_m^{(d)}$ and show how to compute them. Theorem 4.1, which will be proved in that section, gives the rate of exponential growth of the prime Catalan numbers, and it is the only result that is relevant for the earlier sections. In the following, let $C^{(d)}(x) := \sum_{m=0}^{\infty} C_m^{(d)} x^m$ denote the ordinary generating function of the d-dimensional Catalan numbers.

Theorem 4.1. *For any dimension $d \geq 3$, the prime Catalan numbers exhibit the following limit behavior.*

$$\lim_{m\to\infty} \sqrt[m]{P_m^{(d)}} = \gamma_d := \left(\frac{d}{C^{(d)}(1/d^d)}\right)^d$$

Decimal approximations of the numbers γ_d can be computed automatically using any modern computer algebra system. For γ_3 we even obtain a closed formula.

$$\gamma_3 = \frac{27}{(\frac{729\sqrt{3}}{40\pi} - 9)^3} \approx 23.459, \quad \gamma_4 \approx 251.788, \quad \gamma_5 \approx 3119.934 \quad (4.3)$$

Trapezoidal Diagrams. Let P be a set of n points in the plane in general position. This means in particular that all points have distinct x-coordinates, which implies that they can be ordered as $p_1, \ldots, p_n$ from left to right. We then say that a point p_i is *to the left* of another point p_j if $i < j$ holds.

In this chapter, as far as crossing-free geometric graphs are concerned, we restrict our attention to perfect matchings, triangulations and spanning cycles. Even though we tend to omit the adjective crossing-free, all geometric graphs considered here have no crossings.

The *trapezoidal decomposition* of a geometric graph G is a well-known and useful notion—see [57] for a classic application—which is obtained by drawing a vertical *extension* upwards and downwards outgoing from each point in P until a segment of G is hit; if there is no obstruction, then the extension is drawn as an infinite ray. If the extension going upwards (downwards) from a point p hits the segment corresponding to an edge e, then we say that *e sees p below (above)* in G. Clearly, every point can be seen by at most two edges, once from below and once from above.

We now define the *trapezoidal diagram* (or, just *diagram*) of G, where G will be either a perfect matching, a triangulation or a spanning cycle. Informally speaking, the trapezoidal diagram is equivalent to the trapezoidal decomposition except that we discard the coordinates of the vertices.

Definition 4.2. *Let P be a set of n points, and let G be a geometric graph on P. Then, the* trapezoidal diagram *of G, denoted by D_G, is defined as follows.*

(i) D_G is an abstract graph with vertex set $[n] = \{1, 2, \ldots, n\}$ so that there is an edge $\{i, j\}$ in D_G if and only if there is an edge $\{p_i, p_j\}$ in G.

(ii) Every edge in D_G has two distinguished sequences with the indices $i_1, \ldots, i_k$ of the points $p_{i_1}, \ldots, p_{i_k}$ sorted from left to right that the corresponding edge in G can see below and above, respectively.

(iii) There are two additional sequences with the indices of the points sorted from left to right that no edge in G can see below and above, respectively.

If there exists an isomorphism $[n] \to [n]$ between D_{G_1} and D_{G_2} that preserves the structure imposed by (i), (ii) and (iii), then we identify D_{G_1} and D_{G_2}, and we say that G_1 and G_2 have the same trapezoidal diagram.

We typically do not appeal to the above definition directly. Instead, we argue on the basis of a drawing of a given trapezoidal diagram. Incidentally, a *drawing* of D_G is a plane—that is, without any crossings—drawing of the underlying graph and its trapezoidal decomposition, where we allow edges of the graph to be drawn as arbitrary x-monotone Jordan curves. All orientations of edges must however remain the same—that is, a left endpoint remains a left endpoint in the drawing—and all vertical visibility relations must remain identical—that is, the order from left to right in which an edge sees points below and above, respectively, does not change.

We refer to Figure 4.1 for interesting examples. Observe that the geometric graph G combined with its trapezoidal decomposition is an instance of a drawing of D_G. Further note that two distinct

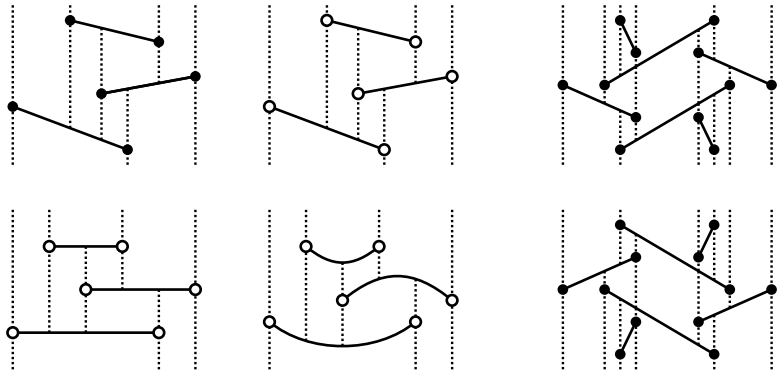

Figure 4.1: On the left, a perfect matching with trapezoidal decomposition and three drawings of its trapezoidal diagram, which are distinguished visually from geometric graphs by leaving vertices blank. On the right, two distinct perfect matchings on the same point set with the same trapezoidal diagram.

perfect matchings M_1 and M_2 on the same point set P may have the same trapezoidal diagram.

Let us remark that trapezoidal diagrams of perfect matchings are related to the well-studied notion of *(directed) bar visibility graphs*; see for example [64] for a definition and further references. However, that class of graphs imposes much coarser equivalence classes on the set of collections of non-intersecting segments in the plane.

For reasons that become clear later, we slightly specialize the definition of trapezoidal diagrams for triangulations.

Definition 4.3. *Let $n > 2$ and assume that P has a triangular convex hull with the edge $\{p_1, p_n\}$ on the lower envelope. The* trapezoidal diagram *of a triangulation T on P, denoted by D_T, is obtained as follows. First, draw an additional edge between p_1 and p_n as an x-monotone curve that goes above all other points and seg-*

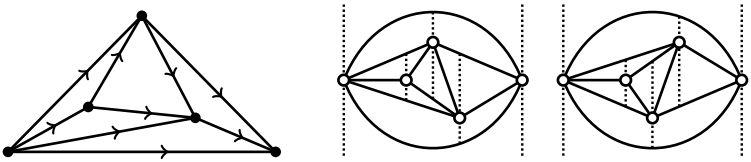

Figure 4.2: An abstract upward (or rather, rightward) triangulation and two corresponding trapezoidal diagrams of geometric triangulations. The second diagram is obtained by a vertical reflection.

ments. Then, D_T is defined analogously to Definition 4.2. For the degenerate case $n = 2$ we define D_T to be a single edge.

In this case, a closely related concept from graph drawing is that of *upward triangulations*. These are abstract maximal planar graphs with directed edges such that there exists a plane embedding where all the edges are drawn as y-monotone Jordan curves pointing upwards. [26] After replacing *upward* with *rightward* and y-monotone with x-monotone, and after looking at Figure 4.2, it becomes clear that every trapezoidal diagram of a triangulation corresponds to a unique upward triangulation—by orienting edges from left to right—and that, depending on the presence or absence of symmetries, every upward triangulation corresponds to one or two such diagrams.

In Section 4.2 we present a generic method for encoding trapezoidal diagrams as strings over a finite alphabet, which then allows us to make deductions about the number of such diagrams. The presented ideas can be applied to any family of geometric graphs. However, we obtain a simple characterization of the set of code words only in the cases of perfect matchings and triangulations.

In order to formulate the following theorem, let $\mathfrak{D}_n^{\mathsf{pm}} = \{D_M\}$ be the set of all diagrams of all perfect matchings on all point sets P of size n. See Table 4.3 for an enumeration of this set for $n = 0, 2, 4$.

$n = 0$	$n = 2$	$n = 4$
$\varnothing$		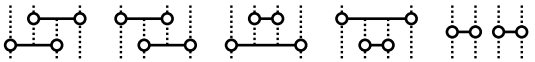

Table 4.3: All non-isomorphic trapezoidal diagrams of perfect matchings for $n = 0, 2, 4$, with $\varnothing$ denoting the empty diagram.

Theorem 4.4. *For any $n = 2m$, the number of trapezoidal diagrams of perfect matchings on n points is equal to the m-th 3-dimensional Catalan number.*

$$|\mathfrak{D}_n^{\mathsf{pm}}| = C_m^{(3)} = \Theta\left(n^{-4}\sqrt{27}^n\right), \qquad \textit{where } \sqrt{27} \approx 5.196$$

Similarly, let $\mathfrak{D}_n^{\mathsf{tr}} = \{D_T\}$ be the set of all diagrams of all triangulations on all sets P of size n as specified in Definition 4.3. An enumeration of this set for $n = 2, 3, 4, 5$ can be seen in Table 4.4.

Theorem 4.5. *For any $n = m + 2$, the number of trapezoidal diagrams of triangulations on n points is equal to the m-th 3-dimensional prime Catalan number.*

$$|\mathfrak{D}_n^{\mathsf{tr}}| = P_m^{(3)} = \Theta^*(\gamma_3^n), \qquad \textit{where } \gamma_3 \approx 23.459$$

The following corollary of the above theorem should be compared with a classic result of Tutte from 1962, which implies that the number of abstract triangulations—that is, maximal planar graphs—on n vertices is $\Theta^*(\alpha^n)$, where $\alpha = 256/27 \approx 9.481$. [66] Moreover, quite curiously, in a side remark of [11] Alvarez and Seidel report an upper bound of 27^n on the number of upward triangulations. As we shall see, the appearance of the exponential base 27 in this context is not at all coincidental.

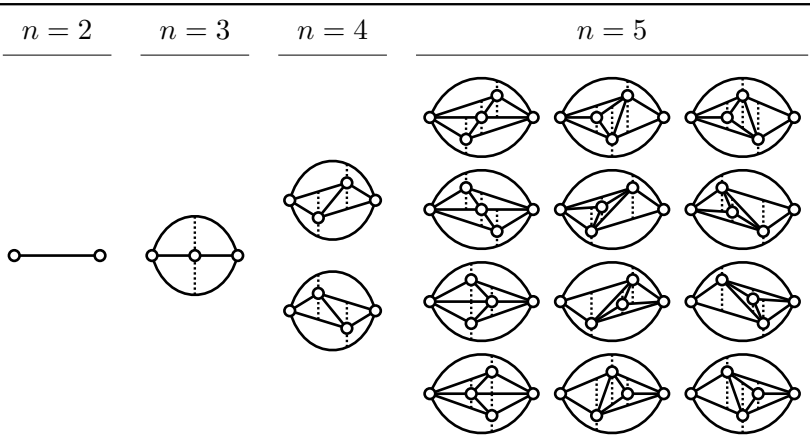

Table 4.4: All trapezoidal diagrams of triangulations. We omit drawing the vertical extensions through vertices 1 and n.

Corollary 4.6. *Let N_n be the number of upward triangulations on n vertices. Then, we have $|\mathfrak{D}_n^{\mathsf{tr}}|/2 \leq N_n \leq |\mathfrak{D}_n^{\mathsf{tr}}|$ and hence also $N_n = \Theta^*(\gamma_3^n)$.*

On a different note, an investigation of Frati, Gudmundsson and Welzl from 2012 shows that the number of upward orientations of any given abstract triangulation is somewhere between $\Omega^*(1.189^n)$ and $O^*(4^n)$, and that it can be as low as $O^*(2^n)$ and as high as $\Omega^*(2.599^n)$ in specific cases. [26] Combined with Tutte's result, the preceding corollary now implies that an abstract triangulation has $\Theta^*(\beta^n)$ upward orientations on average, where $\beta = \gamma_3/\alpha \approx 2.474$ and α is as in Tutte's result.

For graph families other than perfect matchings and triangulations, we do not acquire the same level of understanding. However, the same techniques can be used to obtain at least exponential upper bounds. We shall illustrate this with the example of spanning cy-

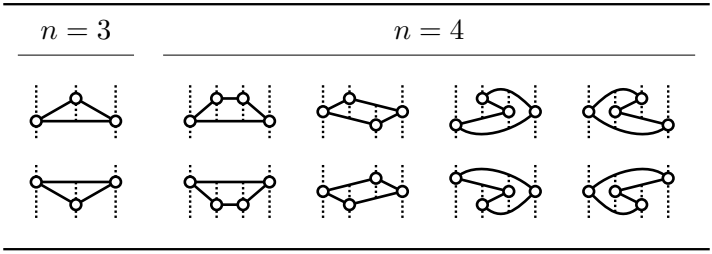

Table 4.5: All trapezoidal diagrams of spanning cycles for $n = 3, 4$.

cles. So, let $\mathfrak{D}_n^{\mathsf{sc}} = \{D_C\}$ be the set of all trapezoidal diagrams of all spanning cycles on all sets P of size n; see Table 4.5 for an enumeration.

Theorem 4.7. *For any $n \geq 3$, it holds that $|\mathfrak{D}_n^{\mathsf{sc}}| \leq 16^n$.*

Embeddings. Our interest in trapezoidal diagrams comes originally from a desire for improved upper bounds on the maximum number of crossing-free geometric graphs. In Section 4.3 we initiate the study of the maximum number of embeddings that a given diagram can have on a fixed point set, by giving two exponential lower bounds. Unfortunately, we do not succeed in proving strong enough upper bounds on the number of embeddings, so as to obtain improved upper bounds on the number of crossing-free geometric graphs.

4.2 Encoding Trapezoidal Diagrams

4.2.1 The Canonical Order

Let G be a crossing-free geometric graph of one of the investigated families. Fix a drawing of D_G and consider the set of all points in the

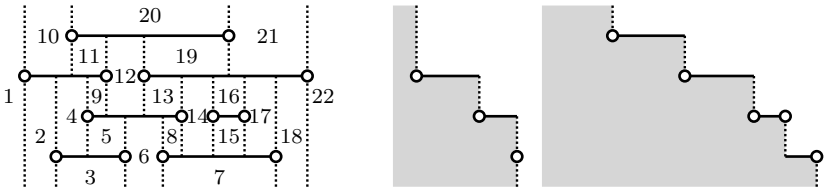

Figure 4.6: On the left, the canonical order of a trapezoidal diagram of a perfect matching. On the right, the boundaries corresponding to the prefixes $1, \ldots, 5$ and $1, \ldots, 15$.

plane which are neither a vertex, nor part of an edge, nor a vertical extension. Then, a *trapezoid* in D_G is defined as the closure of a maximal connected region in that set. Typically, but not always, a trapezoid is bounded from above and below by edges of G, and to the left and right by vertical extensions.

We define a *canonical order* over the trapezoids in D_G in the following recursive manner. Given a prefix of the canonical order, we select as the next element a trapezoid that is either unbounded from below or that is bounded from below by an edge e which is already well-supported, in the sense that all trapezoids having e as their upper boundary occur in the given prefix of the canonical order. If this choice is not unique, then we settle with the left-most option.

By the following observation, which follows by induction over the length of the given prefix, the canonical order is seen to be both well-defined and independent of the fixed drawing of D_G.

Observation 4.8. *Take any proper—that is, both non-empty and incomplete—prefix of the canonical order of D_G, build the union of all trapezoids occurring in that prefix, and consider the boundary of that union. This boundary has a staircase shape as depicted in Figures 4.6 and 4.7. Specifically:*

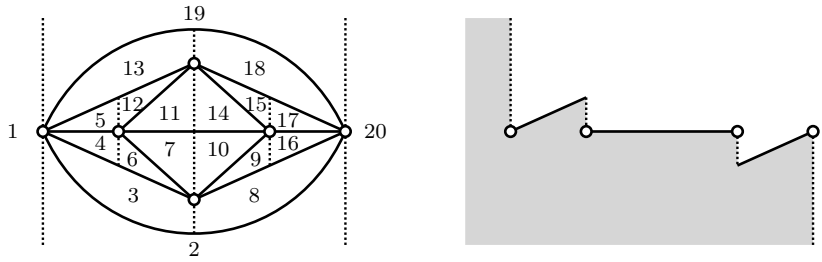

Figure 4.7: On the left, the canonical order of a trapezoidal diagram of a triangulation. On the right, the boundary corresponding to the prefix $1, \ldots, 10$.

- *Starting at positive infinity at the end of a vertical extension that is unbounded from above, the boundary alternates between verticals that go downwards and parts of not necessarily straight edges that go to the right, and it finally ends at negative infinity at the end of a vertical extension that is unbounded from below.*
- *Every vertical on the boundary contains exactly one vertex of G, either (a) at the bottom, (b) in its relative interior, or (c) at the top. When going along the boundary, we first encounter a possibly empty sequence of verticals of type (a), then at most one vertical of type (b), and then a possibly empty sequence of verticals of type (c).*

Further note that the subsequent trapezoid in canonical order must be bounded to the left by the last vertical that is not of type (c).

4.2.2 Perfect Matchings

We are ready to prove the following lemma. Combining it with (4.1) and (4.2) yields Theorem 4.4.

Lemma 4.9. *For any $n = 2m$, there is a bijection between $\mathfrak{D}_n^{\mathsf{pm}}$ and the set of balanced bracket expressions of dimension 3 of size m.*

Proof. For $m = 0$ the claim is trivial. So let $m \geq 1$, and let us define mappings in both directions. Observing that these mappings are inverses of each other will conclude the proof.

From trapezoids to brackets. Let $D = D_M$ be the trapezoidal diagram of any perfect matching M on a set P of n points. We show how to construct the corresponding balanced bracket expression c of size m.

We first enumerate the trapezoids in D in canonical order, where we omit the last trapezoid on the far right. We obtain a sequence of exactly $3m$ trapezoids, each bounded to the right. Indeed, observe that to each edge $e = \{i, j\}$ in D, where $i < j$ are the respective left and right vertices, we can attribute the following three trapezoids.

(i) The unique trapezoid whose right boundary is the vertical extension through i.

(ii) The unique trapezoid whose right boundary is the vertical extension below j.

(iii) The unique trapezoid whose right boundary is the vertical extension above j.

In order to obtain c, we now apply the substitution rules (i) $\mapsto$ '$\langle$', (ii) $\mapsto$ '|', (iii) $\mapsto$ '$\rangle$', based on the three types of trapezoids specified above. The resulting string is a balanced bracket expression of size m because, as is clear from Observation 4.8, for each edge e the three attributed trapezoids occur in the relative order (i), (ii), (iii).

From brackets to trapezoids. Let c be an arbitrary balanced bracket expression of dimension 3 and of size m. We show how

to construct the corresponding trapezoidal diagram $D = D_M$ of a perfect matching M on n points.

We iterate over c and construct a drawing of D by drawing one trapezoid per letter in c. For each bracket we select a different type of trapezoid. More precisely, as follows, we discriminate between the possible locations of the vertex i that lies on the right boundary of the new trapezoid.

(i) For '⟨' we select  ; that is, i is in the interior.

(ii) For '|' we select  ; that is, i is at the top.

(iii) For '⟩' we select  ; that is, i is at the bottom.

In the illustrations above we have omitted to draw the vertices on the respective left boundaries. Also, the trapezoids of types (i) and (ii), but not (iii), might in fact be unbounded from below. Similarly, the trapezoids of type (i) and (iii), but not (ii), might be unbounded from above.

The positioning of individual trapezoids is done as illustrated in Table 4.8, where the labels l and r indicate whether a boundary vertex is a left or right endpoint. Mutations which involve unbounded trapezoids can be handled analogously. Also note that, after each step, the boundary of the union of all drawn trapezoids has a staircase shape as in Observation 4.8, and the order in which we add trapezoids corresponds to the canonical order.

We now have to show that if c is a balanced bracket expression, then each trapezoid can be placed in a coherent way. Assume thus that we have processed a certain prefix of c already. Then, each left endpoint on the current boundary, except for those on a vertical of type (a) directly followed by a vertical of type (c) (as specified in Observation 4.8), is called an *active left endpoint*. In more descriptive terms, an active left endpoint is one whose corresponding

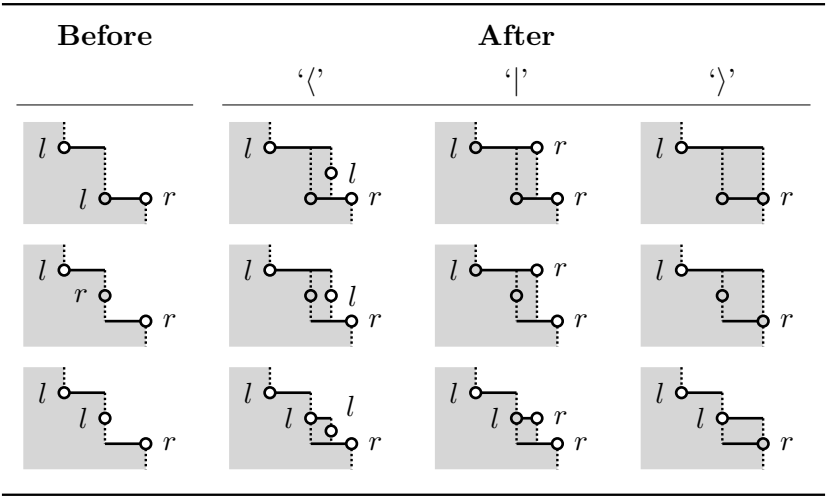

Table 4.8: Constructing the diagram of a perfect matching. Vertices which are not active left or right endpoints are drawn in gray.

right endpoint is not yet part of the drawing. Similarly, each right endpoint on the current boundary, except for those on a vertical of type (b), is called an *active right endpoint*. That is, an active right endpoint is one which has no trapezoid placed on top of it. Let now m_1, m_2 and m_3 be the respective numbers of occurrences of the brackets ‘⟨’, ‘|’ and ‘⟩’ in the processed prefix of c. We claim that we maintain the following invariants.

(I1) The number of active left endpoints on the boundary is equal to $m_1 - m_2$.

(I2) The number of active right endpoints on the boundary is equal to $m_2 - m_3$.

These invariants are a consequence of the following simple observations: Adding a trapezoid of type (i) creates a new active left endpoint. Adding a trapezoid of type (ii) turns a formerly active

left endpoint inactive, and it also creates a new active right endpoint. Adding a trapezoid of type (iii) turns a formerly active right endpoint inactive. We again refer to Table 4.8 for helpful illustrations.

The invariants guarantee that we never get stuck when constructing D. Indeed, if the current bracket to be processed is '$\langle$', then it is always possible to add a trapezoid of type (i). If the current bracket is '$|$', then we can add a trapezoid of type (ii) only if there is an active left endpoint on the boundary, which is guaranteed by (I1) since the already processed prefix of c satisfies $m_1 > m_2$ because c is a balanced bracket expression. If the current bracket is '$\rangle$', then we can add a trapezoid of type (iii) only if there is an active right endpoint on the boundary, which is guaranteed by (I2) because the already processed prefix of c satisfies $m_2 > m_3$.

Also, by invariants (I1) and (I2), when the whole string c has been processed we end up with a boundary that consists of a single vertical extension with one inactive right endpoint. The last trapezoid—that is, the one that is unbounded to the right—can then be added in order to finish the construction of D. □

4.2.3 Triangulations

The proof of the next lemma is very similar to the one before. Combining the lemma with Theorem 4.1 and (4.3) yields Theorem 4.5.

Lemma 4.10. *For any $n = m + 2$, there is a bijection between $\mathfrak{D}_n^{\mathsf{tr}}$ and the set of prime balanced bracket expressions of dimension 3 and of size m.*

Proof. Assume again that $m \geq 1$. We proceed by defining mappings in both directions which are clearly inverses of each other.

From trapezoids to brackets. Let $D = D_T$ be the trapezoidal diagram of a triangulation T on a set of n points, as specified in Definition 4.3. We show how to construct the corresponding balanced bracket expression c of size m.

We start by enumerating the trapezoids in D in canonical order, where we only consider trapezoids that are enclosed by the double edge $\{1, n\}$. In other words, we ignore all four unbounded trapezoids. The reader should not be confused by the fact that all enumerated trapezoids have only one vertical boundary and hence look more like triangles. We further note that we get a sequence of $4m$ trapezoids in this way. Indeed, to each of the m inner vertices $i \in [n] \setminus \{1, n\}$ we can attribute the following four trapezoids.

(i) The unique trapezoid whose right boundary is the vertical extension below i.

(ii) The unique trapezoid whose right boundary is the vertical extension above i.

(iii) The unique trapezoid whose left boundary is the vertical extension below i.

(iv) The unique trapezoid whose left boundary is the vertical extension above i.

As a consequence of Observation 4.8, the trapezoids of type (ii) and (iii) attributed to a common vertex i always appear consecutively in the order (ii), (iii). Therefore, similar to the proof of Lemma 4.9, we construct c by applying the substitution rules (i) $\mapsto$ '$\langle$', (ii),(iii) $\mapsto$ '$|$', (iv) $\mapsto$ '$\rangle$'. Note that in the case of the second rule we effectively replace two trapezoids with one single bracket. Also, by Observation 4.8, the four trapezoids attributed to a common vertex i occur in the relative order (i), (ii), (iii), (iv), implying that c is indeed a balanced bracket expression of size m. In what follows, we shall further see that c is prime.

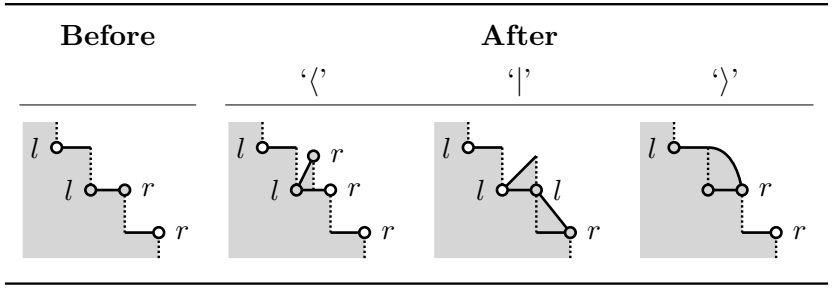

Table 4.9: Constructing the diagram of a triangulation. Vertices which are not active left or right endpoints are drawn in gray.

From brackets to trapezoids. Let c be an arbitrary balanced bracket expression of size m. For the time being, we do *not* make the assumption that c is prime. We shall try—and gracefully fail—to construct the corresponding trapezoidal diagram $D = D_T$ of a triangulation T on n points.

We start by drawing the two initial unbounded trapezoids. We then iterate over c and draw either one or two trapezoids for each letter in c. Depending on the brackets we make the following selections.

(i) For ‘⟨’ we select  ; that is, vertical right, vertex on top.

(ii,iii) For ‘|’ we select  ; that is, a combination of two trapezoids.

(iv) For ‘⟩’ we select  ; that is, vertical left, vertex at bottom.

As for the positioning of individual trapezoids, we do it again in the obvious way by trying to maintain the invariant that, after each step, the boundary has a staircase shape as in Observation 4.8. In fact, if we regard the addition of the two trapezoids of type (ii,iii) as one single step, then the boundary never contains any verticals of type (b) (as specified in Observation 4.8). Helpful illustrations can be seen in Table 4.9.

Assume that we have processed a certain prefix of c already. Then, every vertex on a vertical of type (a), except for the right-most one, is called an *active left endpoint*. Similarly, every vertex on a vertical of type (c), except for the left-most one, is called an *active right endpoint*. For m_1, m_2 and m_3 defined as in the proof of Lemma 4.9, we claim that we maintain the following invariants.

(I1) The number of active right endpoints on the boundary is equal to $m_1 - m_2$.

(I2) The number of active left endpoints on the boundary is equal to $m_2 - m_3$.

These invariants once more follow from simple observations: Adding a trapezoid of type (i) turns a formerly inactive right endpoint active. Adding a pair of trapezoids of type (ii,iii) turns a formerly active right endpoint inactive, and it also turns a formerly inactive left endpoint active. Adding a trapezoid of type (iv) turns a formerly active left endpoint inactive.

The above invariants guarantee that we never get stuck while constructing D, even if c is not prime. Indeed, if the current bracket to be processed is '$\langle$', then it is always possible to add a trapezoid of type (i). If the current bracket is '$|$', then we can add a pair of trapezoids of type (ii,iii) only if there is an active right endpoint, which is guaranteed by (I1) because the already processed prefix of c satisfies $m_1 > m_2$. If the current bracket is '$\rangle$', then we can add a trapezoid of type (iv) only if there is an active left endpoint, which is guaranteed by (I2) because the already processed prefix of c satisfies $m_2 > m_3$.

Furthermore, when c has been processed completely, invariants (I1) and (I2) imply that the boundary consists of a single edge and two unbounded vertical extensions. In other words, the staircase consists of a single step. Hence, we can just add the two final unbounded trapezoids in order to finish the construction of D.

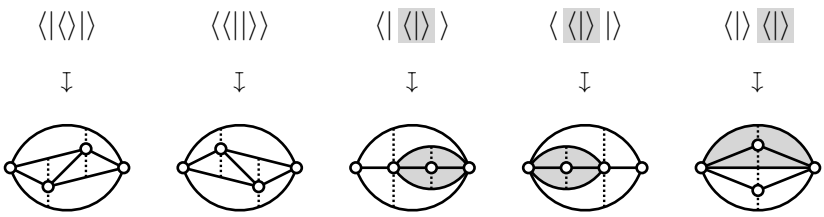

Figure 4.10: Substrings which are balanced bracket expressions lead to unwanted double edges.

Figure 4.10 shows that not every balanced bracket expression c is mapped to a valid trapezoidal diagram. It can happen that unwanted double edges are created. Recall that one double edge between vertices 1 and n is required, but any other double edge or even a triple edge between vertices 1 and n stands in violation of Definition 4.3. All the same, we can now observe that the described reconstruction procedure creates a double edge whenever it finishes processing a substring of c that is itself a balanced bracket expression. Since the described procedure clearly computes the inverse of the earlier described mapping that goes in the other direction, this also implies that all balanced bracket expressions produced by that first mapping are in fact prime.

Lastly, we face the problem of stretchability, namely that the produced drawing D might not correspond to the trapezoidal diagram D_T of an actual triangulation T with straight-line segments. However, it is known that any simple plane graph with edges drawn as non-crossing x-monotone curves can be stretched without changing edge orientations with respect to the x-axis. [38, Theorem 4] If c is prime, it thus follows that also our drawing D is stretchable after removing the upper copy of the double edge $\{1, n\}$. □

4.2.4 Spanning Cycles

Finally, Theorem 4.7 is an easy consequence of the following lemma.

Lemma 4.11. *For any $n \geq 3$ there is an injective map from $\mathfrak{D}_n^{\mathsf{sc}}$ to the set of strings of length $2n$ over the alphabet $\{\mathtt{a}, \mathtt{b}, \mathtt{c}, \mathtt{d}\}$.*

Proof. We define mappings in both directions. The lemma follows after observing that the second mapping is the left inverse of the first. Note that, in fact, the second mapping is only well-defined for outputs produced by the first mapping.

From trapezoids to letters. Let $D = D_C$ be the trapezoidal diagram of a spanning cycle C on a set of n points. By double counting we see that there are exactly $2n+1$ trapezoids in D. Indeed, each of the n vertices is incident with four trapezoids and each trapezoid is incident with two vertices, except for the left-most and right-most trapezoids, which are incident with only one vertex. Hence, the number t of trapezoids must satisfy the equation $4n = 2t - 2$.

We now partition the trapezoids into four distinct groups, where we discriminate between the appearance of the right boundary.

(i) 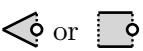 ; that is, vertex in relative interior.

(ii) 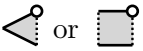 ; that is, vertex on top.

(iii) 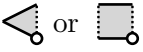 ; that is, vertex at bottom.

(iv)  ; that is, right boundary consists of a single vertex.

Similar to the note in the proof of Lemma 4.9, some of the above trapezoids might in fact be unbounded from above or from below.

Enumerating the trapezoids in canonical order, where we omit the very last trapezoid—that is, the one that is unbounded to the right—

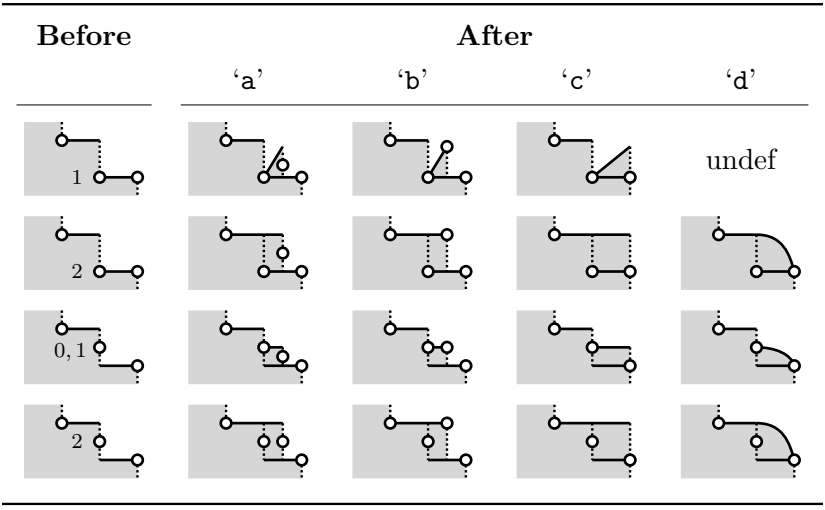

Table 4.11: Constructing the diagram of a spanning cycle.

yields a sequence of $2n$ trapezoids. Based on the types defined above, we then apply the substitution rules (i) $\mapsto$ '`a`', (ii) $\mapsto$ '`b`', (iii) $\mapsto$ '`c`', (iv) $\mapsto$ '`d`' and obtain the desired string.

From letters to trapezoids. Let s be a string of length $2n$ over the alphabet $\{\mathtt{a}, \mathtt{b}, \mathtt{c}, \mathtt{d}\}$ produced by the mapping from the preceding paragraph. This means that there exists a corresponding trapezoidal diagram $D = D_C$ of a spanning cycle C on a set of n points. The reconstruction of D from s can then be done in the usual way by iterating over s and drawing one trapezoid per letter according to the types (i), (ii), (iii), (iv) defined earlier.

All possible cases that only involve bounded trapezoids are illustrated in Table 4.11; all other cases can be dealt with in analogous fashion. Note that the labels 0, 1 and 2 in Table 4.11 indicate the degrees of the respective vertices on the current boundary. The fact

that a vertex may not disappear from the boundary before it has degree two makes the reconstruction unique in all cases. □

4.3 Embeddings of Trapezoidal Diagrams

Fix a diagram D with n vertices and a set P of n points. An *embedding* of D on P is a crossing-free geometric graph G on P with $D_G = D$. Recall from Section 2.2 that for any family of crossing-free geometric graphs, the maximum number of such graphs on any set of n points equals $\overline{\mathrm{nf}}(n) = O^*(u^n)$ for some constant u. If the embedding of D on every P were unique, then Theorems 4.4, 4.5 and 4.7 would imply the improved bounds $u = 5.196$ for perfect matchings, $u = 23.459$ for triangulations and $u = 16$ for spanning cycles. However, since embeddings are not unique in general, a natural follow-up question asks for the maximum number of embeddings. While so far we have not succeeded to obtain adequate upper bounds for these quantities, we can present two simple exponential lower bounds.

4.3.1 Perfect Matchings

As already seen in Figure 4.1, there exists a diagram of a perfect matching with $m = 6$ edges that can be embedded in two different ways on a set of $n = 12$ points. By repeating that construction side by side as illustrated in Figure 4.12, we get the following amplification.

Theorem 4.12. *For any k there exists a planar point set P_k of size $n = 10k + 2$ and a diagram $D \in \mathfrak{D}_n^{\mathsf{pm}}$ with $2^k = \Omega(1.071^n)$ distinct embeddings on P_k.*

Proof. To construct P_k, put k *blocks*, each one consisting of a copy of the point set from Figure 4.1, side by side, but draw the respec-

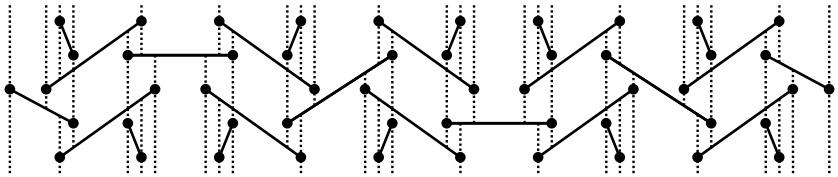

Figure 4.12: A point set where many distinct perfect matchings have the same trapezoidal diagram. Only one of $2^5 = 32$ such perfect matchings is shown.

tive left-most and right-most points only once, as exemplified in Figure 4.12 for $k = 5$. In this way we get ten points per block and two extra points, giving a total of $10k + 2$ points. The diagram D is chosen as a natural extension of the one seen in Figure 4.1. Observe now that for each block we can choose one of two distinct ways of embedding the corresponding part of D. Furthermore, these binary choices can be made independently, implying the desired number of 2^k embeddings. □

4.3.2 Triangulations

For triangulations we present an analogous construction. It is based on the point set depicted in Figure 4.13, which is an adaptation of a point set taken from [11] due to Günter Rote.

Theorem 4.13. *For any k there exists a planar point set P_k of size $n = 12k^2 + 4k + 3$ and a diagram $D \in \mathfrak{D}_n^{\mathsf{tr}}$ with $2^{k^2} = \Omega(1.059^n)$ distinct embeddings on P_k.*

Proof. Define a *block* as a copy of the point set depicted in Figure 4.13. Arrange k^2 such blocks in a honey comb grid, where extreme points of individual blocks may coincide with extreme points of neighboring blocks. Place three additional points such that P_k

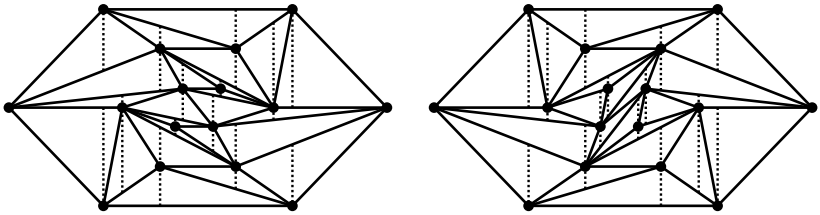

Figure 4.13: A point set and two triangulations which have the same trapezoidal diagram.

has a triangular convex hull. It can be checked that this gives a total of $12k^2 + 4k + 3$ points. The diagram D is chosen accordingly as a honey comb grid consisting of k^2 copies of the diagram depicted in Figure 4.13 and some extra edges for connecting the hull vertices. The desired number of embeddings again follows after observing that we have independent binary choices for embedding individual blocks. □

4.4 Prime Catalan Numbers

In order to make notation less cumbersome when dealing with Catalan numbers of arbitrary dimension, we omit writing the superscripts (d), but we always keep in mind the dependency on d. That is, we write $C_m = C_m^{(d)}$ and $P_m = P_m^{(d)}$. We further define the corresponding ordinary generating functions.

$$C(x) \coloneqq \sum_{m=0}^{\infty} C_m x^m \qquad P(x) \coloneqq \sum_{m=0}^{\infty} P_m x^m \tag{4.4}$$

We shall use a fundamental result of complex function theory called the Lagrange inversion formula. In its classic form, it gives the

Taylor expansion of the inverse of an analytic function at a point where the first derivative does not vanish. In combinatorics, the following formulation is often most useful. [25, Theorem A.2]

Theorem 4.14 (Lagrange Inversion)**.** *Let $A(x) = \sum_{m=0}^{\infty} A_m x^m$ be a formal power series with $A_0 \neq 0$. Define $Z(x) = \frac{x}{A(x)}$. Then, there exists a unique compositional inverse of $Z(x)$; that is, a unique formal power series $X(z) = \sum_{m=0}^{\infty} X_m z^m$ which satisfies $Z(X(z)) = z$. Moreover, the coefficients of $X(z)$ and $X(z)^k$ are as follows.*

$$[z^m]X(z) = \frac{1}{m} \cdot [x^{m-1}]A(x)^m, \quad [z^m]X(z)^k = \frac{k}{m} \cdot [x^{m-k}]A(x)^m$$

We also need a multiplicative variant of Fekete's lemma. For a proof we refer the reader to [67, Lemma 11.6].

Theorem 4.15 (Fekete's Lemma)**.** *Let $A_0, A_1, A_2, \ldots$ be a sequence of non-negative real numbers such that $A_{m+n} \geq A_m A_n$ holds for all m, n. Then, the following limit exists, unless it diverges to infinity.*

$$\lim_{m\to\infty} \sqrt[m]{A_m} = \limsup_{m\to\infty} \sqrt[m]{A_m}$$

We start by proving the following lemma, which establishes a formal relation between $C(x)$ and $P(x)$, and hence between the numbers C_m and P_m.

Lemma 4.16. *For any dimension d, we have that the functional equation $C(x) = P(xC(x)^d)$ holds.*

Proof. Let c be a balanced bracket expression of dimension d. Consider now all inclusion-maximal and contiguous substrings of c which are themselves balanced bracket expressions of dimension d and which start someplace after the first letter of c. Call these substrings $c_1, c_2, \ldots, c_k$ and note that some of them might be empty; see Figure 4.14 for an example for $d = 3$. In fact, by definition, we have $|c_1| = |c_2| = \cdots = |c_k| = 0$ if and only if c is prime.

$$c = \langle\, \langle|\rangle \,|\langle\, \langle|\rangle \,\rangle|\, \langle|\langle|\rangle\rangle \,\rangle\, \langle|\rangle$$

$$\begin{array}{llll} p = \langle|\langle\rangle|\rangle & c_1 = \langle|\rangle & c_2 = \varepsilon & c_3 = \langle|\rangle \\ |p| = 2 & c_4 = \varepsilon & c_5 = \langle|\langle|\rangle\rangle & c_6 = \langle|\rangle \end{array}$$

Figure 4.14: A balanced bracket expression c, and the corresponding factorization consisting of p and $c_1, \ldots, c_6$.

Clearly, for $i \neq j$, c_i and c_j cannot be adjacent in c since they are inclusion-maximal. Nor does c_i contain c_j or vice versa. Nor do they overlap because if that were the case, then both their intersection and their union would be balanced bracket expressions, again contradicting inclusion-maximality.

Therefore, after removing $c_1, \ldots, c_k$ from c, we obtain a balanced bracket expression p that is prime, whose size satisfies $d \cdot |p| = k$, and which yields back c if $c_1, \ldots, c_k$ are plugged back into the k gaps in p in the appropriate order, where we ignore the "gap" before the first letter in p. Loosely speaking, the ordered collection consisting of p and $c_1, \ldots, c_k$ can be seen as a unique factorization of c. Further note that we have $|c| = |p| + |c_1| + \cdots + |c_k|$.

We now have everything that we need. In the following derivation, we let the variables c and $c_1, \ldots, c_k$ run over all balanced bracket expressions of dimension d, and we let the variable p run over all balanced bracket expressions that are prime.

$$\begin{aligned} C(x) &= \sum_{c} x^{|c|} = \sum_{p} \sum_{\substack{c_1,\ldots,c_k \\ k=d\cdot|p|}} x^{|p|+|c_1|+\cdots+|c_k|} \\ &= \sum_{p} x^{|p|} \sum_{\substack{c_1,\ldots,c_k \\ k=d\cdot|p|}} x^{|c_1|+\cdots+|c_k|} = \sum_{p} x^{|p|} C(x)^{d\cdot|p|} = P(xC(x)^d) \end{aligned}$$

□

By combining Lemma 4.16 with the Lagrange inversion formula, we obtain the following efficient method for computing prime Catalan numbers of any dimension.

Lemma 4.17. *For any d, we have* $P_m = \dfrac{1}{1-dm} \cdot [x^m] \dfrac{1}{C(x)^{dm-1}}$.

Proof. Define the following formal power series.

$$A(x) \coloneqq \frac{1}{C(x)^d} \qquad Z(x) \coloneqq \frac{x}{A(x)} = xC(x)^d \tag{4.5}$$

By Theorem 4.14, there is $X(z)$ with $Z(X(z)) = z$. Hence, substituting $X(z)$ for x in Lemma 4.16 yields $C(X(z)) = P(z)$. Observe now that for $m = 0$, the lemma holds trivially because we have $P_0 = C_0 = 1$. For $m > 0$, use the formula from Theorem 4.14 in the fourth step; that is, in the second line of the following derivation.

$$\begin{aligned}
P_m &= [z^m]P(z) = [z^m]C(X(z)) \\
&= \sum_{k=0}^{\infty} C_k \cdot [z^m]X(z)^k = \sum_{k=0}^{\infty} C_k \frac{k}{m} \cdot [x^{m-k}]A(x)^m \\
&= \frac{1}{m} \cdot [x^m]A(x)^m \underbrace{\sum_{k=0}^{\infty} kC_k x^k}_{=xC'(x)} \\
&= \frac{1}{m} \cdot [x^{m-1}] \frac{C'(x)}{C(x)^{dm}} = \frac{1}{m} \cdot [x^{m-1}] \left(\frac{1}{1-dm} \frac{1}{C(x)^{dm-1}} \right)' \\
&= \frac{1}{1-dm} \cdot [x^m] \frac{1}{C(x)^{dm-1}}
\end{aligned}$$

□

Recall from the introduction that for $d = 2$, the prime Catalan numbers do not give us a particularly exciting sequence. For higher dimensions the situation is very different, as shown by the next lemma.

Lemma 4.18. *For any dimension $d \geq 3$, the prime Catalan numbers are super-multiplicative; that is, $P_{m+n} \geq P_m P_n$ holds for all m and n.*

Proof. Let us fix m and n. Consider the two sets of sizes P_m and P_n containing all prime balanced bracket expressions of size m and n, respectively. By combining each pair of such expressions in a certain way, we shall show how to obtain $P_m P_n$ distinct prime balanced bracket expressions of size $m + n$.

Let now p_m and p_n be two arbitrary prime balanced bracket expressions of respective sizes m and n. We may assume that m and n are both non-zero. In that case, however, the two expressions must be of the form $p_m = p'_m\rangle$ and $p_n = \langle p'_n$, where p'_m and p'_n are the prefix and postfix, respectively, of p_n and p_m, containing all but one letter. For the purpose of this proof, we use the brackets $b_1 = \text{`}\langle\text{'}$ and $b_d = \text{`}\rangle\text{'}$, while leaving the remaining $d-2$ brackets unspecified. The expression corresponding to the pair (p_m, p_n) can now be defined as $p = p'_m\langle\rangle p'_n$. Clearly, in this way we obtain $P_m P_n$ distinct balanced bracket expressions of size $m + n$. It only remains to show that p is also prime.

Consider thus a substring c of p that is a balanced bracket expression of dimension d. Since by assumption p_m and p_n do not contain any such substrings, c must run over the central "$\langle\rangle$" between p'_m and p'_n in p. Fittingly, we write $c = c'_m\langle\rangle c'_n$, where c'_m and c'_n are a postfix and prefix, respectively, of p'_m and p'_n. Furthermore, let us consider the expressions $c_m = c'_m\rangle$ and $c_n = \langle c'_n$. The fact that c'_m and c_m are, respectively, a prefix and a postfix of a balanced bracket expression implies that c_m is a balanced bracket expression. By a symmetric argument, c_n is also a balanced bracket expression. Since p_m and p_n are prime, it follows that $c_m = p_m$ and $c_n = p_n$, and thus $c = p$. Since we have shown that an arbitrary subexpression c of p is equal to p, we can conclude that p is prime, indeed. □

Theorem 4.1 from the introduction is a consequence of Lemma 4.18, Theorem 4.15, and the fact that the radius of convergence of the formal power series $P(x)$ is equal to $1/\gamma_d$. The latter is not hard to prove by using Lemma 4.16 and by using that the radius of convergence of $C(x)$ is equal to $1/d^d$.

Theorem 4.1 (restated)**.** *For any dimension $d \geq 3$, the prime Catalan numbers exhibit the following limit behavior.*

$$\lim_{m\to\infty} \sqrt[m]{P_m} = \gamma_d \coloneqq \left(\frac{d}{C(1/d^d)}\right)^d$$

Proof. For any fixed dimension $d \geq 3$, let us write R_C and R_P in order to denote the radii of convergence of the power series $C(x)$ and $P(y)$, respectively. From the hook-length formula and Stirlings's approximation—see equations (4.1) and (4.2) for the 3-dimensional case—we get the following asymptotic estimate for C_m as m tends to infinity.

$$C_m = \Theta\left(m^{-(d^2-1)/2} d^{dm}\right) \tag{4.6}$$

Hence, we also obtain the corresponding radius of convergence R_C by elementary analysis.

$$R_C = 1/d^d \tag{4.7}$$

From equations (4.6) and (4.7) we shall deduce that $R_P = 1/\gamma_d$ holds. This will conclude the proof of the theorem because of Lemma 4.18 and Theorem 4.15.

Firstly, we show that $R_P \geq 1/\gamma_d$. Note that for positive $x < R_C$, the function $C(x)$ is continuous and strictly increasing, since all coefficients are positive. It follows that for every positive $y < 1/\gamma_d = R_C C(R_C)^d$ there exists a unique positive $x < R_C$ with $y = xC(x)^d$ and hence, by using Lemma 4.16, we obtain the following.

$$P(y) = P(xC(x)^d) = C(x) < \infty \tag{4.8}$$

Secondly, we show that $R_P \leq 1/\gamma_d$. Since the radius of convergence does not change under differentiation, it is sufficient to prove that the formal derivative of $P(y)$ of a certain order diverges at the point $y = 1/\gamma_d$. For that, we shall use the following elementary observations.

- The k-th derivative $C^{(k)}(R_C)$ remains convergent for $k < \frac{d^2-1}{2} - 1$, but diverges for all $k \geq \frac{d^2-1}{2} - 1$. This follows from (4.6) by a comparison with hyperharmonic series.
- We have $C^{(k)}(x) > 0$ for any $k \geq 0$ and all positive $x \leq R_C$, simply because all coefficients of $C(x)$ are positive.

Let now $F(x) = xC(x)^d$ and consider the first and k-th derivative of this formal power series.

$$F'(x) = dxC(x)^{d-1}C'(x) + C(x)^d \tag{4.9}$$

$$F^{(k)}(x) = dxC(x)^{d-1}C^{(k)}(x) + \dots \tag{4.10}$$

Note that in (4.10) we have omitted all the additive terms that contain only lower-order derivatives of $C(x)$.

Starting from the equality given by Lemma 4.16, we similarly get the following derivatives.

$$P'(F(x)) = \frac{C'(x)}{F'(x)} \tag{4.11}$$

$$P^{(k)}(F(x)) = \frac{C^{(k)}(x)}{F'(x)^k} - \frac{F^{(k)}(x)C'(x)}{F'(x)^{k+1}} + \dots \tag{4.12}$$

Similar to before, we have omitted all the additive terms that contain only lower-order derivatives of $C(x)$ and $F(x)$. By combining (4.12)

with (4.9) and (4.10) we now obtain the following equations.

$$\begin{aligned} P^{(k)}(F(x)) &= \frac{C^{(k)}(x)}{F'(x)^k}\left(1 - \frac{dxC(x)^{d-1}C'(x)}{F'(x)}\right) + \dots \\ &= C^{(k)}(x) \cdot \frac{C(x)^d}{F'(x)^{k+1}} + \dots \end{aligned} \tag{4.13}$$

Using our two observations from earlier, for $k = \lceil \frac{d^2-1}{2} - 1 \rceil \geq 2$, as x approaches R_C from below, the right hand side of equation (4.13) diverges because $C^{(k)}(x)$ tends to infinity and because all omitted additive terms are bounded. □

As expected, the argument in the proof of Theorem 4.1 breaks down for the case $d = 2$. Indeed, for $d = 2$ we get $k = \lceil \frac{d^2-1}{2} - 1 \rceil = 1$, which means $F'(x)$ is no longer bounded and we cannot conclude that the right hand side of (4.13) tends to infinity. In fact, it is clear that it does not diverge since we have $P(y) = 1 + y$ and $P'(y) = 1$ for the case $d = 2$.

4.5 Experiments

In Tables 4.15 to 4.17 we present some experimental evidence for the asymptotic growth rate of the prime Catalan numbers.

For the case $d = 3$ the corresponding approximations are defined as follows.

$$\tilde{C}_m^{(3)} := m^{-4}3^{3m} \qquad \tilde{P}_m^{(3)} := m^{-4}\gamma_3^m \qquad \gamma_3 = \frac{27}{(\frac{729\sqrt{3}}{40\pi} - 9)^3}$$

In our data we see that the ratio $C_m^{(3)}/\tilde{C}_m^{(3)}$ approaches $\frac{\sqrt{3}}{\pi} \approx 0.551$ as m tends to infinity, as can also be proved with Stirling's approximation. Also the ratio $P_m^{(3)}/\tilde{P}_m^{(3)}$ seems to converge; but neither

can we prove that it converges, nor do we have a guess for the exact value of that limit. Nevertheless, the data suggests quite clearly that the approximation $\tilde{P}_m^{(3)}$ has the right order of growth.

Similarly, for the cases $d = 4, 5$ we define the following approximations.

$$\begin{aligned} \tilde{C}_m^{(4)} &:= m^{-7.5} 4^{4m} & \tilde{P}_m^{(4)} &:= m^{-7.5} \gamma_4^m & \gamma_4 &\approx 251.788 \\ \tilde{C}_m^{(5)} &:= m^{-12} 5^{5m} & \tilde{P}_m^{(5)} &:= m^{-12} \gamma_5^m & \gamma_5 &\approx 3119.934 \end{aligned}$$

Also here the data suggests that the approximations $\tilde{P}_m^{(4)}$ and $\tilde{P}_m^{(5)}$ have the right order of growth.

m	$C_m^{(3)}$	$\tilde{C}_m^{(3)}$	$C_m^{(3)}/\tilde{C}_m^{(3)}$	$P_m^{(3)}$	$\tilde{P}_m^{(3)}$	$P_m^{(3)}/\tilde{P}_m^{(3)}$
1	1.00000e+00000	2.70000e+00001	0.03703	1.00000e+00000	2.34594e+00001	0.04262
2	5.00000e+00000	4.55625e+00001	0.10973	2.00000e+00000	3.43966e+00001	0.05814
4	4.62000e+00002	2.07594e+00003	0.22254	1.07000e+00002	1.18313e+00003	0.09043
8	2.33716e+00007	6.89525e+00007	0.33895	3.00297e+00006	2.23968e+00007	0.13408
16	5.21086e+00017	1.21713e+00018	0.42812	2.30416e+00016	1.28414e+00017	0.17943
32	2.94021e+00039	6.06792e+00039	0.48454	1.46103e+00037	6.75438e+00037	0.21630
64	1.24633e+00084	2.41302e+00084	0.51650	7.19612e+00079	2.98986e+00080	0.24068
128	3.25751e+00174	6.10550e+00174	0.53353	2.38674e+00166	9.37353e+00166	0.25462
256	3.39180e+00356	6.25408e+00356	0.54233	3.86180e+00340	1.47410e+00341	0.26197
512	5.74118e+00721	1.04994e+00722	0.54680	1.54989e+00690	5.83302e+00690	0.26571
1024	2.59965e+01453	4.73472e+01453	0.54906	3.91023e+01390	1.46132e+01391	0.26758
2048	8.47588e+02917	1.54052e+02918	0.55019	3.94041e+02792	1.46749e+02793	0.26851
4096	1.43714e+05848	2.60938e+05848	0.55076	6.36897e+05597	2.36783e+05598	0.26897
8192	6.60059e+11709	1.19783e+11710	0.55104	2.65530e+11209	9.86334e+11209	0.26920
16384	2.22603e+23434	4.03861e+23434	0.55118	7.37501e+22433	2.73834e+22434	0.26932

Table 4.15: Experimental data for 3-dimensional (prime) Catalan numbers.

m	$C_m^{(4)}$	$\tilde{C}_m^{(4)}$	$C_m^{(4)}/\tilde{C}_m^{(4)}$	$P_m^{(4)}$	$\tilde{P}_m^{(4)}$	$P_m^{(4)}/\tilde{P}_m^{(4)}$
1	1.00000e+0000	2.56000e+0002	0.00390	1.00000e+0000	2.51788e+0002	0.00397
2	1.40000e+0001	3.62038e+0002	0.03866	1.00000e+0001	3.50225e+0002	0.02855
4	2.40240e+0004	1.31072e+0005	0.18328	1.67640e+0004	1.22657e+0005	0.13667
8	1.48987e+0012	3.10988e+0012	0.47907	1.05311e+0012	2.72342e+0012	0.38668
16	2.62708e+0029	3.16912e+0029	0.82896	1.70499e+0029	2.43041e+0029	0.70152
32	6.63875e+0065	5.95736e+0065	1.11437	3.36922e+0065	3.50378e+0065	0.96159
64	4.95456e+0140	3.81072e+0140	1.30016	1.49107e+0140	1.31817e+0140	1.13116
128	3.97058e+0292	2.82254e+0292	1.40674	4.14916e+0291	3.37732e+0291	1.22853
256	4.10340e+0598	2.80305e+0598	1.46390	5.14015e+0596	4.01325e+0596	1.28079
512	7.47391e+1212	5.00423e+1212	1.49351	1.34163e+1209	1.02581e+1209	1.30788
1024	4.35558e+2443	2.88718e+2443	1.50859	1.60345e+2436	1.21320e+2436	1.32167
2048	2.63772e+4907	1.73969e+4907	1.51619	4.08128e+4892	3.07180e+4892	1.32862

Table 4.16: Experimental data for 4-dimensional (prime) Catalan numbers.

m	$C_m^{(5)}$	$\tilde{C}_m^{(5)}$	$C_m^{(5)}/\tilde{C}_m^{(5)}$	$P_m^{(5)}$	$\tilde{P}_m^{(5)}$	$P_m^{(5)}/\tilde{P}_m^{(5)}$
1	1.00000e+0000	3.12500e+0003	0.00032	1.00000e+0000	3.11993e+0003	0.00032
2	4.20000e+0001	2.38418e+0003	0.01761	3.70000e+0001	2.37646e+0003	0.01556
4	1.66280e+0006	5.68434e+0006	0.29252	1.53347e+0006	5.64757e+0006	0.27152
8	2.31471e+0017	1.32348e+0017	1.74895	2.19820e+0017	1.30642e+0017	1.68261
16	1.46174e+0042	2.93873e+0041	4.97406	1.38606e+0042	2.86343e+0041	4.84055
32	5.23671e+0094	5.93472e+0093	8.82384	4.85822e+0094	5.63449e+0093	8.62228
64	1.18277e+0203	9.91383e+0201	11.93052	1.04361e+0203	8.93612e+0201	11.67859
128	1.57847e+0423	1.13313e+0422	13.93012	1.25644e+0423	9.20658e+0421	13.64719
256	9.13693e+0866	6.06353e+0865	15.06864	5.91142e+0866	4.00273e+0865	14.76846
512	1.11487e+1758	7.11166e+1756	15.67671	4.76248e+1757	3.09908e+1756	15.36741
1024	6.40765e+3543	4.00703e+3542	15.99101	1.19291e+3543	7.60931e+3541	15.67703
2048	8.41548e+7118	5.21056e+7117	16.15081	2.97532e+7117	1.87901e+7116	15.83445

Table 4.17: Experimental data for 5-dimensional (prime) Catalan numbers.

CHAPTER 5

Explicit Formulas for Wheel Sets

5.1 Introduction

Let $P = H \cup \{w\}$ be a set of $n+1$ points in the plane. Unless stated otherwise, P is assumed to be in general position and the points in H are assumed to be extreme; that is, part of the boundary of the convex hull of P. We say that P is a *wheel set* if all points except w are extreme and, as usual, we say that P is in *convex position* if all points including w are extreme. In any case, if P is either a wheel set or in convex position, then we call P a *conowheel set*. Moreover, we call w the *extra point* of the conowheel set P.

Recall from Section 2.1 that P_{con} denotes a point set in convex position and that P_{sym} denotes a symmetric wheel set. In addition,

we write P_{bar} to denote a *barely-in* wheel set; that is, H is the vertex set of a regular n-gon and the extra point w is sufficiently close to an edge e of that n-gon so that w is contained in the interior of every triangle spanned by e and a third point of H.

Order types. The *order type* of a point set P is a combinatorial description that assigns an orientation—either clockwise or counterclockwise—to every ordered triple of points in P. [29] Two point sets are said to have the same order type if there exists a bijection between the sets that preserves these orientations. We follow the practice of also considering two point sets to have the same order type if there exists a bijection that reverses all orientations.

Many combinatorial properties of a point set can be recovered from its order type. In particular, the order type determines whether two segments with endpoints in P cross, and whether a given point in P is extreme. Moreover, it can be observed that all point sets in convex position have the same order type. However, the following theorem shows that the same is not true for wheel sets.

Theorem 5.1. *The number of distinct order types of conowheel sets of size $n+1$ is given by the following formula.*

$$\frac{1}{4n}\sum_{2\nmid k\mid n}\varphi(k)2^{n/k}+2^{\lfloor(n-3)/2\rfloor}=\Theta(2^n/n)$$

Note that $\varphi(k)$ denotes Euler's totient function, which counts the integers coprime to k that are at most k. The above formula has been obtained first by Perles—as stated, without proof, in [32, Chapter 6.3]—for the number of simplicial polytopes with few vertices; we explain the connection to wheel sets in Section 5.4. Perles also counts so-called distended standard forms of Gale diagrams, which basically correspond to wheel sets with different order types; in Section 5.2 we describe this correspondence.

Frequency vectors. While the order type of P determines the set of crossing-free geometric graphs on P, we show in Section 5.3 that we can rely on the following coarser classification when only considering conowheel sets.

Let $P = H \cup \{w\}$ be a conowheel set and let $h \in H$ be arbitrary. Let $\mathsf{l}(h)$ denote the number of points strictly to the left of the directed line going from w to h, and let $\mathsf{r}(h)$ denote the number of points strictly to the right of that line. The *frequency vector* of P is the vector $F(P) = (F_0, F_1, \ldots, F_{n-1})$ where F_i denotes the number of points $h \in H$ that satisfy $|\,\mathsf{l}(h) - \mathsf{r}(h)| = i$. Consider the following extreme examples for the case $n = 7$.

$$F(P_{\mathsf{con}}) = (1, 0, 2, 0, 2, 0, 2) \tag{5.1}$$

$$F(P_{\mathsf{bar}}) = (1, 0, 2, 0, 4, 0, 0) \tag{5.2}$$

$$F(P_{\mathsf{sym}}) = (7, 0, 0, 0, 0, 0, 0) \tag{5.3}$$

Note that the frequency vector of P can be computed in $O(n \log n)$ time by radially sorting H around w. It is also clear that the order type of P determines the frequency vector $F(P)$. However, the opposite is not true. In Section 5.2 we give a characterization of frequency vectors, which allows us to conclude the following.

Theorem 5.2. *For any $n \geq 1$, the number of frequency vectors realizable by a conowheel set over $n + 1$ points is exactly $2^{\lceil n/2 \rceil - 1}$.*

Given that the number of frequency vectors is significantly smaller than the number of order types, it is a priori unclear how much the frequency vector reveals about a conowheel set. However, we show that for the purpose of counting crossing-free geometric graphs, it is both sufficient and necessary.

There is again a connection to simplicial polytopes with few vertices; in Section 5.4 we see that the number of frequency vectors is equal to the number of f-vectors of polytopes in d-space with at most

$d+3$ vertices including the empty polytope. The latter has been calculated by Linusson using a sophisticated counting of so-called M-sequences. [42]

Geometric graphs. Let $\mathfrak{G}$ be a set of abstract unlabeled graphs, each with $n+1$ vertices. Further let $\mathrm{nf}_{\mathfrak{G}}(P)$ denote the number of crossing-free geometric graphs on P that are isomorphic to a graph in the set $\mathfrak{G}$. For example, if $\mathfrak{M}$ denotes the set that contains all abstract matchings over $n+1$ vertices, then we have $\mathrm{nf}_{\mathfrak{M}}(P) = \mathrm{ma}(P)$.

Theorem 5.3. *Let $\mathfrak{G}$ be arbitrary, and let $P = H \cup \{w\}$ be a conowheel set of size $n+1$. Then, as follows, the number $\mathrm{nf}_{\mathfrak{G}}(P)$ depends only on the frequency vector $F(P) = (F_0, F_1, \ldots, F_{n-1})$.*

$$\mathrm{nf}_{\mathfrak{G}}(P) = \gamma_n - \frac{1}{2}\sum_{h\in H} \lambda_{\mathsf{l}(h),\mathsf{r}(h)} = \sum_{k=0}^{n-1} F_k \Lambda_k$$

In the formula above, γ_n and $\lambda_{l,r} = \lambda_{r,l}$ are integers and Λ_k are rationals that depend on the set $\mathfrak{G}$.

While the latter formula in the above theorem makes the dependency on the frequency vector more obvious, the former turns out to be more natural. The latter follows from the former simply by putting $\Lambda_k = \gamma_n/n + 1/2 \cdot \lambda_{(n+k-1)/2,(n-k-1)/2}$.

We give just one example here, which at the same time makes the connection to the later parts of the chapter. We consider the case $\mathfrak{G} = \{K_4^{\cdots}\}$, where $K_4^{\cdots}$ is obtained by adding $n-3$ additional isolated vertices to the complete graph K_4. The following formula is obtained alongside Theorem 5.3 in Section 5.3.

$$\mathrm{nf}_{\{K_4^{\cdots}\}}(P) = \binom{n}{3} - \frac{1}{2}\sum_{h\in H}\left(\binom{\mathsf{l}(h)}{2} + \binom{\mathsf{r}(h)}{2}\right) \tag{5.4}$$

Let us consider a crossing-free geometric graph on a conowheel set $P = H \cup \{w\}$ that is isomorphic to $K_4^{\cdot\cdot}$. We observe that one of the vertices of the underlying K_4 is the extra point w, while the other three vertices form a triangle that contains w in its interior. Indeed, if all four vertices of K_4 belong to H, then there necessarily is a pair of crossing edges since H is in convex position. With (5.4) we thus have a rather simple formula for the number of *w-embracing triangles*; that is, point triples in H whose convex hull contains w.

Also note that the set of w-embracing triangles does not change if we replace a point $h \in H$ by a point h' somewhere on the ray that starts at w and passes through h. The formula in (5.4) thus generalizes and can be used to count w-embracing triangles on arbitrary point sets P. We note that the algorithm which counts w-embracing triangles in [54] is essentially an implementation of equation (5.4).

Higher dimensions. The concept of a conowheel set can be generalized to arbitrary dimension, where we may again consider sets with at most one non-extreme point. However, even for counting w-embracing tetrahedra in 3-space, the ideas from the proof of Theorem 5.3 do not generalize. Nevertheless, in Section 5.4 we give a generalization of equation (5.4). From that we obtain improved time bounds for computing the *simplicial depth* of a query point w in a set H; that is, the number of w-embracing simplices spanned by points in H, as defined in [43].

Theorem 5.4. *Let $d \geq 3$ be fixed and let H be a set of n points in $\mathbb{R}^d$. Then, the simplicial depth of a point w in H can be computed in $O(n^{d-1})$ time.*

Again, this result is stated for arbitrary sets H and not for conowheel sets only; as far as the simplicial depth is concerned, only the position relative to w is relevant. The algorithm further generalizes to counting all k-element subsets of H whose convex hull contains w.

The simplicial depth of a point has attracted considerable attention as a measure of data depth. Several authors describe how to compute the simplicial depth in the plane. [28, 39, 54] Algorithms that run in time $O(n^2)$ and $O(n^4)$ for $d = 3$ and $d = 4$, respectively, are provided by Cheng and Ouyang, who also point out flaws in previous algorithms. [19] Our result improves over the previously best reported general $O(n^d \log n)$ time algorithm for points in constant dimension d. [1] For arbitrary dimension, the problem can be shown to be $\#\mathcal{P}$-complete and $W[1]$-hard. [1]

Via the Gale dual, the number of facets of a simplicial polytope corresponds to the number of origin-embracing simplices in a dual point set. In Section 5.4 we show how to compute the number of facets of the convex hull of $d + k$ points in general position in $\mathbb{R}^d$ in time $O(n^{\max\{\omega, k-2\}})$, where ω is the exponent for matrix multiplication.

5.2 Combinatorial Descriptions

The purpose of this section is to give an explanation for Table 5.1, which contains the numbers of distinct order types and frequency vectors corresponding to conowheel sets of size $n + 1$. For the sake of completeness, we have also included the respective numbers if equivalence over order types is defined in such a way that reflected order types are considered distinct.

5.2.1 Order Types

Given a set H of $n = 7$ points forming the vertex set of a regular heptagon, it can be seen that there are 8 conowheel sets $P = H \cup \{w\}$ with distinct order types that can be obtained by adding an extra point w. Notice the discrepancy with the number 9 displayed in the seventh row of Table 5.1. In order to obtain the ninth and last

$n = \lvert H \rvert$	**Order Types**		**Frequency Vectors**
	with reflection	without reflection	
1	1	1	1
2	1	1	1
3	2	2	2
4	2	2	2
5	4	4	4
6	5	6	4
7	9	10	8
8	12	16	8
9	23	30	16
10	34	52	16
11	63	94	32
12	102	172	32
13	190	316	64
14	325	586	64

Table 5.1: Number of distinct order types and frequency vectors of conowheel sets over $n + 1$ points.

order type, one first has to deform the point set H before adding w. This necessary deformation of H seems to complicate matters significantly, but only at first sight.

The formula given in Theorem 5.1 for the number of distinct order types of conowheel sets is also known from the context of counting 2-colored *self-dual necklaces* with $2n$ beads and mirrored necklaces identified. [15, 49] These are binary—say, black and white—circular sequences of length $2n$ such that elements at distance n are distinct; meaning that if one bead is black, then the bead on the opposite side must be white, and vice versa.

We give a proof of Theorem 5.1 by using a simple bijection to such necklaces. Also note that the asymptotic estimate is explained by taking the dominant summand with $k = 1$.

Theorem 5.1 (restated)**.** *The number of distinct order types of conowheel sets of size $n + 1$ is given by the following formula.*

$$\frac{1}{4n} \sum_{2 \nmid k \mid n} \varphi(k) 2^{n/k} + 2^{\lfloor (n-3)/2 \rfloor} = \Theta(2^n/n)$$

Proof. Let $P = H \cup \{w\}$ be a conowheel set. Consider a directed line s through w that rotates counterclockwise around w by an angle of 2π. The line passes over each point in H twice, once on the positive ray and once on the negative ray. We record the sequence in which the points $h \in H$ are passed, and indicate for each entry whether the corresponding point h is on the positive or negative ray of the line s. The obtained sequence can be considered cyclic and is known as the local sequence of w. [30] It only depends on the order type of P and it naturally corresponds to a self-dual necklace with $2n$ beads and two colors; in this case, positive and negative.

The defined mapping is seen to be a bijection by considering its inverse. Given a necklace, we can transform it into an order type by placing w at the center of a regular $2n$-gon, by identifying the beads of the necklace with the vertices of the $2n$-gon in circular order, and then by placing a point h on each vertex that corresponds to a positive bead. By construction, the resulting point set $P = H \cup \{w\}$ is a conowheel set. □

We note that a similar and slightly simpler formula is known if mirrored necklaces are not identified. Naturally, such a formula then also counts order types of conowheel sets without reflection.

5.2.2 Frequency Vectors

The following lemma gives a succinct characterization of frequency vectors. The proof is again by letting a line rotate around the extra point w, and by observing how it dissects the point set H during the process. More details can be found in [55].

Lemma 5.5. *A vector $F = (F_0, F_1, \ldots, F_{n-1}) \in \mathbb{N}^n$ is the frequency vector of a conowheel set $P = H \cup \{w\}$ of size $n+1$ if and only if the following properties hold.*

(i) We have $\sum_{k=0}^{n-1} F_k = n$.

(ii) We have $F_k = 0$ for all $k \equiv_2 n$.

(iii) We have that F_k is even for all $k \geq 1$.

(iv) If $F_k \neq 0$ and $k \geq 2$, then $F_{k-2} \neq 0$.

Proof. Let us first prove necessity. From the definition of frequency vectors, (i) and (ii) are immediate. As for (iii) and (iv), let us consider the sequence $s_1, s_2, \ldots, s_n$ of lines that pass through w and one of the n points of H. Suppose further that $s_1, s_2, \ldots, s_n$ are given in radial counterclockwise order around w. Define $n+1$ additional lines $s_{i+1/2}$ that are in between the lines s_i and s_{i+1} in the counterclockwise order. More precisely, $s_{i+1/2}$ may be any of the intermediate lines that are encountered when transforming s_i into s_{i+1} by a counterclockwise rotation around w. Finally, give all lines $s_{1/2}, s_1, s_{1+1/2}, \ldots, s_n, s_{n+1/2}$ a direction by orienting $s_{1/2}$ arbitrarily and then rotating counterclockwise around w by an angle π.

Now, let $\mathsf{l}(s)$ and $\mathsf{r}(s)$ denote the number of points of H strictly to the left and right, respectively, of a directed line s, and let $g(s) = \mathsf{l}(s) - \mathsf{r}(s)$. For any integer i, observe that $g(s_i)$ is the average of $g(s_{i-1/2})$ and $g(s_{i+1/2})$. Moreover, the sequence $\gamma = g(s_{1/2}), g(s_{1+1/2}), \ldots, g(s_{n+1/2})$ is continuous in the sense that any two subsequent elements differ by exactly 2, and cyclic in the sense

that $g(s_{1/2}) = -g(s_{n+1/2})$. Property (iii) now follows because for any integer $k \geq 1$ with $k \not\equiv_2 n$, the sequence γ jumps over $+k$ and $-k$ an even number of times. Note that the same is not true for $k = 0$ if n is odd, as the number of times that γ jumps over 0 is also odd. Property (iv) follows by continuity and because γ jumps over 0 or ± 1 at least once.

As for the other direction, let us fix a vector $F = (F_0, F_1, \ldots, F_{n-1})$ satisfying (i)–(iv), and let us show how to realize it by a conowheel set $P = H \cup \{w\}$ of size $n + 1$. We start by drawing a circle with w at its center, and n distinct lines $s_1, \ldots, s_n$ passing through w in counterclockwise order. We consider the lines directed in such a way that $s_2, \ldots, s_n$ point into the half-space to the left of s_1. As described below, for each line s_i we place one additional point h on one of the two intersections of s_i and the fixed circle around w. We refer to these two possible locations as the *back* and *front* of s_i, so that s_i is directed from the back to the front.

Let $k_{\mathsf{max}} \geq 0$ be the largest integer that satisfies $F_{k_{\mathsf{max}}} \neq 0$. We construct a sequence γ of length $n+1$ which starts with $-(k_{\mathsf{max}}+1)$, which ends with $(k_{\mathsf{max}} + 1)$, in which any two subsequent elements differ by exactly 2, and such that the number of times we jump over a non-negative integer k or its inverse $-k$ is equal to F_k. It is easy to construct such a sequence γ given that (i)–(iv) hold. Indeed, for even n, say, we start with $-(k_{\mathsf{max}} + 1), -(k_{\mathsf{max}} + 1) + 2, \ldots, 0$ and then, for each integer $k = 1, 3, \ldots, k_{\mathsf{max}}$, we jump back and forth over k exactly $F_k - 1$ times. As for the placement of H, if the i-th jump in γ is increasing, then we place a point h at the back of s_i; otherwise, we place h at the front of s_i.

It is clear that the resulting set $P = H \cup \{w\}$ is a conowheel set of size $n + 1$. Moreover, note that γ can be recovered when given only P and the sequence $s_1, \ldots, s_n$, simply by constructing the sequence $g(s_{1/2}), g(s_{1+1/2}), \ldots, g(s_{n+1/2})$ as in the first part of the proof. It follows that P has frequency vector F. □

With this characterization, it is not hard to determine the number of frequency vectors.

Theorem 5.2 (restated)**.** *For any $n \geq 1$, the number of frequency vectors realizable by a conowheel set over $n+1$ points is exactly $2^{\lceil n/2 \rceil - 1}$.*

Proof. For $n = 1$ and $n = 2$ the formula evaluates to 1, which is consistent with the fact that there is only one respective order type for either two or three points. For larger n, we give a proof by induction for odd n, and note that even n can be handled analogously.

So let $n = m+2 \geq 3$ be odd. Using Lemma 5.5, we can characterize the set of frequency vectors that are realizable by $n+1$ points by saying that it contains all vectors $F = (F_0, F_1, \ldots, F_{n-1})$ which have one of the following two mutually exclusive forms.

- $F_0 = 1$, $F_1 = 0$, and $(F_2 - 1, F_3, F_4, \ldots, F_{n-1})$ is any frequency vector realizable by $m+1$ points.
- $F_0 \geq 3$ is odd, $F_{n-2} = F_{n-1} = 0$, and $(F_0 - 2, F_1, F_2, \ldots, F_{n-3})$ is any frequency vector realizable by $m+1$ points.

Therefore, if $2^{\lceil m/2 \rceil - 1}$ is the number of frequency vectors realizable by $m+1$ points, then the corresponding number for $n+1$ points is exactly $2 \cdot 2^{\lceil m/2 \rceil - 1} = 2^{\lceil n/2 \rceil - 1}$. □

5.3 Geometric Graphs

5.3.1 Proof of the Main Theorem

Recall that $\mathrm{nf}_{\mathfrak{G}}(P)$ is the number of crossing-free geometric graphs on P that are isomorphic to a graph in the set $\mathfrak{G}$. Consider now two conowheel sets $P = H \cup \{w\}$ and $P' = H \cup \{w'\}$ which can be transformed into each other by moving the extra point w over the

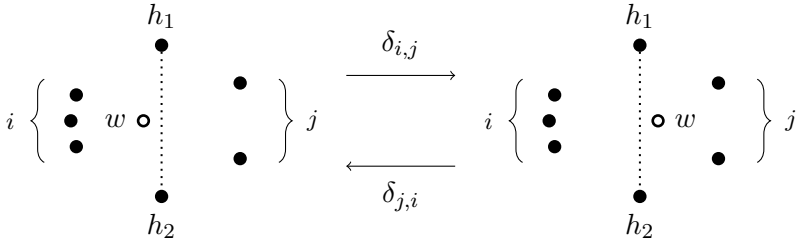

Figure 5.2: Moving the extra point w, drawn in white, over the segment h_1h_2 for the case $i = 3$ and $j = 2$.

segment between two points $h_1, h_2 \in H$, and without encountering any other collinearities in the process. The situation is illustrated in Figure 5.2. Assume that on the w-side of the segment h_1h_2 there are i points of H, and on the w'-side there are j points of H; hence, we have $i + j = n - 2$. Let $\delta_{i,j}$ be the increment of $\mathrm{nf}_{\mathfrak{G}}$ when going from P to P'; that is, $\delta_{i,j} \coloneqq \mathrm{nf}_{\mathfrak{G}}(P') - \mathrm{nf}_{\mathfrak{G}}(P)$.

Lemma 5.6. *For every $\mathfrak{G}$, $\delta_{i,j}$ is well-defined; that is, its value depends only on i, j and $\mathfrak{G}$, but not on the exact placement of H or the location where the extra point w traverses the segment between h_1 and h_2.*

Proof. All geometric graphs that do not contain the edge $\{h_1, h_2\}$ are not affected by the mutation; that is, they are crossing-free on P if and only if they are crossing-free on P'. Therefore, $\delta_{i,j}$ is equal to the number of crossing-free geometric graphs (isomorphic to a graph in $\mathfrak{G}$) on P' containing $\{h_1, h_2\}$ minus the number of crossing-free geometric graphs on P containing $\{h_1, h_2\}$. For the following reasons, these numbers only depend on i, j and $\mathfrak{G}$.

In the case of P, on the w-side we have $i + 3$ points including h_1 and h_2 in a barely-in configuration, for which there exists a unique order type. On the opposite side we have $j + 2$ points including h_1

and h_2 in convex position, for which there also exists a unique order type. Because of the presence of the edge $\{h_1, h_2\}$ any other edges must be completely contained in one of the two sides, and the claim follows. In the case of P', an analogous argument works. □

Example, embracing triangles. Consider the case $\mathfrak{G} = \{K_4^{\cdots}\}$, as already discussed in the introduction. Recall that any crossing-free embedding of $K_4^{\cdots}$ on P uses w as the inner vertex of the underlying K_4. Furthermore, if the embedding uses the edge $\{h_1, h_2\}$, which implies that h_1 and h_2 are outer vertices of the K_4, then any one of the i points on the left hand side can be used as the third outer vertex of K_4. This gives i crossing-free embeddings of $K_4^{\cdots}$ on P that use the edge $\{h_1, h_2\}$. Similarly, we get j for the corresponding number on P'. Therefore, $\delta_{i,j} = j - i$ for $\mathfrak{G} = \{K_4^{\cdots}\}$.

Having Lemma 5.6 at our disposal, we are now ready to prove our main theorem.

Theorem 5.3 (restated)**.** *Let $\mathfrak{G}$ be arbitrary, and let $P = H \cup \{w\}$ be a conowheel set of size $n+1$. Then, as follows, the number $\mathrm{nf}_{\mathfrak{G}}(P)$ depends only on the frequency vector $F(P) = (F_0, F_1, \ldots, F_{n-1})$.*

$$\mathrm{nf}_{\mathfrak{G}}(P) = \gamma_n - \frac{1}{2} \sum_{h \in H} \lambda_{\mathrm{l}(h),\mathrm{r}(h)} = \sum_{k=0}^{n-1} F_k \Lambda_k$$

In the formula above, γ_n and $\lambda_{l,r} = \lambda_{r,l}$ are integers and Λ_k are rationals that depend on the set $\mathfrak{G}$.

Proof. We proceed by choosing the numbers $\lambda_{l,r}$ such that the validity of the formula is preserved under continuous motion of P, and then choose γ_n such that it holds for some arbitrary starting configuration. To be more concrete, we allow continuous motion of P where all points are allowed to move if P is in convex position, and only w is allowed to move if P is a wheel set. At discrete moments in time we allow collinearity of three points, the one in the

middle being w. Note that in this way, any two conowheel sets can be transformed into each other.

Let now P and P' be as in Figure 5.2. Note that the values $\mathsf{l}(h)$ and $\mathsf{r}(h)$ do not change for any $h \in H \setminus \{h_1, h_2\}$ when going from P to P'. For h_1 and h_2 the corresponding values are as follows.

$$\begin{array}{lll} P: & \mathsf{l}(h_1) = \mathsf{r}(h_2) = i & \mathsf{r}(h_1) = \mathsf{l}(h_2) = j+1 \\ P': & \mathsf{l}(h_1) = \mathsf{r}(h_2) = i+1 & \mathsf{r}(h_1) = \mathsf{l}(h_2) = j \end{array}$$

We therefore preserve the validity of the formula as long as the numbers $\lambda_{l,r} = \lambda_{r,l}$ are chosen in such a way that the following equality holds.

$$\delta_{i,j} = \frac{1}{2}(\lambda_{i,j+1} + \lambda_{j+1,i}) - \frac{1}{2}(\lambda_{i+1,j} + \lambda_{j,i+1}) = \lambda_{i,j+1} - \lambda_{i+1,j}$$

The definition $\lambda_{l,r} := \delta_{n-2,0} + \delta_{n-3,1} + \cdots + \delta_{l,r-1} + c_n$ satisfies this constraint. Moreover, the assumed symmetry $\lambda_{l,r} = \lambda_{r,l}$ follows from the skew-symmetry $\delta_{i,j} = -\delta_{j,i}$. Note that $l+r = n-1$ always holds, and that c_n is an arbitrary integer independent of l and r; for the proof to go through one could simply fix $c_n = 0$.

Finally, γ_n is chosen in such a way that the formula holds for some conowheel set. The most natural choice for anchoring the formula is a set in convex position.

$$\gamma_n := \mathrm{nf}_{\mathfrak{G}}(P_{\mathsf{con}}) + \frac{1}{2} \sum_{l,r:\ l+r=n-1} \lambda_{l,r} \qquad \square$$

Computing the frequency vector is possible in $O(n \log n)$ time. Given the values Λ_k, computing the number $\mathrm{nf}_{\mathfrak{G}}(P)$ then requires only $O(n)$ additional arithmetic operations.

Example continued, embracing triangles. We have already argued that $\delta_{i,j} = j - i$ holds for $\mathfrak{G} = \{K_4^{\cdot\cdot}\}$. This now gives rise to the following values for $\lambda_{l,r}$ if we choose $c_n = \binom{n-1}{2}$.

$$\begin{aligned}\lambda_{l,r} &= \delta_{n-2,0} + \delta_{n-3,1} + \cdots + \delta_{l,r-1} + c_n \\ &= \sum_{j=0}^{r-1} j - \left(\binom{n-1}{2} - \sum_{i=0}^{l-1} i\right) + c_n = \binom{l}{2} + \binom{r}{2}\end{aligned}$$

It can be checked that $\mathrm{nf}_{\mathfrak{G}}(P_{\mathsf{con}}) = 0$. Hence, we get the following value for γ_n.

$$\gamma_n = \mathrm{nf}_{\mathfrak{G}}(P_{\mathsf{con}}) + \frac{1}{2}\sum_{l,r} \lambda_{l,r} = 0 + \frac{1}{2}\sum_{l=0}^{n-1}\binom{l}{2} + \frac{1}{2}\sum_{r=0}^{n-1}\binom{r}{2} = \binom{n}{3}$$

After putting everything together we obtain the exact formula displayed earlier in equation (5.4).

5.3.2 Further Examples

The following two simple applications are insensitive in the sense that the number of corresponding crossing-free geometric graphs is the same on all wheel sets; but it may be different for sets in convex position.

Spanning cycles. Consider the case where $\mathfrak{G}$ contains a single cycle over $n+1$ vertices. Then, we have $\delta_{i,j} = 0$ because no crossing-free spanning cycle can use the edge $\{h_1, h_2\}$; that is, unless $i = 0$ or $j = 0$, in which case we have $\delta_{0,n-2} = -\delta_{n-2,0} = n - 1$. For anchoring we use $\mathrm{nf}_{\mathfrak{G}}(P_{\mathsf{con}}) = 1$. It follows that all wheel sets over $n+1$ points have n crossing-free spanning cycles, which is of course not hard to see directly.

Spanning paths. If $\mathfrak{G}$ contains a single path over $n+1$ vertices, then we also get $\delta_{i,j} = 0$ unless $i = 0$ or $j = 0$, but for a different reason. On P there are $2 \cdot 2^i \cdot 2^{j-1}$ crossing-free spanning paths that use the edge $\{h_1, h_2\}$, since there are 2 choices for deciding which one of h_1 and h_2 is connected to the left hand side, 2^i choices for completing the left hand side to a path and 2^{j-1} choices for completing the right hand side to a path. Likewise, on P' there are $2 \cdot 2^{i-1} \cdot 2^j$ spanning paths, which is the same number. Using a similar argument, the following can also be verified.

$$\delta_{0,n-2} = 2 \cdot (2^{n-2} + \sum_{k=1}^{n-2} 2^{k-1} \cdot 2^{n-2-k}) - 2 \cdot 2^{n-3} = (n-1)2^{n-2}$$

For anchoring we make the simple observation that $\mathrm{nf}_{\mathfrak{G}}(P_{\mathsf{con}}) = (n+1)2^{n-2}$, which then implies that $\mathrm{nf}_{\mathfrak{G}}(P) = \mathrm{sp}(P) = n2^{n-1}$ holds for any wheel set P.

The next two applications are sensitive in the sense that different wheel sets have different numbers of corresponding crossing-free geometric graphs. The running example with embracing triangles is also of this kind.

Matchings. Let $\mathfrak{G} = \mathfrak{M}$, the set of not necessarily perfect matchings over $n+1$ vertices. From Section 2.1 we know that $\mathrm{nf}_{\mathfrak{M}}(P_{\mathsf{con}}) = M_{n+1} := \sum_{k=0}^{\lfloor (n+1)/2 \rfloor} \binom{n+1}{2k} C_k$, the $(n+1)$-th Motzkin number. It is easy to compute $\delta_{i,j} = M_i M_{j+1} - M_{i+1} M_j$ since, as always, we only have to worry about graphs that use the edge $\{h_1, h_2\}$. This gives $\lambda_{l,r} = M_l M_r$ and $\gamma_n = M_{n+1} + \frac{1}{2} \sum_{l,r} M_l M_r$. After simplifying we obtain the following formula.

$$\mathrm{nf}_{\mathfrak{M}}(P) = \mathrm{ma}(P) = \frac{3M_{n+1} - M_n}{2} - \frac{1}{2} \sum_{h \in H} M_{\mathsf{l}(h)} M_{\mathsf{r}(h)} \qquad (5.5)$$

Spanning trees. Let $\mathfrak{G} = \mathfrak{T}$, the set of all abstract trees over $n+1$ vertices. We shall use $\mathrm{nf}_{\mathfrak{T}}(P_{\mathsf{con}}) = T_{n+1} \coloneqq \frac{1}{2n+1}\binom{3n}{n}$. Furthermore, we also use the following hypergeometric identity.

$$\sum_{k=0}^{i} T_{k+1}T_{i-k+1} = \frac{1}{i+1}\binom{3i+1}{i}$$

Consider the set P as in Figure 5.2. To complete the left side into a spanning tree, we build two disjoint trees rooted at h_1 and h_2, respectively. There are 2 choices for assigning w either to the upper or lower tree, and there are $i+1$ choices for distributing the i points on the left among the two trees. Indeed, observe that the k, say, out of i points assigned to h_1 have to appear consecutively with h_1 on the convex hull as otherwise we get a crossing. Once the points have been distributed, we are left with two point sets of size $k+1$ and $i-k+2$ in convex position. For completing the right side into a spanning tree, a simpler argument can be used without the additional complication of w. The set P' is handled analogously.

$$\begin{aligned}
\delta_{i,j} &= 2\sum_{k=0}^{j} T_{k+1}T_{j-k+2} \cdot \sum_{k=0}^{i} T_{k+1}T_{i-k+1} \\
&\qquad - 2\sum_{k=0}^{i} T_{k+1}T_{i-k+2} \cdot \sum_{k=0}^{j} T_{k+1}T_{j-k+1} \\
&= 2\left(\frac{2}{j+2}\binom{3j+3}{j} \cdot \frac{1}{i+1}\binom{3i+1}{i}\right. \\
&\qquad \left. - \frac{2}{i+2}\binom{3i+3}{i} \cdot \frac{1}{j+1}\binom{3j+1}{j}\right)
\end{aligned}$$

For this application, we do not know if a simple closed form expression exists for $\lambda_{l,r}$. Still, note that if one were to compute $\mathrm{nf}_{\mathfrak{T}}(P)$, the numbers $\delta_{i,j}$ could be summed up in linear time and the value of γ_n could be computed on the fly for any given n.

Related applications. Observe that, for example, a triangulation on P_{con} can also be embedded as a crossing-free geometric graph on P_{bar}. However, this embedding is no longer a triangulation since it is not edge-maximal. Hence, there is no natural choice for $\mathfrak{G}$ such that $\mathrm{nf}_{\mathfrak{G}}(P)$ is the number of geometric triangulations on any conowheel set P. There are other families of geometric graphs whose number on a conowheel set P cannot be expressed easily in the form $\mathrm{nf}_{\mathfrak{G}}(P)$—such as crossing-free convex partitions—but for which the argument behind the proof of Theorem 5.3 is still applicable and leads to similarly simple formulas. All that is required is a specialized version of Lemma 5.6.

Furthermore, we note that Theorem 5.3 generalizes to crossing-free hypergraphs, where crossing-free means that the convex hulls of any two hyperedges intersect in an at most 1-dimensional set.

5.3.3 The Symmetric Wheel Set Maximizes

In what follows, we give a sufficient condition that allows us to prove that among all conowheel sets, the symmetric wheel set P_{sym} maximizes the number of geometric graphs of many families. Recall that the set P_{sym} is constructed by taking the vertex set of a regular n-gon and by adding the extra point w at the center. For the case that n is even, we slightly perturb the position of w in order to obtain a point set in general position.

Lemma 5.7. *Let $\mathfrak{G}$ be any set of abstract graphs for which $\delta_{i,j} \geq 0$ holds for all $i < j$. Then, the number $\mathrm{nf}_{\mathfrak{G}}(P)$ is maximized for $P = P_{\mathsf{sym}}$.*

Proof. We start with a point set that contains the vertices of a regular n-gon and the extra point w added in such a way that the whole set is in convex position. We then let w move on a straight line

towards its final position in P_{sym}, which gives the following relation.

$$\mathrm{nf}_{\mathfrak{G}}(P_{\mathsf{sym}}) = \mathrm{nf}_{\mathfrak{G}}(P_{\mathsf{con}}) + \sum_{\substack{i,j\colon i<j \\ i+j=n-2}} (i+1)\cdot\delta_{i,j}$$

Note that, for the case that n is even, we always have $\delta_{i,j} = 0$ whenever $i = j$ by symmetry. Hence, we need not worry about how w was perturbed in P_{sym}.

For an arbitrary conowheel set P, we wish to prove that $\mathrm{nf}_{\mathfrak{G}}(P) \leq \mathrm{nf}_{\mathfrak{G}}(P_{\mathsf{sym}})$ holds. We start with a point set that is a copy of P except that the extra point w has been moved in such a way that the whole set is again in convex position. By letting w move on a straight line to its final position in P, we now obtain the following equation.

$$\begin{aligned}\mathrm{nf}_{\mathfrak{G}}(P) &= \mathrm{nf}_{\mathfrak{G}}(P_{\mathsf{con}}) + \sum_{\substack{i,j\colon i<j \\ i+j=n-2}} \alpha(i)\underbrace{\delta_{i,j}}_{\geq 0} + \sum_{\substack{i,j\colon i>j \\ i+j=n-2}} \alpha(i)\underbrace{\delta_{i,j}}_{\leq 0} \\ &\leq \mathrm{nf}_{\mathfrak{G}}(P_{\mathsf{sym}})\end{aligned}$$

In the formula above, the number $\alpha(i)$ indicates, for any fixed i, how often an (i,j)-transition occurs during this process. The last inequality follows after observing that $\alpha(i) \leq i+1$. □

It is easy to see that the condition in Lemma 5.7 holds for our running example with embracing triangles. By making use of the fact that Motzkin numbers are log-concave [7], it can also be shown to hold for crossing-free matchings. For the case of crossing-free spanning trees, on the other hand, by starting from the computed formula for $\delta_{i,j}$ and by doing some elementary calculations, one can derive the following equivalence.

$$\delta_{i,j} \geq 0 \iff \frac{(i+1)(i+\frac{2}{3})}{(i+2)(i+\frac{3}{2})} \leq \frac{(j+1)(j+\frac{2}{3})}{(j+2)(j+\frac{3}{2})}$$

Assuming $i < j$, we see that the factor $\frac{i+1}{i+2}$ is dominated by the factor $\frac{j+1}{j+2}$. The same can be said for the other two factors, and hence we conclude that $\delta_{i,j} \geq 0$.

Corollary 5.8. *When restricted to conowheel sets, the number of embracing triangles, crossing-free matchings and crossing-free spanning trees, respectively, is maximized for the symmetric wheel set.*

5.3.4 Embracing Sets Determine Frequency Vector

We generalize the notion of embracing triangles to larger sets. Consider a conowheel set $P = H \cup \{w\}$ of size $n+1$. A subset $A \subseteq H$ is a *w-embracing k-set* if w is in the convex hull of A and $|A| = k$. For simplicity, we shall consider $w = \mathbf{0}$ and call A an *origin-embracing k-set*, or simply *embracing k-set*.

We can show that the number of embracing k-sets is determined by the frequency vector of P for any k, and not just for $k = 3$ as seen earlier in equation (5.4). Indeed, since H is in general position, for every non-embracing k-set $A \subseteq H$ there exists a unique point $h \in A$ such that the convex hull of A is in the closed halfplane to the left of the directed line through w and h. Observe that for any choice of $h \in H$ we can construct $\binom{\mathsf{l}(h)}{k-1}$ such non-embracing k-sets, and thus it is possible to get a generalization of (5.4). Interestingly, the reverse also turns out to be true.

Lemma 5.9. *The sequence $(\mathsf{embr}_k)_{k=3}^{n}$, where embr_k is the number of embracing k-sets in a conowheel set $P = H \cup \{w\}$ of size $n+1$, determines the frequency vector of P.*

Proof. Let $E = (\mathsf{embr}_k)_{k=3}^{n}$. Consider the vector $L = (L_j)_{j=1}^{n-1}$ where L_j is the number of points $h \in H$ with $\mathsf{l}(h) = j$. Clearly, L determines the frequency vector of P. It thus suffices to show that E determines L.

As argued earlier, the number embr_k of embracing k-sets can be written as follows.

$$\mathsf{embr}_k = \binom{n}{k} - \sum_{h \in H} \binom{\mathsf{l}(h)}{k-1}$$

The above equation also holds for $k = 2$. We can thus define a vector $E' = (e_i)_{i=1}^{n-1}$ with $e_i = \binom{n}{i+1} - \mathsf{embr}_{i+1}$ and a square matrix $A = (a_{i,j})_{i,j=1}^{n-1}$ with $a_{i,j} = \binom{j}{i}$, such that $E' = AL$ holds. Since the matrix A is unitriangular, it has an inverse, from which we can conclude that E' determines L. □

Corollary 5.10. *Let P and P' be two conowheel sets. Then, we have that $\mathrm{nf}_{\mathfrak{G}}(P) = \mathrm{nf}_{\mathfrak{G}}(P')$ holds for every graph class $\mathfrak{G}$ if and only if $F(P) = F(P')$.*

Proof. We already know from Theorem 5.3 that the frequency vector determines the number of crossing-free geometric graphs. For the other direction, we reconstruct the number of embracing k-sets by appropriately choosing the graph classes $\mathfrak{G}$. After that, the frequency vector is determined by Lemma 5.9.

The number of embracing triangles is equal to the number $\mathrm{nf}_{\{K_4^{\cdots}\}}(P)$ and therefore, by assumption, the same for both P and P'. We now simply generalize to k-wheels; that is, we consider a set $\mathfrak{G}$ that contains a single cycle with k vertices, each adjacent to one additional vertex. All that is left to observe is that for such $\mathfrak{G}$ the number $\mathrm{nf}_{\mathfrak{G}}(P)$ is equal to the number of embracing k-sets in P, and hence the same for both P and P'. □

5.4 Higher Dimensions

As noted in the introduction, the concept of a conowheel set can be generalized to higher dimension. However, already in $\mathbb{R}^3$ we face

certain challenges. For example, the number of tetrahedralizations of $n+1$ points in convex position in $\mathbb{R}^3$ does not only depend on n, in contrast to the 2-dimensional case. Even when considering simpler structures, like the set of w-embracing tetrahedra, the ideas from the proof of Theorem 5.3 do not generalize. Intuitively, the argument of w passing over a segment does not work in 3-space, as it can pass over but also beside a triangle.

Oriented simplices. Given a set A of d affinely independent points in $\mathbb{R}^d$, its convex hull $\mathsf{CH}(A)$ is a $(d-1)$-simplex and its affine hull is a hyperplane. We want to be able to refer to the two sides of this hyperplane by identifying a positive and a negative side. For that, consider a sequence $p_1p_2\ldots p_d$ of d affinely independent points. The corresponding affine hull can be described as the set of points q with $\sigma(q, p_1p_2\ldots p_d) = 0$, where

$$\sigma(q, p_1p_2\ldots p_d) := \det(p_1 - q, p_2 - q, \ldots, p_d - q).$$

We call the set of points q with $\sigma(q, p_1p_2\ldots p_d) > 0$ the *positive side* of $p_1p_2\ldots p_d$, and the set of points q with $\sigma(q, p_1p_2\ldots p_d) < 0$ the *negative side*. Note that for $d = 2$, the positive side of p_1p_2 is the set of points left of the line through p_1 and p_2, directed from p_1 to p_2. Also note that the positive side of p_1p_2 coincides with the negative side of p_2p_1. For $d \geq 3$, distinct orderings of the given d points may have identical positive sides; this happens if and only if the orderings can be obtained from each other by an even number of transpositions.

An *oriented* $(d-1)$*-simplex* is a sequence $p_1p_2\ldots p_d$ of d affinely independent points, with the convex hull as its associated $(d-1)$-simplex and with corresponding positive and negative sides as defined above. Two such oriented $(d-1)$-simplices are defined to be equivalent if their sequences can be obtained from each other by an even number of transpositions.

Via oriented simplices, the concept of an order type generalizes to arbitrary dimension. Similar to the 2-dimensional case, the order type of a set $P = H \cup \{w\}$ in $\mathbb{R}^d$ determines the set of points on the positive side of the oriented $(d-1)$-simplex $wh_1 \dots h_{d-1}$, for each $(d-1)$-tuple in H. We denote by $\mathsf{l}(h_1 \dots h_{d-1})$ the number of such points, and we denote by $\mathsf{r}(h_1 \dots h_{d-1})$ the number of points on the negative side.

5.4.1 Embracing Sets

Generalizing the approach of counting embracing k-sets from Section 5.3.4 to higher dimension fails already in 3-space. Indeed, consider the set of non-embracing tetrahedra for a set $H \subseteq \mathbb{R}^3$ in convex position. Observe now that any such tetrahedron has either three or four edges that form a tangent plane through w.

Instead, consider a partition $B \dot\cup W = H$ defined by a plane ϕ through w that is disjoint from H. Then, the set of non-embracing k-sets consists of those completely contained in B and W, respectively, and those intersected by ϕ. For the latter, consider the intersection of $\mathsf{CH}(A)$ of such a set A with ϕ. There is again a unique tangent point $t = pq \cap \phi$ such that $\mathsf{CH}(A) \cap \phi$ is on the left side of the line wt on ϕ. Hence, the number of embracing k-sets in 3-space can be written as follows.

$$\mathsf{embr}_k = \binom{n}{k} - \binom{|B|}{k} - \binom{|W|}{k} - \sum_{pq \in B \times W} \binom{\mathsf{l}(pq)}{k-2}$$

In the following lemma, we generalize the above approach to arbitrary dimension.

Lemma 5.11. *Let H be a set of n points in $\mathbb{R}^d$, with $H \cup \{\mathbf{0}\}$ in general position, and let ψ be a generic 2-flat that contains the origin. Let* $\mathrm{proj} : \mathbb{R}^d \to \mathbb{R}^{d-2}$ *be a projection that maps all of ψ to*

$\mathbf{0} \in \mathbb{R}^{d-2}$. *Then, the number of embracing k-sets in H is given by the following formula.*

$$\mathsf{embr}_k(\mathrm{proj}(H)) - \frac{1}{2} \sum_{\substack{\rho \in \binom{H}{d-1} \\ \mathsf{CH}(\rho) \cap \psi \neq \emptyset}} \left(\binom{\mathsf{l}(\rho)}{k-d+1} + \binom{\mathsf{r}(\rho)}{k-d+1} \right)$$

Proof. Clearly, any embracing k-set is also an embracing k-set in the projection, so we only have to subtract the number of non-embracing k-sets which happen to be embracing in the projection. Let A be such a set. Since $\mathbf{0} \in \mathrm{proj}(\mathsf{CH}(A))$, we have $\mathsf{CH}(A) \cap \psi \neq \emptyset$. In the 2-dimensional subspace defined by ψ, there is a unique point t on the boundary of $\mathsf{CH}(A) \cap \psi$ such that $\mathsf{CH}(A) \cap \psi$ is in the left closed halfplane defined by $\mathbf{0}t$. Since ψ is generic, t is the intersection of ψ with a $(d-2)$-simplex defined by a tuple ρ of $d-1$ points of A, and the oriented $(d-1)$-simplex $\mathbf{0}\rho$ has all points of $A \setminus \rho$ either on its positive or negative side. We are thus counting each such non-embracing k-set twice and the claim follows. □

With the previous lemma at hand, it is now a simple task to give a proof of our main computational result.

Theorem 5.4 (restated)**.** *Let $d \geq 3$ be fixed and let H be a set of n points in $\mathbb{R}^d$. Then, the simplicial depth of a point w in H can be computed in $O(n^{d-1})$ time.*

Proof. The proof of Lemma 5.11 is constructive apart from the choice of ψ, which can be done generically using the techniques in [21]. Whether a $(d-1)$-simplex intersects ψ can be computed in $O(d^d)$ time. It thus remains to compute the values of $\mathsf{l}(\rho)$ for the $(d-1)$-tuples ρ. While a brute-force approach takes $O(n^d)$ time, we can consider the points in H as vectors representing points in the $(d-1)$-dimensional projective plane. We compute the dual hyperplane arrangement in $O(n^{d-1})$ time, which allows us to extract the values of $\mathsf{l}(\rho)$ within the same time bounds, as discussed in [22]. □

5.4.2 Polytopes with Few Vertices

Through the so-called Gale transform [68, 69], origin-embracing triangles are in correspondence with facets or $(n-4)$-faces of simplicial $(n-3)$-polytopes with at most n vertices. More generally, subsets of size i that contain the origin in their convex hull correspond to $(n-i-1)$-faces. Therefore, some of our results connect to such simplicial d-dimensional polytopes with at most $d+3$ vertices.

Gale duality. For $n > d$, we call a matrix $A \in \mathbb{R}^{n\times d}$ *legal* if A has full rank d and $A^\top \mathbf{1}_n = \mathbf{0}_d$. Let $S_A = (p_1, p_2, \ldots, p_n)$ be the sequence of points in $\mathbb{R}^d$ with the coordinates of p_i obtained from the i-th row of A. Legal thus means that S_A is not contained in a hyperplane and that the origin is the centroid of S_A. For legal matrices $A \in \mathbb{R}^{n\times d}$ and $B \in \mathbb{R}^{n\times n-d-1}$, we call B an *orthogonal dual* of A, in symbols $A \perp B$, if $A^\top B = \mathbf{0}$. S_B is called a *Gale dual* or *Gale transform* of S_A. In other words, if $A \perp B$ then all columns of B are orthogonal to all columns of A; together with the legal condition, this means that the columns of B span the space of all vectors orthogonal to the columns of A and to $\mathbf{1}_n$.

Proposition 5.12 ([45, page 111])**.** *Let $A \perp B$ such that $S_A = (p_1, p_2, \ldots, p_n)$, $S_B = (p_1^*, p_2^*, \ldots, p_n^*)$. For every $I \subseteq [n]$, the set $\{p_i : i \in I\}$ is contained in a facet of $\mathsf{CH}(S_A)$ if and only if $\{p_i^* : i \notin I\}$ is embracing.*

For a d-dimensional polytope $\mathcal{P}$, the *f-vector of $\mathcal{P}$* is defined as $f(\mathcal{P}) = (f_{-1}, f_0, \ldots, f_{d-1})$, where $f_i(\mathcal{P})$ is the number of i-faces of $\mathcal{P}$; the empty face is the unique (-1)-face, 0-faces are vertices, 1-faces are edges, $(d-1)$-faces are facets. A property of the Gale dual is that the points in S_A are in general position if and only if the rows in B are linearly independent. [45, page 111] Thus, if $S = \{p_1, p_2, \ldots, p_n\}$ is a set of n points in general position, if $\mathcal{P} = \mathsf{CH}(S)$, and if Q is the set $\{p_1^*, p_2^*, \ldots, p_n^*\}$, then $f_i(\mathcal{P})$ equals the number of embracing

$(n-i-1)$-sets in Q. Computing the f-vector can thus be done by computing the Gale dual and by using Proposition 5.12.

Proposition 5.13. *Given a legal matrix $A \in \mathbb{R}^{n\times d}$, an orthogonal dual can be computed in time $O(n^\omega)$, where ω is the exponent for matrix multiplication over $\mathbb{R}$.*

Proof. Note that $(A\mathbf{1}_n) \in \mathbb{R}^{n\times d+1}$ also has full rank $d+1$ because the extra column $\mathbf{1}_n$ is orthogonal to all columns in A. Recall that, therefore, there exists a factorization $(A\mathbf{1}_n)^\top = LUP$ where $L \in \mathbb{R}^{d+1\times d+1}$ is lower triangular, $U = (U_1, U_2) \in \mathbb{R}^{d+1\times d+1} \times \mathbb{R}^{d+1\times n-d-1}$ is upper triangular (in particular, this means that all entries in the diagonals of L and U_1 are non-zero and that these matrices are invertible), and $P \in \mathbb{R}^{n\times n}$ is a permutation matrix. [16, Theorem 16.4] Also recall that such a factorization can be computed in time $O(n^\omega)$. [16, Theorem 16.5].

Given such a factorization, it is now easy to compute an orthogonal dual $B \in \mathbb{R}^{n\times n-d-1}$. Indeed, for unknown $B_1 \in \mathbb{R}^{d+1\times n-d-1}$ and identity matrix $I \in \mathbb{R}^{n-d-1\times n-d-1}$, write the rows in B such that the following equation holds.

$$PB = \begin{pmatrix} B_1 \\ I \end{pmatrix}$$

The equality $\mathbf{0} = (A\mathbf{1}_n)^\top B = LUPB$ is satisfied if and only if $\mathbf{0} = UPB = U_1B_1 + U_2$, which in turn holds if and only if we have $B_1 = -U_1^{-1}U_2$. B has full rank since the columns are linearly independent. Lastly, the inverse U_1^{-1} can be computed in time $O(d^\omega)$. [16, Proposition 16.6] □

Corollary 5.14. *For a set S of $n = d+k$ points in general position in $\mathbb{R}^d$, the number of facets of the simplicial polytope $\mathsf{CH}(S)$ can be computed in time $O(n^{k-2})$ for $k \geq 5$ and in $O(n^\omega)$ otherwise, where ω is the exponent for matrix multiplication over $\mathbb{R}$.*

The asymptotic number of facets may be as large as n^k. A generalization of Corollary 5.14 to sets not necessarily in general position is possible for $k = 3$. Our efficient computation of the number of embracing k-sets thus lets us obtain not only the f-vector of a polytope, but also related vectors like the h- and the g-vector.

Bibliography

[1] P. Afshani, D. R. Sheehy, and Y. Stein. Approximating the Simplicial Depth in High Dimensions. In *Proc. 32nd European Workshop on Computational Geometry*, 2016.

[2] O. Aichholzer. The Path of a Triangulation. In *Proc. 15th Symposium on Computational Geometry*, pages 14–23, 1999.

[3] O. Aichholzer, V. Alvarez, T. Hackl, A. Pilz, B. Speckmann, and B. Vogtenhuber. An Improved Lower Bound on the Minimum Number of Triangulations. In *Proc. 32nd Symposium on Computational Geometry*, pages 7:1–7:16, 2016.

[4] O. Aichholzer, F. Aurenhammer, C. Huemer, and B. Vogtenhuber. Gray Code Enumeration of Plane Straight-Line Graphs. *Graphs and Combinatorics*, 23(5):467–479, 2007.

[5] O. Aichholzer, T. Hackl, C. Huemer, F. Hurtado, H. Krasser, and B. Vogtenhuber. On the Number of Plane Geometric Graphs. *Graphs and Combinatorics*, 23(1):67–84, 2007.

[6] O. Aichholzer, V. Kusters, W. Mulzer, A. Pilz, and M. Wettstein. An Optimal Algorithm for Reconstructing Point

Set Order Types from Radial Orderings. *International Journal of Computational Geometry and Applications*, 27:57–83, 2017.

[7] M. Aigner. Motzkin Numbers. *European Journal of Combinatorics*, 19(6):663 – 675, 1998.

[8] M. Ajtai, V. Chvátal, M. M. Newborn, and E. Szemerédi. Crossing-free subgraphs. *Annals Discrete Mathematics*, 12:9–12, 1982.

[9] V. Alvarez, K. Bringmann, R. Curticapean, and S. Ray. Counting Triangulations and Other Crossing-Free Structures via Onion Layers. *Discrete & Computational Geometry*, 53(4):675–690, 2015.

[10] V. Alvarez, K. Bringmann, S. Ray, and R. Seidel. Counting triangulations and other crossing-free structures approximately. *Computational Geometry: Theory and Applications*, 48(5):386–397, 2015.

[11] V. Alvarez and R. Seidel. A Simple Aggregative Algorithm for Counting Triangulations of Planar Point Sets and Related Problems. In *Proc. 29th Symposium on Computational Geometry*, pages 1–8, 2013.

[12] A. Asinowski and G. Rote. Point sets with many non-crossing matchings. *Computational Geometry: Theory and Applications*, 68:7–33, 2018.

[13] D. Avis and K. Fukuda. Reverse search for enumeration. *Discrete Applied Mathematics*, 65:21–46, 1996.

[14] S. Bespamyatnikh. An efficient algorithm for enumeration of triangulations. *Computational Geometry: Theory and Applications*, 23(3):271–279, 2002.

[15] A. E. Brouwer. The enumeration of locally transitive tournaments. Technical Report Report ZW 138/80, Mathematisch Centrum, Amsterdam, 1980.

[16] P. Bürgisser, T. Lickteig, M. Clausen, and A. Shokrollahi. *Algebraic Complexity Theory*. Springer Berlin Heidelberg, 1996.

[17] J. Cardinal, M. Hoffmann, V. Kusters, C. D. Tóth, and M. Wettstein. Arc diagrams, flip distances, and Hamiltonian triangulations. *Computational Geometry: Theory and Applications*, 68:206–225, 2018.

[18] E. Catalan. Note sur une équation aux différences finies. *Journal de Mathématiques Pures et Appliquées*, 3:508–516, 1838.

[19] A. Y. Cheng and M. Ouyang. On Algorithms for Simplicial Depth. In *Proc. 13th Canadian Conference on Computational Geometry*, pages 53–56, 2001.

[20] A. Dumitrescu, A. Schulz, A. Sheffer, and C. D. Tóth. Bounds on the Maximum Multiplicity of Some Common Geometric Graphs. *SIAM Journal on Discrete Mathematics*, 27(2):802–826, 2013.

[21] H. Edelsbrunner and E. P. Mücke. Simulation of simplicity: a technique to cope with degenerate cases in geometric algorithms. *ACM Transactions on Graphics*, 9(1):66–104, 1990.

[22] H. Edelsbrunner, J. O'Rourke, and R. Seidel. Constructing Arrangements of Lines and Hyperplanes with Applications. *SIAM Journal on Computing*, 15(2):341–363, 1986.

[23] L. Euler. Letter to Goldbach, dated September 4, 1751. Published as "Lettre CXL, Euler à Goldbach". In *Leonhard Euler Briefwechsel*, volume I, page 159.

[24] P. Flajolet and M. Noy. Analytic combinatorics of non-crossing configurations. *Discrete Mathematics*, 204:203–229, 1999.

[25] P. Flajolet and R. Sedgewick. *Analytic combinatorics*. Cambridge University Press, Cambridge, 2009.

[26] F. Frati, J. Gudmundsson, and E. Welzl. On the number of upward planar orientations of maximal planar graphs. *Theoretical Computer Science*, 544:32–59, 2014.

[27] A. García, M. Noy, and J. Tejel. Lower bounds on the number of crossing-free subgraphs of K_n. *Computational Geometry: Theory and Applications*, 16(4):211–221, 2000.

[28] J. Gil, W. L. Steiger, and A. Wigderson. Geometric medians. *Discrete Mathematics*, 108(1-3):37–51, 1992.

[29] J. E. Goodman and R. Pollack. Multidimensional Sorting. *SIAM Journal on Computing*, 12(3):484–507, 1983.

[30] J. E. Goodman and R. Pollack. Semispaces of configurations, cell complexes of arrangements. *Journal of Combinatorial Theory Series A*, 37(3):257–293, 1984.

[31] K. Górska and K. A. Penson. Multidimensional Catalan and related numbers as Hausdorff moments. *Probability and Mathematical Statistics*, 33(2):265–274, 2013.

[32] B. Grünbaum. *Convex Polytopes*. Springer, 2nd edition, 2003.

[33] M. Hoffmann, A. Schulz, M. Sharir, A. Sheffer, C. D. Tóth, and E. Welzl. Counting Plane Graphs: Flippability and Its Applications. *Thirty Essays on Geometric Graph Theory*, pages 303–325, 2012.

[34] C. Huemer and A. de Mier. Lower bounds on the maximum number of non-crossing acyclic graphs. *European Journal of Combinatorics*, 48:48–62, 2015.

[35] F. Hurtado and M. Noy. Counting triangulations of almost-convex polygons. *Ars Combinatoria*, 45:169–179, 1997.

[36] M. Karpinski, A. Linga, and D. Sledneu. A QPTAS for the base of the number of crossing-free structures on a planar point set. *Theoretical Computer Science*, 711:56–65, 2018.

[37] N. Katoh and S.-I. Tanigawa. Fast Enumeration Algorithms for Non-crossing Geometric Graphs. *Discrete & Computational Geometry*, 42:443–468, 2009.

[38] D. Kelly. Fundamentals of planar ordered sets. *Discrete Mathematics*, 63(2-3):197–216, 1987.

[39] S. Khuller and J. S. B. Mitchell. On a Triangle Counting Problem. *Information Processing Letters*, 33(6):319–321, 1990.

[40] G. Lamé. Extrait d'une lettre de M. Lamé à M. Liouville sur cette question: Un polygone convexe étant donné, de combien de manières peut-on le partager en triangles au moyen de diagonales? *Journal de Mathématiques Pures et Appliquées*, 3:505–507, 1838.

[41] J. B. Lewis. Pattern avoidance for alternating permutations and Young tableaux. *Journal of Combinatorial Theory Series A*, 118(4):1436–1450, 2011.

[42] S. Linusson. The Number of M-Sequences and f-Vectors. *Combinatorica*, 19(2):255–266, 1999.

[43] R. Y. Liu. On a notion of data depth based on random simplices. *Annals of Statistics*, 18:405–414, 1990.

[44] D. Marx and T. Miltzow. Peeling and Nibbling the Cactus: Subexponential-Time Algorithms for Counting Triangulations and Related Problems. In *Proc. 32nd Symposium on Computational Geometry*, pages 52:1–52:15, 2016.

[45] J. Matoušek. *Lectures on Discrete Geometry.* Springer, 2002.

[46] T. Motzkin. Relations between hypersurface cross ratios, and a combinatorial formula for partitions of a polygon, for permanent preponderance, and for non-associative products. *Bulletin of the American Mathematical Society*, 54(4):352–360, 1948.

[47] J.-C. Novelli, I. Pak, and A. V. Stoyanovskii. A direct bijective proof of the hook-length formula. *Discrete Mathematics and Theoretical Computer Science*, 1(1):53–67, 1997.

[48] I. Pak. History of Catalan Numbers. Accessed: April 12, 2018. URL: `http://www.math.ucla.edu/~pak/papers/cathist4.pdf`.

[49] E. M. Palmer and R. W. Robinson. Enumeration of self-dual configurations. *Pacific Journal of Mathematics*, 110(1):203–221, 1984.

[50] A. Pilz, E. Welzl, and M. Wettstein. From Crossing-Free Graphs on Wheel Sets to Embracing Simplices and Polytopes with Few Vertices. In *Proc. 33rd Symposium on Computational Geometry*, pages 54:1–54:16, 2017.

[51] D. Randall, G. Rote, F. Santos, and J. Snoeyink. Counting Triangulations and Pseudo-Triangulations of Wheels. In *Proc. 13th Canadian Conference on Computational Geometry*, pages 149–152, 2001.

[52] S. Ray and R. Seidel. A Simple and Less Slow Method for Counting Triangulations and for Related Problems. In *Proc. 20th European Workshop on Computational Geometry*, 2004.

[53] A. Razen and E. Welzl. Counting Plane Graphs with Exponential Speed-Up. *Rainbow of Computer Science*, pages 36–46, 2011.

[54] P. J. Rousseeuw and I. Ruts. Bivariate Location Depth. *Journal of the Royal Statistical Society Series C*, 45(4):516–526, 1996.

[55] A. J. Ruiz-Vargas and E. Welzl. Crossing-Free Perfect Matchings in Wheel Point Sets. *A Journey through Discrete Mathematics: A Tribute to Jiri Matousek*, pages 735–764, 2017.

[56] J. A. Segner. Enumeratio modorum quibus figurae planae rectilineae per diagonales dividuntur in triangula. *Novi Commentarii Academiae Scientiarum Imperialis Petropolitanae*, 7:203–210, 1761.

[57] R. Seidel. Reprint of: A simple and fast incremental randomized algorithm for computing trapezoidal decompositions and for triangulating polygons. *Computational Geometry: Theory and Applications*, 43(6-7):556–564, 2010.

[58] M. Sharir and A. Sheffer. Counting Triangulations of Planar Point Sets. *Electronic Journal of Combinatorics*, 18(1):1–74, 2011.

[59] M. Sharir and A. Sheffer. Counting Plane Graphs: Cross-Graph Charging Schemes. *Combinatorics, Probability and Computing*, 22:935–954, 2013.

[60] M. Sharir, A. Sheffer, and E. Welzl. Counting plane graphs: Perfect matchings, spanning cycles, and Kasteleyn's technique. *Journal of Combinatorial Theory, Series A*, 120:777–794, 2013.

[61] M. Sharir and E. Welzl. On the Number of Crossing-Free Matchings, Cycles, and Partitions. *SIAM Journal on Computing*, 36(3):695–720, 2006.

[62] R. P. Stanley. *Enumerative Combinatorics Volume 2*. Cambridge Studies in Advanced Mathematics. Cambridge University Press, Cambridge, 1999.

[63] R. A. Sulanke. Generalizing Narayana and Schröder numbers to higher dimensions. *Electronic Journal of Combinatorics*, 11(1):54, 2004.

[64] R. Tamassia and I. G. Tollis. A unified approach to visibility representations of planar graphs. *Discrete & Computational Geometry*, 1(4):321–341, 1986.

[65] G. T. Toussaint. Movable Separability of Sets. In *Computational Geometry*, pages 335–375. North-Holland, 1985.

[66] W. T. Tutte. A census of planar triangulations. *Canadian Journal of Mathematics*, 14:21–38, 1962.

[67] J. H. van Lint and R. M. Wilson. *A course in combinatorics*. Cambridge University Press, Cambridge, second edition, 2001.

[68] U. Wagner and E. Welzl. A Continuous Analogue of the Upper Bound Theorem. *Discrete & Computational Geometry*, 26(2):205–219, 2001.

[69] E. Welzl. Entering and Leaving j-Facets. *Discrete & Computational Geometry*, 25(3):351–364, 2001.

[70] M. Wettstein. Algorithms for Counting Crossing-free Configurations. Master's thesis, ETH Zürich, April 2013.

[71] M. Wettstein. Counting and Enumerating Crossing-free Geometric Graphs. In *Proc. 30th Symposium on Computational Geometry*, pages 1–10, 2014.

[72] M. Wettstein. Counting and Enumerating Crossing-free Geometric Graphs. *Journal of Computational Geometry*, 8(1):47–77, 2017.

[73] M. Wettstein. Trapezoidal Diagrams, Upward Triangulations, and Prime Catalan Numbers. *Discrete & Computational Geometry*, 58(3):505–525, 2017.

Curriculum Vitae

Manuel Wettstein

born 29 June 1987
citizen of Fislisbach, Aargau, Switzerland
Canale d'Agordo, Veneto, Italy

2003–2007	Swiss Gymnasial Matura Physics and Applied Mathematics Kantonsschule Wettingen
2007–2008	Military Service Rettungstruppen/Katastrophenhilfe
2008–2012	B.Sc. in Computer Science ETH Zürich
2011–2013	M.Sc. in Theoretical Computer Science ETH Zürich
2013–2018	Ph.D. in Theoretical Computer Science ETH Zürich